Hanse-Studien / Hanse Studies

Hanse-Wissenschaftskolleg (HWK) –
Institute for Advanced Study

**Band
Volume 6**

Manfred Herrmann / Christiane M. Thiel (Eds.)

Center for Advanced Imaging (CAI) · Bremen

Topics in Advanced Imaging

Hanse-Studien / Hanse Studies
Hanse-Wissenschaftskolleg Delmenhorst
Hanse Institute for Advanced Study

herausgegeben von
Gerhard Roth und Uwe Opolka

In der Reihe *Hanse-Studien / Hanse Studies* erscheinen – in deutscher oder englischer Sprache – unveröffentlichte Forschungsarbeiten, die am HWK in Delmenhorst entstanden sind, sowie Berichte über vom HWK durchgeführte Konferenzen.

Das HWK wurde 1995 gegründet und ist eine gemeinnützige Stiftung bürgerlichen Rechts der Länder Bremen und Niedersachsen sowie der Stadt Delmenhorst. Seine Hauptaufgabe besteht in der Stärkung des national und international anerkannten Forschungspotentials der umliegenden Universitäten und Forschungseinrichtungen, insbesondere der Universitäten Oldenburg und Bremen. Seine derzeitigen Arbeitsschwerpunkte liegen auf den Gebieten Meeres- und Klimaforschung, Neuro- und Kognitionswissenschaften, Sozialwissenschaften, Materialforschung sowie auf interdisziplinären Projekten. In diesen Bereichen beruft es Gastwissenschaftler (Fellows) und führt Tagungen durch.

Table of Contents

I.   Affective Neuroscience

II.   MR-Physics and Neuroimaging Methods

III.   Monkey Neurophysiology and Functional MRI

IV.   Functional MRI in Visual Psychophysics

V.   Functional MRI in Auditory Processing

VIII.   Various Topics

The Bremen MRI Perspective in Neuroscience

Willy Lemke, Senator for Education and Science

Free Hanseatic City of Bremen

Cognitive neuroscience is considered as a high priority topic within the framework of the Science Plan 2010 both with respect to research and teaching facilities promoted by the Senator for Education and Science.

The particular importance of the Cognitive Neuroscience derives from the broad fascination of its research topic – not only for scientists but also for wide parts of the public - as well as from the medical need to understand brain function. Only a clear and detailed understanding of the basic principles of brain function will provide the necessary knowledge to understand it's pathological deviations and the resulting neurological and psychiatric diseases. Moreover future treatments for these diseases will be only possible if physiology and pathophysiology of the brain are well understood. The demographic development with the increase in life expectancy will continuously raise the number of patients suffering from severe illnesses of the brain which directly affect and degrade the neurological condition as well as emotion and affect, personality traits, and the cognitive functions of our brains.

Cognitive Neuroscience at Bremen University covers a broad field of research and teaching activities which are carefully coordinated by the Center for Advanced Imaging (CAI). Its major goal is to understand the basic mechanisms of brain function and for that purpose it combines detailed investigations in animals, with theoretical modeling and human psychophysics and neuropsychology.

In this regard, the CAI plays an important role for the transfer of the results of fundamental research derived from experimental studies into the human brain by applying fMRI both in non-human and in human subjects.

Based on this research strategy the MRI facilities at Bremen University are expected to reduce, refine and finally replace invasive animal studies.

Neuroimaging at Bremen University

Prof. Dr. Angelika Bunse-Gerstner, Deputy Rector (Research)

University of Bremen

Over the last two decades, the University of Bremen has evolved into an excellent institution for research renowned in Germany and beyond for its work in various disciplines. This development, which may have seemed astonishing from the outside perception, was achieved by strictly focusing on specific innovative lines of research, on hiring excellent scholars at an early stage of their career and by strongly supporting the best interdisciplinary fields of research.

These interdisciplinary research foci are fundamental components of our past and future development and Cognitive Sciences is one of them. By now, it is a well established field of research at the University of Bremen, conducting highly rewarding cooperation with other Universities and Institutes in the north western region of Germany. A key feature is its Centre for Research in Cognition (ZKW) which has been attracting researchers from four different faculties of the University for more than ten years now. From 1996 to 2005, the Centre organized the Collaborative Research Centre on Neuro-Cognition (CRC 517) in cooperation with researchers from Oldenburg University. More recently, another outstanding example of the quality of research in this field is the Centre for Advanced Imaging (CAI) which in close cooperation with the University of Magdeburg has been established in 2002. Funded by the Federal Ministry of Education and Research (BMBF) within the Neuroimaging Centre of Excellence program, it exhibits a truly interdisciplinary approach combining researchers from the departments of psychology, biology, informatics, mathematics and chemistry.

This Centre covers a broad variety of topics, including MR methodology and technology, fMRI in non-human primates and in humans, affective neuroscience, visual and auditory neuroscience, clinical neurology, and others and the research work has of course a strong international background with cooperation with the Universities of Sydney (Australia), Barcelona (Spain), Exeter (UK), Northumbria (UK), and MIT (US), to name but a few.

Neurosciences are held in high esteem at our university, becoming evident most recently by the fact that a new building, the *Cognium*, has been put up for the neuroscience groups. In the past widely distributed over the university campus, they now can move into this new building, which besides the different research groups will also house the MR facilities thus allowing for a new feeling of a short-distance "door to door" cooperation in cognitive neuroscience at Bremen University. This will also facilitate and invigorate the ongoing work of the Centre for Advanced Imaging (CAI) whose results of five years of research will be presented at this conference and the accompanying publication.

Neuroimaging at Oldenburg University

Prof. Dr. Reto Weiler, Vice President for Research

University of Oldenburg

Neuroimaging methods such as functional magnetic resonance imaging (fMRI) have only recently been established at the Carl von Ossietzky University of Oldenburg. As a tool which enables us to study neural processes involved in sensory and cognitive functions in humans, it has become an important technique for one of the major research foci in Oldenburg: Neurosensory Science. Neuroimaging methods complement animal and psychophysical experiments investigating neuronal mechanisms and models of neurosensory processing in health and disease. Such mechanisms and models are investigated in several research networks including a DFG funded international research training group "Neurosensory Science, Systems and Applications" (GRK 591), an interdisciplinary Research Centre for Neurosensory Science (FZN), a DFG funded research unit "Dynamic and stability of retinal processing" (FOR 701), and a transregional collaborative research centre "The Active Auditory System" (TR-SFB 31).

Neuroimaging techniques further play a central role in a recent BMBF funded initiative at Oldenburg University that aims at combining educational research - one of the other major research foci in Oldenburg - with neuroscience research. These and other projects presented in the present reader demonstrate that neuroimaging may be one promising neuroscientific tool in interdisciplinary cooperations with the humanities including educational and social sciences or philosophy.

The symposium "Topics in Advanced Imaging" provides an up to date overview of the research investigated by means of neuroimaging at the Universities of Bremen and Oldenburg and the Hanse Institute for Advanced Study in Delmenhorst. It demonstrates the varieties of expertise and synergies present at the sites and will help to foster the cooperation in cognitive neuroscience in the Northwest.

The Center for Advanced Imaging (CAI)

Prof. Dr. Hans-Jochen Heinze, Main Coordinator CAI

University of Magdeburg

The Center for Advanced Imaging (CAI) was established in 2002 as an integrated neuroscientific research center for the Department of Neurology II at the Otto-von-Guericke University in Magdeburg (the coordinating institution), the Leibniz Institute for Neurobiology in Magdeburg, the Center for Neurosciences (ZeN) in Bremen, and the Hanse Institute for Advanced Study in Delmenhorst. In 2002, the Federal Ministry of Education and Research (BMBF) selected the CAI as one of five outstanding regional imaging centers to be designated as a "Center of Excellence". Since then, the CAI has been a major recipient of government funding. The CAI and its affiliate organizations focus on the integration of the results of human and animal experimental procedures, and on the application of multimodal imaging in the various areas of Cognitive Neuroscience. An additional shared goal is the development of new neuroimaging and visualization techniques. Thanks to the support of the Federal Ministry of Education and Research and the States of Saxony-Anhalt and Bremen, the CAI has extensive brain-imaging laboratories at its disposal including several research only magnetic resonance imaging (MRI) units as well as a whole-head MEG apparatus with an integrated EEG. The CAI concentrates on investigations of the control of higher brain functions in the following three areas: visual and auditory perception, memory, and decision-making and activity control. The comparison of human and animal experimental results allows for an enhanced understanding of brain imaging outcomes. An additional central objective of the CAI is to support the training of young scientists. In Magdeburg and Bremen, the members of the CAI coordinate the curricula of various neurobiology, cognitive neuroscience, and psychology programs.

The cooperation between participating scientists from Magdeburg and Bremen (the latter including those at the Hanse Institute for Advanced Study in Delmenhorst and at the University of Oldenburg) has a long tradition that

began well before the establishment of the CAI, but which was massively broadened and extended by the advent of BMBF funding. The Bremen location brings to the CAI's profile its internationally recognized expertise in the area of functional magnetic resonance imaging and spectroscopy, and in image processing and animal brain imaging, and contributes to optimal support for the neurosciences at both locations. In the area of cognitive brain research, the research groups in Bremen, Delmenhorst, Oldenburg, and Magdeburg focus their efforts on investigations of emotion, auditory and visual information processing, and executive function. Finally, as also demonstrated by the program of this conference, the participating CAI colleagues in Bremen are increasingly turning to the investigation of clinical research questions.

The conference "Topics of Advanced Imaging" gives a comprehensive overview of the wide range of themes investigated by participating local CAI research groups, and impressively demonstrates the success of the BMBF's funding initiative.

I.   Affective Neuroscience

Affective Neuroscience

Roth, G.[1,2] and Herrmann, M.[2,3]

[1]Hanse Institute for Advanced Study (HWK), Delmenhorst, [2]Center for Advanced Imaging (CAI) – Bremen, [3]Department of Neuropsychology and Behavioral Neurobiology, University of Bremen

Experimental research on affective neuroscience was established by the installation of the research group "Neuroscience of Emotion". This research group was a joint initiative between the Hanse Institute for Advanced Study (HWK) and the Center for Advanced Imaging (CAI) at Bremen University. Located at the HWK, it offers (young) scientists the possibility to conduct experimental studies using both the MR imaging and EEG recording facilities at Bremen University and the stimulating infrastructure at the Hanse Institute. The studies from Lars Kuchinke (Free University of Berlin) and Daniel Wiswede (Magdeburg University, now HWK fellow) are illustrative examples of the fruitful cooperation between HWK and CAI Bremen in this "Neuroscience of Emotion" project.

The studies by Sina Trautmann and Thorsten Fehr present new methodological approaches to the investigation of the neurobiological foundation of affect and emotion. Both authors used dynamic instead of static stimuli to analyze the neuronal structures which subserve the processing of affective information.

Trautmann and coworkers clearly demonstrate that the use of emotional expressions based on dynamic faces evokes a significantly stronger and more widespread neuronal response than static faces. This data emphasize the relevance of ecologically valid stimulus material in order to investigate the neuronal networks involved in the perception of emotional information derived from human faces.

Fehr presents a joint HWK and CAI approach to the investigation of the perception of aggressive behavior in male and female subjects. This group also used dynamic stimuli in terms of video clips presenting short sequences of ego-centered reactive aggressive behavior. Based on this newly developed

and evaluated stimulus material (BRAIN - BRemen Aggression INventory) Fehr and co-authors show preliminary fMRI data which point to gender-specific neuronal correlates of coping with aggressive and potentially threatening everyday life behavior.

Lars Kuchinke introduced an affective lexical decision task (LDT) to investigate the neuronal networks underlying the incidental processing of the emotional valence in single words. Besides a well-described activation pattern resulting from a word vs. non-word contrast and obviously reflecting semantic word knowledge [2], the authors also found distinct orbitofrontal and prefrontal activations possibly reflecting emotional intensity. Further studies on the same topic (not detailed here but reported elsewhere [3]) showed a valence-dependent dissociation during emotional word recognition in the right prefrontal cortex. These findings demonstrates that emotions modulate cognitive performance.

The last two presentations by Sascha Frühholz and Daniel Wiswede follow this line of investigation and particularly focus on the emotional modulation of interference resolution induced by competing information streams.

Frühholz and co-authors studied contextual distraction from face perception with negative, positive, and neutral facial expressions. They found an increased interference effect in negative and neutral incongruent (i.e. distracting) trials. The inhibition of distracting information in a negative emotional context was associated with distinct signal enhancements in the antero-medial cuneus and superior temporal sulcus, whereas inhibition with neutral facial expressions activated more ventrally located brain areas in the lingual and fusiform gyrus.

Wiswede and his colleagues also used an interference paradigm to investigate the emotion effect on the error-related negativity (ERN), an ERP component emerging early after an erroneous trial. In three experiments they induced different emotions via pictures, facial feedback through muscle innervation, and behavioral feedback. In all experiments negative emotion increased the ERN amplitude, a fact which the authors suppose to be induced by an alteration of dopaminergic activity transmitted via the medial forebrain bundle. Both the investigations by Frühholz and Wiswede demonstrate that the emotional modulation of cognitive processes obviously take place at a very early stage of (visual) information processing.

[1]   Lück, M., Strüber, D., & Roth, G. (2005). *Psychobiologische Grundlagen aggressiven und gewalttätigen Verhaltens*. Hanse-Studien, Bd. 5, Oldenburg: bis-Verlag.

[2]   Kuchinke, L., Jacobs, A.M., Grubich, C., Võ, M.L.H., Conrad, M., & Herrmann, M. (2005). Incidental effects of emotional valence in single word processing: an fMRI study, *NeuroImage*, 28, 1022-1032.

[3]   Kuchinke, L., Jacobs, A.M., Võ, M.L.H., Conrad, M., Grubich, C., & Herrmann, M. (2006). Modulation of PFC activation by emotional words in recognition memory. *Neuroreport*, 17, 1037-1041.

Correspondence. Gerhard Roth, Hanse-Wissenschaftskolleg, Lehmkuhlenbusch 4, 27753 Delmenhorst; gerhard.roth(at)h-w-k.de; Manfred Herrmann, Institute for Cognitive Neuroscience (ICN), University of Bremen, Grazerstr. 6, D-28359 Bremen; manfred.herrmann(at)uni-bremen.de

FMRI Investigations of the Perception of Dynamic and Static Emotional Expressions

Trautmann, S.A.[1,2], Fehr, T.[1,2] and Herrmann, M.[1,2]

[1]Department of Neuropsychology and Behavioral Neurobiology, University of Bremen, [2]Center for Advanced Imaging (CAI) - Bremen

Introduction. Emotions are studied mostly by static emotional faces or scenes and have been a widely discussed topic in cognitive neuroscience for the past 15 years. Only few imaging studies have used dynamic stimuli [1, 2, 3] and revealed larger and more widespread activation patterns in emotion, face and biological motion sensitive areas (such as limbic areas, the fusiform face area (FFA) and the superior temporal sulcus (STS) area, respectively). There has been no study to date dealing with emotional dynamic face perception of disgust. The goal of the current study was (1) to reveal networks for the perception of faces of each positive (smile) and negative (disgust) valence with a new database including static and dynamic stimuli and (2) to analyze modality-specific activation patterns.

Methods. Sixteen healthy, right-handed female volunteers (mean age: 21.6 years, SD: 2.3, 19-27 years) with normal or corrected to normal vision and no history of neurological or psychiatric disorders participated in our study. We introduced a newly developed stimulus set consisting of videos of actresses (black background, N=40) with neutral facial expressions looking to the left or right with an angle of 90° for 1 sec, turning to the front (~1 sec), facing the camera frontally and presenting each a neutral (= ne, control), disgusted (= di) and smiling (= sm) face for around 1.5 sec; other basic emotions like surprise, fear, anger, laugh, sadness, and other sex are also available, but not included in the present study. Static stimuli were captured from the videos at the apex of each frontally presented neutral or emotional expression. The emotional expression was presented and analyzed for the static (= s) and dynamic (= d) condition with a mean duration of 1.5 sec and with an ISI of 3 ± 0.3 sec. Subjects were asked to watch the videos and photographs (a total of 120 stimuli in each modality; 40 disgust, 40 smile, and 40 neutral, respectively) and to empathize the emotional expression.

Dynamic and static stimuli were presented in separate runs and alternated with a simple stimulus-incompatibility task in order to maintain an appropriate vigilance level during scanning. Post-hoc evaluation of arousal, valence, and authenticity was applied after the scanning procedure to ensure that subjects classified the stimuli appropriately. Imaging was performed on a 3-T Magnetom Allegra® System (Siemens, Erlangen / Germany) using a $T2^*$-weighted gradient EPI sequence. We analyzed both simple contrasts (i.e. d_di>d_ne, s_di>s_ne) revealing emotion effects for the different modalities separately, and the interaction (enhanced emotion by motion effect (i.e. [d_di>d_ne]>[s_di>s_ne]) to examine neural activation patterns during emotional information processing in dynamic compared to static stimuli.

Results. A 2 (d, s) x 3 (emotion: sm, di, ne) x 2 (sequence: d, s counterbalanced) showed a significantly better recognition of d_dis compared to s_dis and a significant main effect for emotion with a higher arousal for both smile and disgust compared to neutral faces. Therefore, different activation patterns are unlikely to be evoked by different arousal of the stimuli. By the use of the same threshold, simple contrasts of static smile and disgust revealed left inferior frontal activation (BA45, 46) for the disgust condition only, whereas the dynamic emotion effect of disgust resulted in activations in right posterior cingulate cortex (PCC), in left fusiform gyrus (FG, ~FFA), bilateral middle temporal gyri (MTG), superior TG (STG, both ~STS spreading to ~MT^+/V5), supplementary motor area (SMA) and distinct bilateral parahippocampal gyri (PHG) including the amygdala and bilateral inferior frontal gyri (FrG; see fig 1 (A)). Smile showed similar activations in bilateral dorso-ventral occipital areas, left angular and bilateral posterior MTG, bilateral PCC comprising PHG areas, bilateral more posterior FG, bilateral SMA, left medial FrG, left hippocampus and claustrum.

Interaction analysis indicated enhanced processing for disgust by motion in right occipital areas, left FFA, bilateral STS regions (larger in the left hemisphere and spreading posteriorly to V5/MT^+), left inferior FrG (FrG)/ventral PMA (BA45) and OFC, bilateral PHG activations including the uncus and amygdala (see fig. 1 (B) upper row).

Perception of smile enhanced by motion yielded signal increase in occipital, inferior, posterior middle temporal, temporal pole, orbitofrontal cortex (OFC) and medial frontal areas (see fig. 1 (B) lower row).
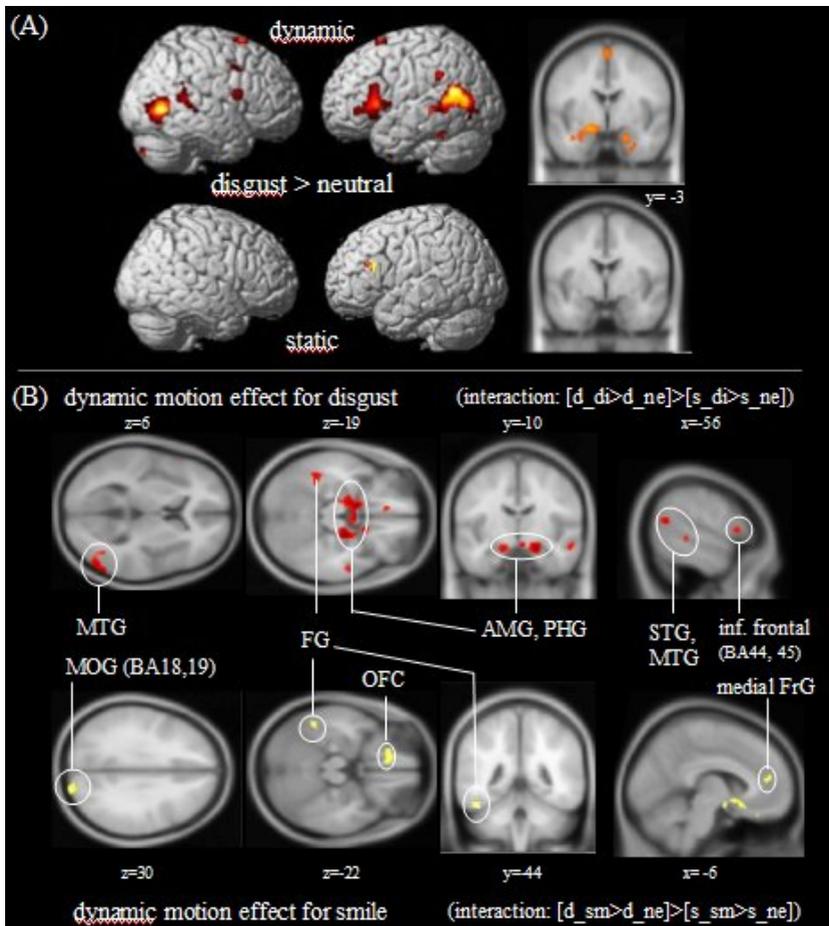
Figure 1. (A) emotion effect of disgust vs. neutral for the dynamic and static modality; (B) distinct activations of motion enhanced disgust (red) and smile (yellow) (all p=.001, k=20; MNI coordinates; for abbreviations see text).

Discussion. Dynamic compared to static presentation of emotional faces revealed stronger and more widespread but distinct activations for dynamic faces. Dynamic facial expressions have been described to convey very complex, redundant and rapid changing cues of information and to be more

natural, powerful and hence, more ecologically valid facilitating the recognition of emotions and enhancing neural activity [1, 2, 3]. The present study showed different neural structures underlying the perception of static and dynamic faces [1]. Motion modulated both emotions, but in disgust stronger than in smile (STS region and left FG), and - exclusively for disgust - in the left inferior frontal gyrus and the parahippocampal complex comprising the amygdala. In this context, the amygdala was suggested to be part of identifying and processing negative, salient, meaningful stimuli signalling a potential threat [2] and thus orienting attention towards the possible source of danger. Because of multiple connections to all stages of the visual information processing stream, the amygdala might play a crucial role in enhancing activity of the FG and the STS area [2], here predominantly in a negative context. Detailed analysis of invariant facial features was related to the FG, while the processing of changeable aspects of the face (i.e. eye gaze, mouth movements etc.) was associated with the STS area [2, 3] consequently enhancing a more detailed feature analysis of a threatening faces in the dynamic modality.

By introducing a new stimulus database, we were able to confirm stronger and more widespread activations for dynamic compared to static emotional facial expressions. These present results support the results of previous studies [1, 2, 3] which showed that dynamic emotional expressions facilitate emotion recognition probably reflecting ecologically more valid stimulus material.

[1]   Kilts, C.D., Egan, G., Gideon, D.A., Ely, T.D., & Hoffman, J.M. (2003). Dissociable neural pathways are involved in the recognition of emotion in static and dynamic facial expressions. *NeuroImage*, 18, 156-168.

[2]   LaBar, K.S., Crupain, M.J., Voyvodic, J.T., & McCarthy, G. (2003). Dynamic perception of facial affect and identity in the human brain. *Cereb Cortex*, 13, 1023-1033.

[3]   Sato, W., Kochiyama, T., Yoshikawa, S., Naito, E., & Matsumura, M. (2004). Enhanced neural activity in response to dynamic facial expressions of emotion: an fMRI study. *Brain Res Cogn Brain Res*, 20, 81-91.

Correspondence. Sina Alexa Trautmann, Department of Neuropsychology and Behavioral Neurobiology, Institute for Cognitive Neuroscience (ICN), University of Bremen, Grazer Strasse 6, D-28359 Bremen; sina(at)uni-bremen.de

Neuronal Correlates of Perceiving Aggressive Behavior

Fehr, T.[1,2], Strüber, D.[3], Lück, M.[3], Herrmann, M.[1,2] and Roth, G.[2,3]

[1]Department of Neuropsychology and Behavioral Neurobiology, University of Bremen, [2]Center for Advanced Imaging (CAI) - Bremen, [3]Hanse Institute for Advanced Study (HWK) - Delmenhorst

Introduction. Criminological statistics of physical aggressive behaviors reported that males are clearly the more aggressive part in most societies [1]. But the story seems to be more complicated because only a sub-group of individuals in the society become delinquent and not all forms of aggression are considered in criminological statistics. Physical aggression peaks between 2 and 4 years of age and decreases monotonously during life for the majority of all individuals [2]. Serotonin metabolism has been discussed to play an important role as it modulates arousal inhibiting top-down processing which in turn has been supposed to be modulated by pre-frontal brain regions. These brain regions might be tuned down in particular for males because of a relatively lower serotonin metabolism [1] resulting in a more pronounced physical aggression in males. To investigate the neuronal correlates of perceived aggressive behavior, we developed a new stimulus inventory (BRAIN - BRemen Aggression INventory) based on short video

Figure 1. Video clips (ego-view) with aggressive, neutral and positive contents.

clips. We expected lower brain activation in pre-frontal regions for male than for females during the presentation of situations showing reactive physical aggression.

Methods. Data were obtained from 17 healthy adults (6 male; mean age: 22.1±4.4 yrs.; 19-26 yrs.; all right handed). One Hundred Twenty short film clips showing reactive aggressive (e.g. being attacked and defending actively, 40 clips), social positive (friendly person is joined in a friendly way, 40 clips) and emotional neutral (40 clips) situations were presented in a pseudo-randomized non-stationary probabilistic sequence (with 3 s fixation between video clips). Participants were asked to observe the scenes as they would have been involved in the displayed action. Scenes were filmed from an ego-view perspective in a way that the observer is involved in the scene from the camera position (see fig. 1). Post hoc evaluation of the stimuli included ratings of arousal (10 level scale) and valence (4 major categories: anger, fear, friendliness and neutral). FMRI data were obtained from a Siemens 3 T Head Scanner (Allegra®, gradient EPI sequence covering 44 axial (AC-PC), interleaved slices (3 mm thickness) encompassing the entire cerebrum and cerebellum; TR/TE = 2500/30 ms; FOV 192 x 192 mm) while participants watched the video clips.

reactive aggression > neutral			
male (n=6)			
lobe	region	Talairach (x y z)	T
frontal	L middle frontal gyrus	-34 -3 63	10.2
		-26 0 46	8.8
		-38 2 50	6.2
	R medial frontal gyrus	8 -11 48	8.7
parietal	L postcentral gyrus	-32 -29 44	17.3
		-48 -19 43	11.4
		-12 -45 67	11.6
		-24 -43 68	8.2
	L postcentral/superior parietal	-32 -47 65	9.7
	R postcentral gyrus	32 -25 38	10.7
		26 -32 50	9.6
		22 -43 65	10.0
	L inferior parietal lobule	-55 -29 35	39.4
	R inferior parietal lobule	55 -43 24	16.7
		61 -28 25	14.6
		57 -24 31	12.1
temporal	L middle temporal gyrus	-50 -58 7	23.2
	R middle temporal gyrus	50 -56 3	28.2
		53 -63 18	9.1
other	L brainstem (midbrain)	-2 -31 -5	18.4
		0 -14 -18	8.5
	R brainstem (pons)	12 -13 -28	16.2
female (n=11)			
lobe	region	Talairach (x y z)	T
parietal	L postcentral gyrus	-24 -45 67	4.2
	R postcentral gyrus	30 -36 59	5.5
	L inferior parietal lobule	-30 -40 55	5.5
		-51 -30 25	4.6
occ.-temp.	L occipital/middle temporal	-42 -63 14	5.8
occipital	L cuneus	-14 -86 21	11.5
		-22 -88 30	7.8
		-10 -75 6	4.5
		-6 -83 6	4.2
	L middle occipital gyrus	-51 -74 0	11.9
	R cuneus	14 -84 34	16.4
	R middle occipital gyrus	53 -72 7	7.7
	R lingual gyrus	14 -68 3	4.3

Table 1. Anatomical regions, Talairach-coordinates and T-scores of significant activation peaks for males and females separately for the contrast reactive aggressive > neutral situations (p<.001, uncorr., k=9).

Results. Behavioral data: post hoc evaluation of the stimuli showed highest arousal values for film clips with aggressive content (7.8±1.0) followed by emotional positive (6.2±1.0) and neutral (4.6±1.0) film clips. Stimuli of different categories were consistently rated in relation to the valence category: aggressive videos induced fear or anger (45.9±31.2% and 45.7±29.1%), social positive videos induced friendly mood (73.5±20.8%) and neutral videos predominantly induced neutral mood (59.0±23.5%).

FMRI data: for illustrations of the fMRI-data see tab. 1 and fig 2. Both males and females showed activations in bilateral postcentral and left inferior parietal regions for the contrast reactive aggressive vs. neutral situations. Males showed an additional activation pattern in left middle and right medial frontal, right inferior parietal, left and right middle temporal regions and left and right brainstem. Females showed additional activations in occipital regions and in the occipito-temporal junction.
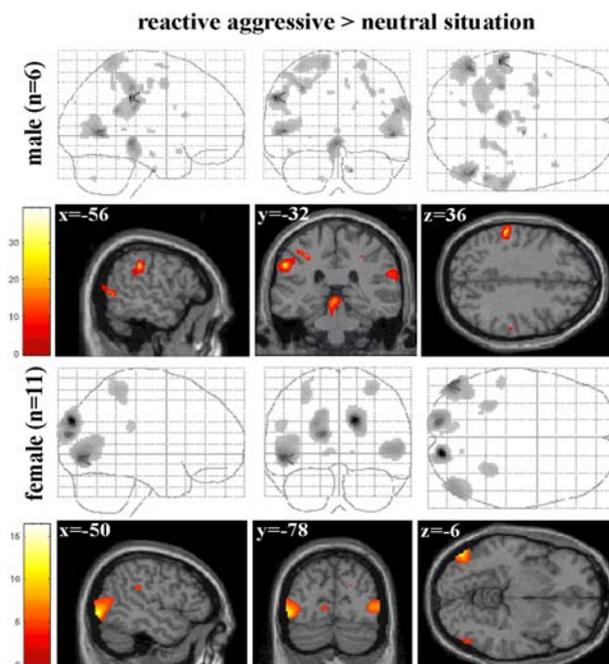
Figure 2. Glass-brain views and superimposed statistics on an individual brain (normalized) for the contrast reactive aggressive vs. neutral situations.

Discussion. Preliminary data of the present study showed differences between males and females at a descriptive level, and conclusions should only be drawn with respect to the unbalanced and small sample size, especially for the male group. Both males and females showed activations in postcentral and inferior parietal regions for reactive aggressive situations in contrast to neutral ones. This activation pattern might be interpreted in terms of physical contact expectations. Females showed occipital and occipito-temporal activations possibly reflecting a more intense analysis of the situation, whereas males showed a relatively more anterior distribution of activations in temporal and frontal brain regions. Most interestingly, only male participants showed bilateral brain stem activation what might be linked to tendencies of attack behavior [3]. The original assumptions of reduced frontal brain activation in males and an enhanced frontal brain activation in females confronted with aggressive actions could not be verified in this preliminary analysis.

[1] Lück, M., Strüber, D., & Roth, G. (2005). *Psychobiologische Grundlagen aggressiven und gewalttätigen Verhaltens*. Hanse-Studien, Bd. 5, Oldenburg: bis-Verlag.

[2] Archer, J. & Cote, S. (2005). Sex differences in aggressive behavior: a developmental and evolutionary perspective. In: Tremblay, R. E., Hartup, W. W. & Archer, J. *Developmental Origins of Aggression*. NY: Guilford.

[3] Gregg, T.R. & Siegel, A. (2001). Brain structures and neurotransmitters regulating aggression in cats: implications for human aggression. Progress in *Neuro-Psychopharmacology and Biological Psychiatry*, 25, 91-140.

Correspondence. Thorsten Fehr, Department of Neuropsychology and Behavioral Neurobiology, Institute for Cognitive Neuroscience (ICN), University of Bremen, Grazer Strasse 6, D-28359 Bremen; fehr(at)uni-bremen.de

Incidental Effects of Emotional Valence in Single Word Processing*

Kuchinke, L.[1], Jacobs, A.M.[1], Grubich, C.[2,3], Võ, M.[1], Conrad, M.[1] and Herrmann, M.[2,3]

[1]Department of Psychology, Free University of Berlin, Germany, [2]Department of Neuropsychology and Behavioral Neurobiology, University of Bremen, [3]Center for Advanced Imaging (CAI) - Bremen

Introduction. Previous research suggested that in situations where previously encoded information is subsequently processed without any conscious recollection subjects' performance is not affected by the emotional valence of words [1] as is the case in the affective lexical decision task (LDT). Using well controlled stimulus material in a functional imaging study we wanted to overcome previous heterogeneous literature findings regarding performance in the LDT [2]. Assuming that incidental processing of emotional valence in visual word recognition is subserved by at least partially the same brain regions known to be involved in explicit emotional memory tasks, we expected to find valence-specific activations in anterior and dorsolateral prefrontal regions, the amygdala and the hippocampus.

Methods. Twenty right-handed young adults (mean age 26.3 yrs., 20 – 36 yrs., 12 female) from Bremen University were employed in the study. All were native German speaker who reported no history of neurological or psychiatric illness. Subjects indicated by button press whether a presented letter string represents a correct German word or not. Stimulus material consisted of 50 positive, 50 neutral and 50 negative words selected from the BAWL [3], and 150 orthographically legal and pronounceable non-words. Word lists were matched for mean word frequency, number of letters and syllables, number and frequency of orthographic neighbors, and imageability. Positive and negative words were chosen to be homogeneously rated on the valence dimension and to be comparable on absolute valence ratings. Stimuli were presented in the center of the screen for 500ms with an interstimulus interval of 2800ms (+/- 200ms jitter). Imaging was performed on a 3-T Magnetom Allegra® System (Siemens, Erlangen / Germany) using a

T2*-weighted gradient EPI sequence comprising volumes with 38 slices and 3 mm thickness covering the whole brain.

Results. Repeated measures ANOVA revealed that words and non-words differed significantly in their response latencies in both subject analysis ($F_{1[1,19]} = 15.395$, $P = 0.001$) and item analysis ($F_{2[1,298]} = 77.300$, $P < 0.001$), due to faster responses for words. Additionally, an effect of emotional valence was observed for subjects ($F_{1[2,38]} = 9.994$, $P < 0.001$), and items ($F_{2[2,147]} = 7.222$, $P = 0.001$) due to fastest responses to positive words (negative and neutral words did not differ). A number of brain areas showed greater activity in response to words than to non-words. Significant effects were elicited in left middle and superior frontal gyrus (BA 8, 9), bilateral temporal lobe (BA 20, 22), bilateral angular gyrus (BA 39), medial frontal gyrus (BA 10, 25) and bilateral posterior cingulate gyrus and precuneus (BA 23, 31, see fig. 1). These activations correspond closely to those reported in lexical decision studies indicating involvement of neural networks responsible for processing semantic word knowledge.

Nonspecific valence effects were observed in orbitofrontal (BA 11) and bilateral inferior frontal gyrus (BA 45/46) with greater activation to emotional than to neutral words (fig. 2). Additional analyses revealed that the orbitofrontal activation is associated with the processing of positive words and the right hemisphere activation in BA 45 with that of negative words. A valence-specific positive > negative contrast yielded significant clusters in anterior and posterior cingulated gyrus, lingual gyrus and the hippocampus.
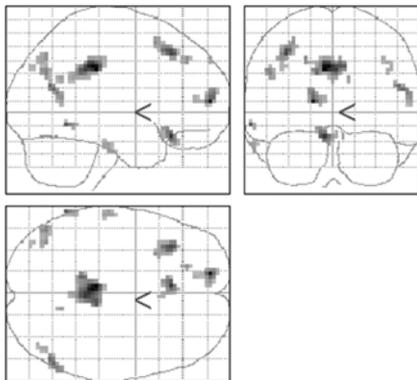
Figure 1. Maximum intensity projections illustrating voxels common to word > non-word contrast (thresholded at P < 0.001, uncorrected).

Discussion. The behavioral data clearly indicate an advantage for positive words compared with neutral or negative words in the LDT in the response latencies. The LDT does not require emotionally valenced responses to be made, nor does it require subjects (fully) to identify the meaning of the words. While dissociating between positive and negative emotional stimuli, our behavioral data strongly support the idea of an early affective evaluation process in word recognition [2].

The functional imaging results indicate differences in the way the brain processes words and non-words, allowing to conclude that the activated neural networks may reflect the activation of semantic word knowledge as well as partial activations of orthographic and phonological codes [4]. As a second result, the processing of emotional words leads to distinct prefrontal activations which are often reported in explicit memory on emotion. Orbitofrontal regions have more generally been discussed to support the processing of positive information and reward, while right ventrolateral PFC functioning has been related to memory retrieval. Since none of these regions survived the valence-specific positive vs. negative comparison, it is probable that it is the words' emotional intensity (and not emotional valence) that accounts for these results. For the valence-specific contrast (positive over negative words) we identified several other regions which previous research has shown to support emotional processing, including anterior and posterior cingulate gyrus and hippocampus. Activity in posterior cingulate gyrus has been related to evaluation of an external stimulus with emotional salience and is suggested to play a crucial role in interaction with the
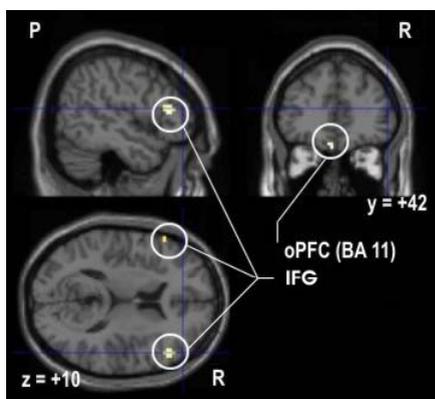
Figure 2. Orbitofrontal (oPFC) and bilateral inferior frontal gyrus (IFG) activity identified in the valence independent emotional > neutral contrast (P < 0.001, uncorrected) in Talairach space, R = right, P = posterior.

hippocampus formation in emotional memory retrieval. Surprisingly, we did not observe amygdala activation in any of the emotional contrasts. Amygdala has been indicated as an important interface between episodic memory and affect. Because most studies reported amygdala activation during encoding and explicit retrieval of emotional pictures, faces and words, its role in visual word recognition remains unclear. The amygdala may be critical in automatically evaluating an affective stimulus, but other areas like inferior frontal or orbitofrontal gyrus may also subserve these automatic processes [5]. Still, we cannot rule out that our failure to find amygdala activation might be due to the low temporal resolution of the fMRI.

[1] Danion, J.-M., Kauffmann-Muller, F., & Grangé, D. (1995). Affective valence of words, explicit and implicit memory in clinical depression. *Journal of Affective Disorders*, 34, 227-234.

[2] Windmann, S., Daum, I., & Günturkün, O. (2002). Dissociating prelexical and postlexical processing of affective information in the two hemispheres: effects of the stimulus presentation format. *Brain and Language*, 80, 269-286.

[3] Vo, M.-L., Jacobs, A.M., & Conrad, M. (2006). Crossvalidating the Berlin affective word list (BAWL). *Behavior Research Me*thods, 38, 606-609.

[4] Binder, J.R., McKiernan, K.A., Parsons, M.E., Westbury, C.F., Possing, E.T., Kaufman, J.N., & Buchanan, L. (2003). Neural correlates of lexical access during visual word recognition. *Journal of Cognitive Ne*uroscience, 15, 372-393.

[5] Anderson, A.K. & Phelps, E.A. (2001). Lesions of the human amygdala impair enhanced perception of emotionally salient events. *Nature*, 411, 305–309.

Correspondence. Lars Kuchinke, Department of Psychology, Freie Universität Berlin, Habelschwerdter Allee 45, 14195 Berlin, Germany; kuchinke(at)zedat.fu-berlin.de

Interference Processing in Emotional Face Perception is Modulated by the Emotional Valence

Frühholz, S.[1,2], Fehr, T.[1,2] and Herrmann, M.[1,2]

[1]Department of Neuropsychology and Behavioral Neurobiology, University of Bremen, [2]Center for Advanced Imaging (CAI) - Bremen

Introduction. Recently, Righart and de Gelder demonstrated that emotional (in-)congruency of facial expressions and surrounding contexts might affect early components of visual evoked potentials (i.e. N170 [1]). Despite functional investigations of selectively attending to facial expressions in, for instance, face-house stimulus compounds [2], there are no functional MRI studies which investigated contextual distraction from emotional face processing. Here, we analyzed the functional correlates of interference resolution during valence categorization of negative (fear), neutral and positive expressions (happiness). We used colored backgrounds which presumable compete with face perception in early extrastriate regions.

Methods. We examined 20 healthy, right-handed female volunteers (mean age 22.7, SD 2.25, range 20-29) with no history of neurologic, psychiatric or vision disorders. In a first experimental run subjects were asked to rate (1) the arousal and (2) the emotional valence (negative, neutral, positive) of 90 pictographically reduced pictures of emotional faces. The emotional valence of faces was systematically combined with distinct background colors (red = negative, blue = neutral, and yellow = positive facial expressions). During a second experimental run subjects were asked for a fast forced-choice categorization of 360 facial expressions. In 30 percent of facial pictures the background-color was changed (incongruent trials), thus inducing conflicting emotional information compared to the implicitly learned color-emotion association. Imaging was performed on a 3-T Magnetom Allegra® System (Siemens, Erlangen / Germany) using a $T2^*$-weighted EPI sequence. In the second experimental run, stimuli were presented for 1400 msec with an interstimulus interval of 3600 msec (+/- 200 msec jitter) while subjects made fast valence judgments of depicted faces.

Results. Incongruent trials induced substantial interference effects which was indicated by a 3 (emotion) x 2 ((in-)congruency) repeated measure ANOVA, and paired t-tests revealed strong effects of emotional incongruence both for reaction times and error rates. These effects were most evident for incongruent neutral expressions (see fig. 1). A conjunction analysis computing interference resolution over all emotional categories revealed a common fronto-parietal activation pattern. Contrasting incongruent with congruent trials in each emotional category (i.e. [negative incongruent] > [negative congruent]) showed a specific effect of interference resolution in different emotions. Interference resolution in positive trials exclusively activated left frontal areas (BA 4, 6) whereas the analysis of interfering neutral and negative conditions resulted in a fronto-parietal activation pattern. These different functional profiles are also reflected in distinct signal enhancements for negative and neutral interference trials in extrastriate visual regions pointing to early control mechanisms for the processing of competing information streams. An interaction analysis for interference resolution in negative trials revealed a dorso-ventral extending activation cluster centered bilaterally in the antero-medial cuneus covering part of the dorsal visual stream (with an additional activation cluster in right middle occipital (~V5/MT+) and middle temporal gyrus (~STS; see fig. 2, top row)). Interference resolution in neutral facial expressions was associated with a more ventrally located activation cluster in the lingual and fusiform gyrus spreading from early visual areas in the ventro-posterior lingual gyrus along the ventral processing stream, with an additional activation cluster in right
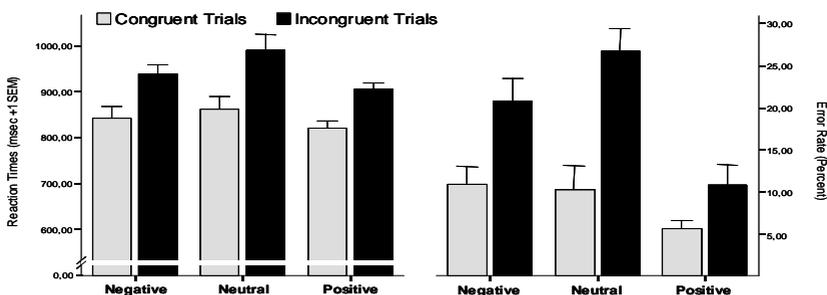
Figure 1. Reaction times (left) and error rates (right) for congruent and incongruent trials with different emotional expressions. Error means misclassification of facial expressions.

anterior frontal regions. In positive facial expressions inhibition of distracting information was not associated with specific activations as indicated by missing interaction effects.

Discussion. We suppose that the distinct emotion-related activation patterns of interference resolution are associated with different demands of information processing in neutral compared to negative or positive facial expressions (such as differences in cognitive processing load). The perception of emotional faces strongly captures attentional resources and is processed in an almost pre-attentive manner. Therefore, the influence of interfering information might be reduced. On the other hand, the perception of neutral facial expression is often ambiguous and thus interference processing might be even enhanced when provided with background colors containing distracting information. The increased interference effect for neutral incongruent trials is reflected in both behavioral and fMRI data. The latter showed a (ventrolateral) prefrontal activation pattern, and additionally a signal enhancement in early striate and extrastriate areas. This finding
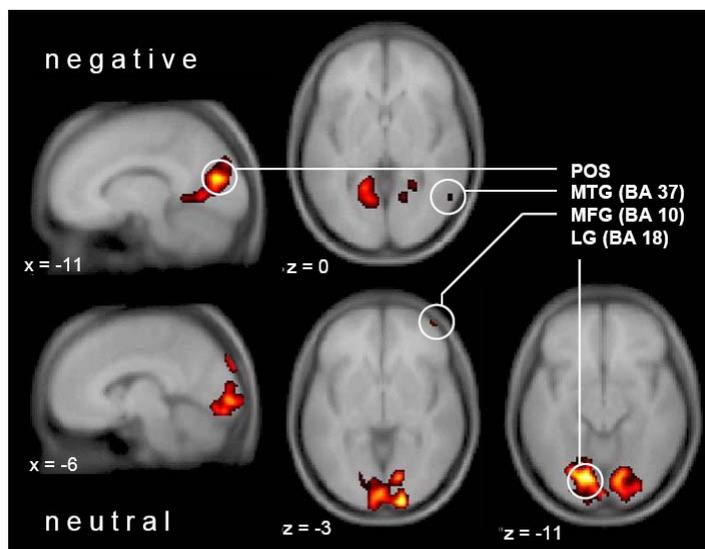
Figure 2. Distinct activations of negative (top row) and neutral incongruent trials (bottom row) (p<.001, k=20; MNI coordinates). *POS,* parieto-occipital sulcus; *MTG,* middle temporal gyrus; *MFG,* middle frontal gyrus; *LG,* lingual gyrus.

might reflect feed-forward and re-entrant information processes underlying deeper re-analysis of facial features (as also indicated by activations of the fusiform face area possibly back-projecting onto the occipital face area (see [3]). This hypothesis is furthermore corroborated by a significant signal increase in bilateral ventral V4 region (posterior fusiform gyrus) which we suppose to reflect the processing of interfering task-irrelevant color information. In contrast, the attention capturing nature of emotional facial expressions makes them less prone to interference effects which is most obvious for positive incongruent trials. Unlike the fast and holistically nature of positive facial expression, negative facial displays, though almost processed in an pre-attentive manner, still contain some ambiguity (e.g. approach vs. withdrawal behavior). We suppose that this type of ambiguity resolution needs more interference control than positive expressions but no deeper feature analysis as induced by neutral faces.

Taken together the present results confirm existing electrophysiological data [1] which indicate early modulatory effects of an emotional context during the processing of facial expressions. Furthermore, the present data give evidence that interference resolution in emotional face processing is associated with both an activation of a common network of attentional control and specific brain areas involved in early face processing.

[1]   Righart, R. & de Gelder, B. (2006). Context influences early perceptual analysis of faces – An electrophysiological study. *Cerebral Cortex*, 16, 1249-1257.

[2]   Vuilleumier, P., Armony, J.L., Driver, J., & Dolan, R.J. (2001). Effects of attention and emotion on face processing in the human brain: An event-related fMRI study. *Neuron*, 30, 829-841.

[3]   Schiltz, C., Sorger, B., Caldara, R., Ahmed, F., Mayer, E., Goebel, R., & Rossion, B. (2006). Impaired face discrimination in acquired prosopagnosia is associated with abnormal response to individual faces in the right middle fusiform gyrus. *Cerebral Cortex*, 16, 574-586.

Correspondence. Sascha Frühholz, Department of Neuropsychology and Behavioral Neurobiology, Institute for Cognitive Neuroscience (ICN), University of Bremen, Grazer Strasse 6, D-28359 Bremen; fruehholz(at)uni-bremen.de

Interactions of Executive Functions and Emotional Processes

Wiswede, D.[1,2], Rüsseler, J.,[1,3] and Münte, T.F.[1]

[1]Otto-von-Guericke Universität Magdeburg, [2]Hanse Wissenschaftskolleg (HWK), Delmenhorst, [3]Philipps-University Marburg

Introduction. One critical aspect of adaptive control of behavior is the ability to monitor one's own cognitive performance. The error-related negativity (ERN) component of the event-related brain potential (ERP) is a well-known electrophysiological signature of performance monitoring [1]. The ERN is a negativity seen for incorrect, but not for correct responses that emerges around the time of an erroneous response, and peaks 50-100 ms later. Source localization studies propose that the ERN is generated in the anterior cingulate cortex (ACC). Researchers have shown that emotional context affects performance monitoring as reflected by the ERN. In general, the ERN-amplitude is larger in affectively distressed groups (obsessive-compulsive disorder, depression, subjects with subclinically high negative affect). The influence of positive affect on ERN amplitude is hardly examined. The purpose of the present studies is to investigate the modulatory role of positive and negative emotions on ERN amplitude. Unlike others, we employed healthy subjects in within group designs (experiment 1 and 2) or arbitrary allocated to affective groups (experiment 3). The findings were integrated in the framework of reinforcement learning theory [2].

Methods. All three experiments were based on a flanker task. Subjects were required to respond as fast and as correct as possible to either a central H or S in a five-letter string. The strings were either congruent (SSSSS or HHHHH, 60%) or incongruent (SSHSS or HHSHH, 40%). Experiments differed in how emotions were induced.

Experiment 1: Emotions were induced by short-term presentation of a neutral, pleasant or unpleasant IAPS (International Affective Picture System) picture (mean IAPS valence values, 5.0, 8.5, 1.6, respectively) directly prior to the flanker stimulus.
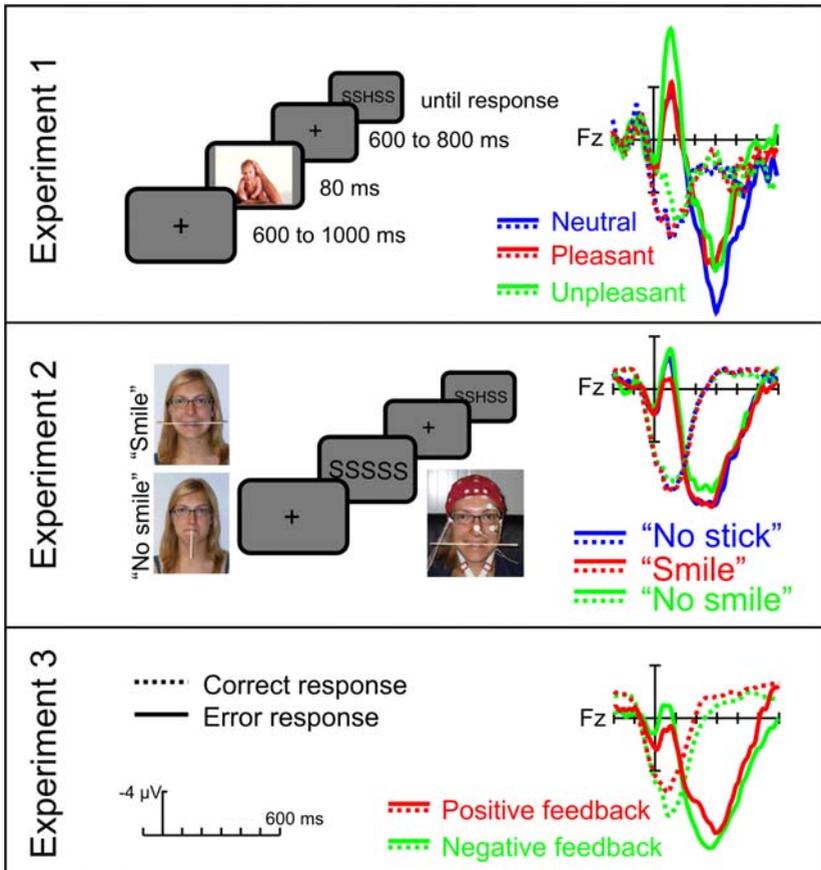
Figure 1. Left panel: experimental setup for all three experiments. Right panel: response- locked ERPs on frontocentral electrode FZ. Solid lines depict erroneous responses, dotted lines correct responses. Emotions are color-coded.

Experiment 2: Positive emotions were induced via Facial Feedback, the zygomaticus major muscle was innervated by placing a chop stick horizontally in the mouth ("Smile" condition). To prevent from smiling, the subjects were required to hold the stick either vertically ("no smile" condition) or remove the stick from the mouth ("no stick" condition). A

cover story veiled the purpose of emotion induction. Stick position was changed blockwise after 210 trials (see fig. 1).

Experiment 3: Subjects were randomly assigned to a negative or positive feedback group. Feedback was based on the subject's reaction times during the preceding block. The negative feedback group received feedback only when performance decreased, the positive feedback group received feedback only when performance increased. Affective changes were assessed by completing a current state questionnaire prior to and after the experiment.

EEG was recorded in all three experiments on electrode positions including all 10/20 channels, referenced to the tip of the nose. Eye artifacts were corrected using a second-order blind identification algorithm.

Results. Behavioral data: Across all experiments, subjects responded faster and more accurate to congruent compared to incongruent flankers. Erroneous responses were given faster than correct responses. Induced emotion did not impact error rates, reaction times or post-error slowing. The questionnaire in experiment 3 showed that negative affect was induced in the negative feedback group, but there was no increased positive affect in the positive feedback group. ERP data: Experiment 1: ERN was increased following negative, but not positive IAPS pictures. Experiment 2: ERN was decreased in the "smile condition". Experiment 3: ERN was increased in the "negative feedback condition" (see fig. 1).

Discussion. The three experiments showed that negative affect increases ERN amplitude, whereas positive affect decreases ERN amplitude. Based on assumptions derived from the reinforcement learning theory [2], we propose that affect modulates performance monitoring by changing dopamine level in mesencephalic structures. Negative affect changes ERN amplitude towards greater negativity (experiment 1 and 3), probably by changes in dopaminergic level. Short term negative affect might lead to a phasic decrease in dopamine release in mesencephalic structures and basal ganglia. According to the reinforcement learning hypothesis [2], a dopamine decrease causes decreased inhibition of the anterior cingulate cortex [2], measurable by a increase of ERN amplitude. Positive affect has the opposite effect on ERN amplitude. Thus, in line with previous research [3], we conclude that positive affect increases dopaminergic activity in frontal areas and the mesencephalic dopaminergic system, which leads to increased inhibition of the ACC and an decreased ERN amplitude. However, experiment 1 and 3

indicates that negative emotions are easier to induce. Thus, further research should focus on scrutinizing positive affect modulations on performance monitoring.

[1]   Falkenstein, M., Hoormann, J., Christ, S., & Hohnsbein, J. *(*2000). ERP components on reaction errors and their functional significance: a tutorial. *Biological Psychology*, 51, 87-107.

[2]   Holroyd, C.B. & Coles, M.G. (2002). The neural basis of human error processing: reinforcement learning, dopamine, and the error-related negativity. *Psychological Review*, 109, 679-709.

[3]   Ashby, F.G., Isen, A.M., & Turken, A.U. (1999) A neuropsychological theory of positive affect and its influence on cognition. *Psychological Review*, 106, 529-550.

Correspondence. Daniel Wiswede, Hanse Wissenschaftskolleg, Lehmkuhlenbusch 4, 27753 Delmenhorst; dwiswede(at)h-w-k.de

II. MR-Physics and Neuroimaging Methods

MR-Physics and Neuroimaging Methods

Leibfritz, D.[1,2] and Peitgen, H.-O.[2,3]

[1]University of Bremen, Institute of Organic Chemistry, [2]Center for Advanced Imaging (CAI) – Bremen, [3]MeVis Research, Bremen

Among the methods for medical imaging, magnetic resonance (MR) techniques are the least invasive ones and by far the best with respect to contrast variability and diagnostic impact. Morphological contrast (spin density, relaxation times T1 and T2), physiological contrast (diffusion, perfusion, flow (angiography), functional imaging, contrast reagents, saturation transfer etc.) and metabolic contrast (spectroscopic imaging, single voxel spectroscopy) are established methods on clinical scanners, but also on high field research systems. Nonetheless, there is an insatiable demand to make perfect existing methods with respect to spatial and temporal resolutions to increase the information contents of the measured data and to improve patients' comfort, but also to develop new acquisition sequences with novel contrast mechanisms and/or improved performance to increase and extend the diagnostic use of MR tools.

However, it is and will be equally important to dig out the maximum of information from physical data by numerical post-processing tools, last but not least as MR methods are prone to various kinds of interferences (motion artifacts, statistical noise, imperfect data mining, spatial ambiguities, tissue heterogeneities etc.).

MR spectroscopy: While magnetic resonance imaging (MRI) records tissue water and its physical properties to generate images, metabolite signals within living organism will reflect their metabolic status. However, their concentrations are at least four orders of magnitude smaller than tissue water concentration. This means uncomfortably long data acquisition times for single voxel spectroscopy and spectroscopic imaging requesting the ultimate efforts to improve sensitivity and speed. Based on the fast imaging techniques using the condition of steady state free precession fast spectroscopic imaging versions have been developed to acquire free induction decay signals as well as spin-echo signals. The sequences were

designed on a 4.7 Tesla animal scanner and adopted to 3 Tesla and 7 Tesla human scanner within the CAI program.

Functional MRI: For functional MRI (fMRI), various pulse sequences are well established to record brain activity. However, fMRI could further benefit from an improved sensitivity and flexibility of T2* and T2 and/or diffusion weighting. Therefore, various protocols using spin echoes (SE) as well as stimulated echoes (STE) were designed to gain sensitivity. STE versions yield high signal changes in fMRI experiments and may allow fast 3D fMRI. SE and particularly STE based fMRI will have higher benefits from high field systems than T2* based fMRI.

Alternatively to the BOLD effect (T2* contrast) conventionally used to record brain activity, activated areas can be monitored by the inflow of contrast agents. Thus paramagnetic manganese with the comparable ion size of calcium is able to follow up influx of the second messenger calcium. After injection of nontoxic manganese concentrations, T1 weighted MRI was used to monitor brain activation caused by passive forepaw movement in rats.

Diffusion tensor imaging (DTI): Anisotropic water diffusion in the proximity of nerve fibers is recorded for follow up the anisotropic connections of nerve bundles. However, diffusion tensor measurements suffer from limited signal-to-noise ratio of the measured data and from serious ambiguities during numerical postprocessing. In cooperation between mathematicians and physicists robust algorithms are developed to improve postprocessing and to trace automatically fiber bundles. By this means also a quality assessment is achieved to quantify the uncertainty of fiber reconstructions. These are demanding prerequisites for using DTI to prepare neurosurgery of neoplastic tissues or epileptic foci as well as to improve the diagnosis of neurological disorders as MS or ALS.

Correspondence. Dieter Leibfritz, Institute of Organic Chemistry, University of Bremen, Leobener Str. NW 2 C, D-28359 Bremen; leibfr@chemie.uni-bremen.de

Heinz-Otto Peitgen, MeVis Research, Universitätsallee 29, D-28359 Bremen; peitgen@mevis.de

A Comparison Between Steady-State Free Precession Based Fast Spectroscopic Imaging Methods

Dreher, W.[1,2], Schuster, C.[1,2] and Leibfritz, D.[1,2]

[1]Institute of Organic Chemistry, University of Bremen, [2]Center for Advanced Imaging (CAI) - Bremen

Introduction. Among the various methods that have been developed for fast ^{1}H spectroscopic imaging (SI) of the brain, pulse sequences based on the condition of steady state free precession (SSFP) have gained considerable interest, primarily because of their potential to realize both a short minimum total measurement time (T_{min}) and a high signal-to-noise ratio (SNR) per unit measurement time (SNR_t) [1-7]. Two different signal types are generated in SSFP based pulse sequences: the FID-like signal S1 and the echo-like signal S2. In the original papers in which fast ^{1}H SSFP based SI was introduced [1, 2], three types of pulse sequences were proposed: "spectroscopic FAST" where S1 is detected while S2 is suppressed, "spectroscopic CE-FAST" where S2 is detected while S1 is suppressed, and "spectroscopic FADE" where S1 and S2 are detected in two separate acquisition windows positioned between consecutive RF pulses. Another SSFP based fast SI sequence, "spectroscopic missing pulse SSFP" (spMP-SSFP), was proposed where every third RF pulse is omitted and an echo-like signal is detected with the echo maximum occurring at the time of the missing pulse [5].´All SSFP based SI sequences have different advantages and drawbacks. They can be implemented with different types of RF pulses and combined with oscillating read gradients to reduce T_{min} even further [3]. It is the purpose of this contribution to compare these SSFP based fast SI sequences, particularly with regard to their use for metabolic imaging at 3 Tesla.

Methods. All experiments were performed on a 3T Magnetom Allegra head scanner (Siemens, Erlangen, Germany) equipped with a standard circularly polarized RF head coil and standard B_0 gradient system with a maximum gradient strength of 40 mT/m and a maximum slew rate of 400 mT/m/ms. Measurements were performed on phantoms and healthy volunteers.

The pulse sequences were implemented using chemical shift selective composite pulses to excite and refocus all metabolite signals of interest and to simultaneously improve water and lipid suppression. In the basic approach, the composite pulses, e.g., 1-2τ-5.4-τ-5.4-2τ-1 or 1-τ-1-τ-8-τ-8-τ-1-τ-1, consisted of rectangular RF pulses. Alternatively, the rectangular pulses can be replaced by slice selective RF pulses enabling spectral-spatial selectivity. Furthermore, the SNR_t and the detection of metabolites were improved by optimising the following parameters: (a) interpulse delay T, (b) total flip angle of the composite or spectral-spatial pulses, (c) water and lipid suppression, (d) minimum total measurement time T_{min}, (e) options for spatial preselection, (f) robustness and complexity of data processing and data evaluation.

Results. In vivo ^{1}H SI data were acquired for spCE-FAST [6], spMP-SSFP [5], and, most recently, by spFAST [7]. spFADE, which was successfully used at 4.7T was not implemented yet at 3T because the achievable spectral resolution was not adequate for interpulse delays being short enough to achieve a sufficient SNR.
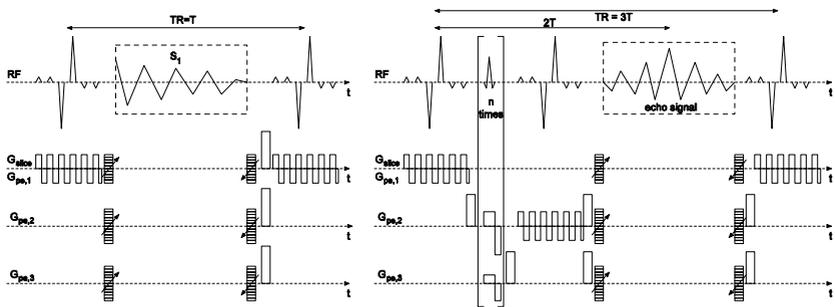
Figure 1. Scheme of the fast 3D SI sequences (left) spFAST and (right) spMP-SSFP (not to scale).

(a) The interpulse delay T results from a trade-off between high SNR and high spectral resolution. Typically T values of 60-80 ms proved to be a good compromise if optimized apodisation was applied to suppress Gibbs ringing artifacts. Considerably shorter T values require data processing by extrapolation methods or model fitting. The longer detection time used in spMP-SSFP does not lead to a better spectral resolution compared to spFAST or spCE-FAST because of information redundancy of both halves of the echo.

(b) The total flip angle was optimized considering typical T, T_1 and T_2 values as described in [2,5]. Rather low optimal flip angles of 20°-50° are advantageous with respect to the specific RF absorption rate (SAR). The rather high optimal flip angles (40°-65°) needed for spMP-SSFP are compensated for by the fact that every third pulse is missing.

(c) In all sequences, water and lipid suppression is realized by the chemical shift selectivity of the used composite or spectral-spatial RF pulses. Additional spatially selective saturation pulses are easily integrated into spMP-SSFP, while for spFAST and spCE-FAST with a given T, the acquisition length must be shortened causing to a reduced spectral resolution.

(d) For a given delay T and a given number of spatial encoding steps N_{cod} and dummy steps N_d used to establish the steady state, T_{min} equals $(N_d+N_{cod})*T$ for spFAST and spCE-FAST, but $(N_d+3*N_{cod})*T$ for spMP-SSFP. Thus the longer T_{min} is a major disadvantage of spMP-SSFP. However, since 3D spatial preselection is possible, a smaller FOV may be used in spMP-SSFP and thus a smaller number of encoding steps is required. Additionally, T_{min} can be reduced for all SSFP based SI sequences by using an oscillating read gradient [3].

(e) The main advantage of spMP-SSFP is the option of 3D spatial preselection achieved by two orthogonal slice selective RF pulses and presaturation pulses [5] (cf. fig.1). Currently, slice selection in only one direction is achieved in spFAST and spCE-FAST and additional spatial saturation is only possible at the cost of prolonged T or reduced acquisition duration between consecutive RF pulses. Thus, reduced FOVs can hardly be realized and lipid and water suppression are more difficult, particularly for spFAST, while the problem is less critical for spCE-FAST because of the rather short T_2 values of lipid and water signals.

(f) With regard to robustness and low complexity of data processing spMP-SSFP is the method of choice. Since full echoes are acquired, the spectra can be calculated in the magnitude mode without any loss in spectral resolution, making an automatic phase correction obsolete. Additionally, fewer problems with baseline correction occur because of the superior water and lipid suppression and the T_2 decay of signals from macromolecules.

Discussion. Considering the general properties of SSFP based fast SI sequences, two sequences seem to be of highest interest for fast SI at 3T: spMP-SSFP and spFAST. spMP-SSFP has proved to be a robust fast SI method which requires minimal user interaction and allows the detection of

signals of both uncoupled and J-coupled spins. However, the SNR is considerably lower (factor of 3-4) as compared to spFAST. Therefore, if the technical challenges of spFAST can be met (water and lipid suppression, robust automatic postprocessing) and 3D preselection is not required, spFAST should be preferred.

[1]   Dreher, W., Geppert, C., Althaus, M., Spektroskopisches Bildgebungs-verfahren sowie Verwendung desselben zur Materialcharakterisierung, German patent: DE10243830B4 (applied: 13.09.2002; granted: 16.11.2006) and international patent: Europe: EP03757665.9, Japan: JP2004-536851 (2005-537896), USA: 10/527,382 (US-2006-0-0139027-A1).

[2]   Dreher, W., Geppert, C., Althaus, M., & Leibfritz, D. (2003). Fast proton spectroscopic imaging using steady-state free precession methods. *Magn Reson Med*, 50, 453-460.

[3]   Althaus, M., Dreher, W., Geppert, C., & Leibfritz, D. (2006). Fast 3D echo-planar SSFP based ^{1}H spectroscopic imaging: demonstration on the rat brain in vivo. *Magn Reson Imaging*, 24, 549-555.

[4]   Geppert, C., Dreher, W., Althaus, M., & Leibfritz, D. (2006). Fast ^{1}H spectroscopic imaging using steady state free precession and spectral-spatial RF pulses, *MAGMA* 19, 196-201.

[5]   Schuster, C., Dreher, W., Geppert, C., & Leibfritz, D. (2007). Fast 3D ^{1}H spectroscopic imaging at 3 Tesla using spectroscopic missing-pulse SSFP with 3D spatial preselection. *Magn Reson Med*, 57, 82-89.

[6]   Geppert, C., Dreher, W., Althaus, M., Schuster, C., & Leibfritz, D. (2005). SSFP based fast ^{1}H spectroscopic imaging on the human brain at 3T using k-space weighted acquisition. In: *Proc 13th Ann Sci Meet ISMRM,* Miami, p. 723.

[7]   Schuster, C., Dreher, W., & Leibfritz, D. (2007). Very fast 2D proton MR spectroscopic imaging of the in vivo human brain at 3 Tesla with high spatial resolution using the SSFP based sequence "spectroscopic FAST", In: *Proc 15th Ann Sci Meet ISMRM*, Berlin, May 2007.

Correspondence. Wolfgang Dreher, University of Bremen, Institute of Organic Chemistry, 28359 Bremen, Germany; dreher(at)tomo.uni-bremen.de

On The Use of Spin Echo and Stimulated Echo Based Functional MRI Sequences

Dreher, W.[1,2], Meier, M.[3], Erhard, P.[1,2] and Leibfritz, D.[1,2]

[1]Institute of Organic Chemistry, University of Bremen, [2]Center for Advanced Imaging (CAI) – Bremen, [3]Department of Neurology II, University of Magdeburg

Introduction. Spin echo (SE) based pulses sequences can be used for functional MRI (fMRI) with reduced image distortions and higher regional specificity as compared to T_2^* based fMRI [1-3]. Signal changes observed in SE fMRI experiments at different B_0 field strengths have been explained by exchange and diffusion models [4, 5]. Data characterizing the dependence of the measured T_2 on the refocusing interval t_{180} showed that T_2 still decreases with increasing t_{180} at rather long t_{180} values. Therefore, we compared SE images with stimulated echo (STE) images to examine whether activation induced signal changes can be increased by choosing an appropriate mixing time (TM) in STE MRI. Measurements were performed using SE or STE variants of echo planar imaging (EPI) and ultrafast low angle RARE (U-FLARE). As the contrast of U-FLARE images has negligible T_2' contributions, it was possible to determine whether the effects observed in SE/STE-EPI images are due to remaining T_2' contributions caused by static B_0 inhomogeneities. The results were presented in part in [6].

Methods. All experiments were performed on a 4.7T Biospec animal scanner (Bruker Biospin, Ettlingen, Germany) equipped with a saddle-type RF coil (98 mm i.d.) for RF transmission, an 18-mm surface coil for signal reception and self-shielded B_0 gradients with 170 mT/m maximum gradient strength and 350 mT/m/ms maximum slew rate. Measurements were performed on 10 healthy adult Wistar rats (200-300g), which were anesthetized by α-chloralose (40 mg/kg) after an initial (10 min) anesthesia by 1.5% halothane. The animals were fixed in a stereotactic headholder. The respiration rate and the body temperature, which was maintained by a warm water blanket, were monitored. Electrodes were positioned subcutaneously in the right or left forepaw. The block design consisted of five 30-s periods (off-on-off-on-off) with an electrical stimulation (square pulses, 0.3 ms, 1.5 Hz, 2 mA) in the

on-periods. The slice position (~5 mm posterior to the rhinal fissure) was optimized by maximizing the fMRI signal changes. *Pulse Sequences:* Four fMRI pulse sequences were implemented: (a) a spin echo EPI (SE-EPI) with asymmetric read gradients and (b) stimulated echo EPI (STE-EPI) where images from both the primary spin echo (prSE) and the stimulated echo (STE) were acquired. The EPI parameters were: FOV: 48(x, read)*24(y, PE) mm^2, matrix size: 64(x)*32(y), slice thickness: 2 mm, interecho spacing: 1.5 ms, echo time TE=(56-144) ms, mixing time TM=(60-500) ms, repetition time TR of 3 s for SE-EPI and 3s+TM for the STE-EPI to yield a constant relaxation delay. The first two RF pulses were spatially selective to allow slice selection (z) and a reduced FOV in phase encoding (y) direction. The third 90° pulse in the STE sequence was not spatially selective to reduce in-flow/out-flow effects. Additionally, (c) SE and (d) STE variants of displaced U-FLARE were implemented with FOV: 48*48 mm^2, matrix size: 64*64, slice thickness: 2 mm, 135° Gaussian refocusing pulses, interecho spacing: 5 ms, TE$_{min}$=36 ms. In STE-UFLARE, images of the prSE and the STE may not be acquired simultaneously but in subsequent measurements. In all experiments, the spoiler gradients were minimized to reduce diffusion effects in external gradients (e.g., in STE-EPI b<50 s/mm^2 for TM=200 ms). Furthermore, inversion recovery (IR) variants of SE-EPI (IR-SE-EPI, inversion time TI=10-750 ms) and snapshot-FLASH (IR-snapshot-FLASH; 64*64 matrix, FOV: 48*48 mm^2, 2 mm slice, α=9°,TR=3 s, ΔTE=5.5 ms, spatially non-selective inversion, TI=200 ms) were performed to examine whether T$_1$ changes occur during stimulation.

Data processing: The images were reconstructed using sine-bell apodization prior to 2D FFT. The signal evolution was analyzed in each pixel without any averaging, additional filtering or motion correction. Two average images were calculated for the rest period and stimulation period, respectively, neglecting the first three images of each period to avoid transition effects. Statistical significance of signal changes was determined by a paired t-test.

Results. Activation induced signal changes were clearly observed in all animals, with only minor motion artifacts in some images. In the centre of activated regions, the relative signal change (I$_{stim}$-I$_{rest}$)/I$_{rest}$ in the SE-EPI experiment was about 3-5% at TE=56 ms, increasing with increasing TE up to 11% at TE=140 ms. A similar behavior was observed in SE-U-FLARE images where the relative signal changes increased from 2% at TE=36 up to
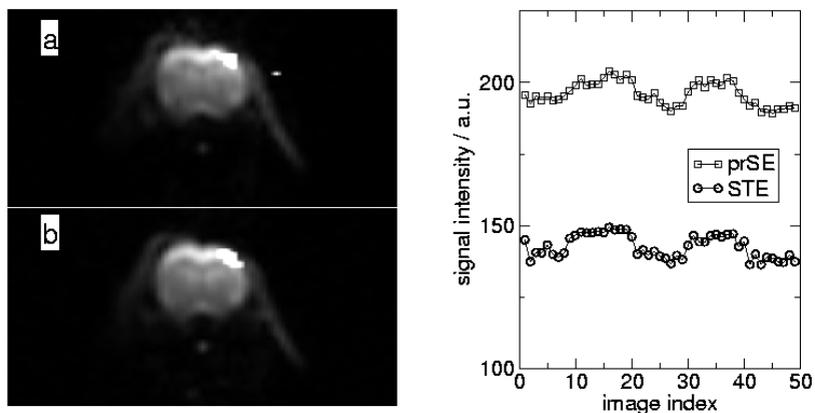
Figure 1. STE-EPI (TE=56ms, TM=200ms) images of the rat brain using (a) prSE and (b) STE with activated areas ($p<10^{-6}$) overlaid in white. (c) Time courses in a central voxel of the activated region for prSE and STE.
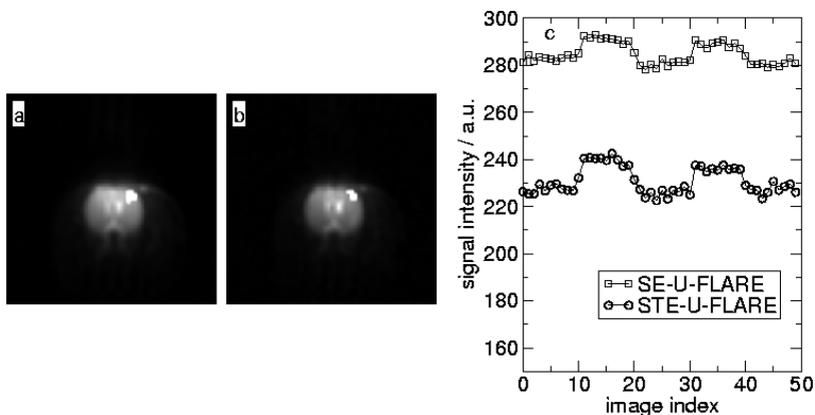
Figure 2. (a) SE-U-FLARE (TE=56ms) and (b) STE-U-FLARE (TE=56ms, TM=200ms) images of the rat brain with activated area ($p<10^{-9}$) overlaid in white. (c) Time courses in the same central voxel of the activated region.

6.5% at TE=136 ms. The larger relative signal changes in SE-EPI than in SE-U-FLARE images may be due to remaining T_2' contributions in the EPI sequence (data acquisition within +/-24 ms around TE). However, a direct

comparison with the EPI results is not possible because of the inherent T_1/T_2 weighting of U-FLARE images. In STE-EPI, as expected, the relative signal changes observed in prSE images were similar to those measured in SE-EPI. However, the STE-EPI images acquired at the same TE=56ms and with TM values of 100-500ms yielded significantly larger relative signal changes and improved statistical significance compared to the prSE data, despite reduced signal intensity (cf. fig.1). The ratio between the relative signal changes, i.e. $[(I_{stim}-I_{rest})/I_{rest}]_{STE}/[(I_{stim}-I_{rest})/I_{rest}]_{prSE}$, was 1.3-1.8. This ratio did not increase systematically with increasing TM. Increased relative signal changes were also observed in STE-U-FLARE images as compared to prSE-U-FLARE images (cf. fig. 2), indicating that the observed effect does not result from specific properties of SE/STE-EPI (e.g. T_2' contributions). To exclude that T_1 changes cause the larger signal changes in STE images, IR measurements were performed (IR-SE-EPI and IR-snapshot-FLASH). However, no statistically significant changes were observed between images measured with or without inversion. Furthermore, since the diffusion weighting of the sequences was low (b<50 s/mm^2 for TM=200ms), ADC changes [7], i.e. altered diffusion processes in external gradients can also not account for the observed findings. The increased sensitivity to flow effects of the STE image as compared to the SE image should reduce the STE signal thus causing the opposite effect. Although the reason why the relative signal changes are higher in STE images than in prSE images remains still unclear, changed diffusion processes in internal gradients are compatible with the described observations if the "long-echo limit" is not valid for the used TE [5]. The fact that in other studies [8] signal changes in STE images were smaller than in prSE images may be due to the higher B_0 and the longer TM values used in the present study.

Conclusion: Higher relative signal changes were observed in STE images compared to prSE images in fMRI experiments at 4.7T using electrical forepaw stimulation of rats. Although these changes do not compensate for the inherent 50% SNR loss of STE images and thus do not lead to higher statistical significance than SE-MRI, these findings are of importance because (a) STE based pulse sequences can be used for high temporal resolution of multislice 2D or 3D fMRI, (b) STE experiments may help to evaluate models of fMRI signal changes, (c) diffusion studies based on STE experiments where the prSE and STE images are used for different b-values (e.g., [9]) should be carefully evaluated to avoid misinterpretations. Our

findings were confirmed in [10] showing STE based fMRI is of increasing importance at higher B_0 fields than the 4.7 T used in the present study [10].

[1]   J.M.E. Oja et al., MRM 42:617 (1999).

[2]   S.-P. Lee et al., MRM 42:919 (1999).

[3]   G. Nair et al., MRM 52:430 (2004).

[4]   J.H. Jensen et al., MRM 44:144 (2000).

[5]   R.A. Brooks et al., MRM 45:1014 (2001).

[6]   W. Dreher et al., ISMRM (2005), p.1394.

[7]   A. Darquie et al., PNAS 98:9391 (2001).

[8]   T. Jochimsen et al. MRM 53:470 (2005)

[9]   U. Goerke et al., ISMRM (2004), p.1240.

[10] U. Goerke et al., ISMRM (2005), p.121 and ISMRM (2006), p.663.

Correspondence. Wolfgang Dreher, University of Bremen, Institute of Organic Chemistry, 28359 Bremen, Germany; dreher(at)tomo.uni-bremen.de

"Snapshot" Functional MRI of Behavior in Small Rodents

Küstermann, E.[1,2,3], Meier, M.[3,4], Scheich, H.[3,5] and Leibfritz, D.[1,3]

[1]Institute of Organic Chemistry, University of Bremen, [2]Department of Neuropsychology and Behavioral Neurobiology, University of Bremen, [3]Center for Advanced Imaging (CAI) – Bremen, [4]Department of Neurology II, University of Magdeburg, [5]Leibniz Institute for Neurobiology (IfN) – Magdeburg

Introduction. This project is aiming for the development of a non-invasive method to image brain activation in unrestrained moving and behaving animals at high spatial resolution in order to get hold of brain activation patterns representing cognitive processes. In vivo imaging of functional brain activation in rodents by means of the well established functional magnetic resonance imaging (fMRI) is currently feasible with anesthetized animals only. In this method, stimulus-dependent activated brain areas are detected by means of temporal correlation of mostly positive signal changes corresponding to the given stimuli [1]. Thus, for BOLD (Blood Oxygen Level Dependent) effects the animals head has to be kept within the scanner during the course of the experiment which is feasible with anesthetized animals only. This, however, precludes the usage of fMRI to investigate cognitive functions since they can be studied only in behavioral experiments. A less restrictive method to tag activated brain regions uses the calcium analog manganese. During stimulation, Mn^{2+}-ions are taken up into activated neuronal cells mediated by voltage gated Ca^{2+}-channels [2, 3]. Since manganese exhibits strong paramagnetic properties, it serves as a T_1-relaxation agent thus enabling the measurement of neuronal activity by T_1-weighted MR-imaging at very high spatial resolution. With this method, the dynamic information of brain activity, as partly preserved in the BOLD-signal, is given up for a more precise localized "snapshot" of brain activity representing all activated areas at the time of the experiment. The measuring time is spent to increase the isotropic spatial resolution thus enabling the resolution of small functional partitions such as substructures of the amygdala. In order to reliably demarcate task dependent activated brain areas, it is essential to deliver Mn^{2+}-ions to the brain (i) uniformly and (ii) exclusively within the experimental time window - otherwise, the labeling

will become task-unspecific. Since the diffusion of Mn^{2+}-ions from blood into brain parenchyma across the blood brain barrier (BBB) is too slow to achieve useful concentrations, it needs to be facilitated by other agents [4, 5]. The established method for transiently opening the BBB is the intraarterial infusion of a hyperosmotic mannitol solution. This highly invasive intervention is, however, definitely not compatible with our minimal invasive approach. Therefore, activities were focused on the development of a suitable minimal invasive protocol for the Mn^{2+}-application with these requirements: (i) minimal interference with the animal: it should be able to move freely and participate in the behavioral test; (ii) it must be applicable repetitively in order to be compatible with long-term studies. Current efforts focus on a bolus application of the manganese solution in combination with DMSO as an agent to accelerate the diffusion of Mn^{2+}-ions across the BBB [6, 7].

Methods. Rats were anesthetized with isoflurane. The tail vein was punctured and a $MnCl_2$-solution of up to 180mM with 15% DMSO was applied at infusion rates ranging between 180 and 600µl/h. Animals were stimulated under isoflurane anesthesia by passive movement of the left forepaw. A stick was taped to the paw and moved back and forth along the body axis at a frequency of about 1Hz manually. Afterwards, the anesthetized animal was transferred to the magnet (4.7T, Bruker Biospec) and the isoflurane anesthesia continued under permanent monitoring of rectal temperature and breathing. The success of the manganese application and brain activity was judged by means of T1-weighted MR-images at a rather course spatial resolution of isotropic 250µm: (i) 3D-gradient-echo imaging, TE/TR=3.6/20-50ms, 250kHz receiver bandwidth, sinc-shaped excitation pulses of 1-2ms and 15°-50° excitation angles; (ii) 3D-MDEFT, TE/TRecho/TR/TI= 4.0/21/1000-2000/900-1400ms, sinc-shaped excitation pulses of 1-2ms at 15°. For reasons of optimal signal-to-noise ration (SNR) per unit time and the ability of intermodal coregistration, only 3D-imaging techniques at isotropic resolution were considered.

Results. As shown in the figures, in T_1-weighted MR-images areas with enhanced signal intensity can be detected upon passive movement under manganese infusion. The signal enhancement is clearly more intense on the contralateral side (right) to the moved paw (left) and thus in good agreement with the classical experiment of electrical forepaw stimulation [3]. Comparing the areas of signal enhancement in fig. 1 with fig. 2, there is a

tendency to stronger signal enhancement under higher manganese concentrations reflecting the higher accumulation of Mn^{2+} ions, although the stimulation period was much shorter.
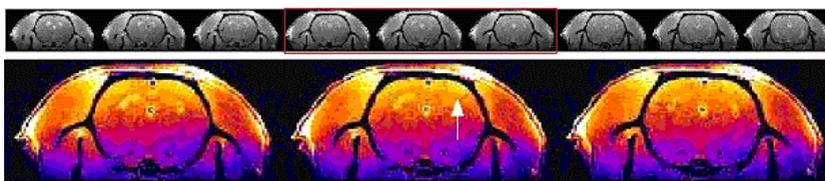
Figure 1. Top row: Consecutive axial slices of rat brain after 20min of passive left forepaw movement under 180mM $MnCl_2$-infusion at 600µl/h. An area of enhanced signal is detected in the corresponding somatosensory cortex of the right hemisphere. Bottom row: Consecutive axial slices (center of top row) in false color enhancing the signal increase in the right somatosensory cortex.
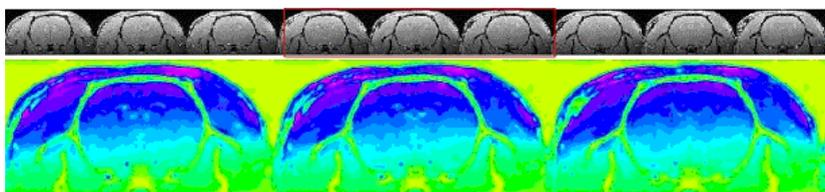
Figure 2. Top row: Consecutive axial slices of rat brain after 60min of passive left forepaw movement under 90mM $MnCl_2$-infusion at 180µl/h. Again, enhanced signal is detected in the somatosensory cortex of the right hemisphere. Bottom row: Consecutive slices (center of top row) in false color enhancing the signal increase in the right somatosensory cortex.

Discussion. These results show that brain activation under isoflurane anesthesia can be detected with such a simple and completely non-invasive stimulation paradigm of passive forepaw movement. This moderate non toxic Mn and DMSO concentrations can be applied under unrestrained conditions via a remotely operated implanted pump. This kind of setup will make it possible to apply the necessary substances in the time window for cognitive "actions" and will allow to monitor brain activity in freely moving animals.

60

[1] Logothetis, N.K., Pauls, J., Augath, M., Trinath, T., & Oeltermann, A. (2001). Neurophysiological investigation of the basis of the fMRI signal. *Nature*, 412, 150-157.

[2] Drapeau, P., & Nachshen, D.A. (1984). Manganese fluxes and manganese-dependent neurotransmitter release in presynaptic nerve endings isolated from rat brain. *J Physiol*, 348, 493-510.

[3] Duong, T.Q., Silva, A.C., Lee, S.-P., & Kim, S.G. (2000). Functional MRI of calcium-dependent synaptic activity: cross correlation with CBF and BOLD measurements. *Magn Reson Med,* 43, 383-92.

[4] Lin, Y.J. & Koretsky A.P. (1997). Manganese ion enhances T1-weighted MRI during brain activation: an approach to direct imaging of brain function. *Magn Reson Med,*. 38, 378-88.

[5] Silva, A.C., Lee, J.H., Aoki, I., & Koretsky, A.P. (2004). Manganese-enhanced magnetic resonance imaging (MEMRI): methodological and practical considerations. *NMR Biomed*, 17, 532-543.

[6] Broadwell, R.D., Salcman, M., & Kaplan, R.S. (1982). Morphologic effect of dimethyl sulfoxide on the blood-brain barrier. *Science*, 217, 164-166.

[7] Kleindienst, A., Dunbar, J.G. Glisson, R., Okuno, K., & Marmarou, A. (2006). Effect of dimethyl sulfoxide on blood-brain barrier integrity following middle cerebral artery occlusion in the rat. *Acta Neurochir Suppl*, 96, 258-262.

Correspondence. Ekkehard Küstermann, c/o Department of Organic Chemistry, University of Bremen, Leobener Strasse NW2/C, D-28359 Bremen; ek(at)tomo.uni-bremen.de

Uncertainty and Reproducibility of Quantitative DTI and Fiber Tracking of the Human Brain

Klein, J.[1,], Schlüter, M.[1], Rexilius, J.[1], Konrad, O.[1], Erhard, P.[2], Stieltjes, B.[3], Althaus, M.[1], Dreher, W.[2], Leibfritz, D.[2], Hahn, H.K.[1] and Peitgen, H.-O.[1]

[1]MeVis Research, Bremen, [2]FB 2 Chemistry and Center for Advanced Imaging (CAI) - Bremen, [3]Dept. of Radiology, German Cancer Research Center, Heidelberg

Introduction. Diffusion tensor imaging (DTI) techniques like fiber tracking (FT) or quantification of DTI related parameters have the potential to identify major white matter tracts afflicted by an individual pathology or tracts at risk for a given surgical approach. However, the reliability and reproducibility of these techniques are known to be limited by the quality of acquired data, the underlying models and algorithms, and by the methods for reporting and displaying the results. We show how different image resolutions of the acquired data influence the quantification and fiber tracking process, derive a relationship between the diffusion anisotropy (DA) and the orientation uncertainty (OU) by considering image noise, and present methods to assess and visualize the uncertainty of fiber reconstructions. As a consequence, we are able to develop and evaluate robust preprocessing, fiber tracking, and quantification algorithms which take partial volume effects into account and which are able to compute DTI parameters along fiber bundles automatically. Our optimized color-coding scheme for DTI data as well as our fiber clustering algorithm address the problem of presenting the results to the clinicians in such a way that uncertainties in the interpretation are reduced and the perception of the visualization is enhanced.

Methods. We acquired echo planar diffusion tensor data from both 1.5T and 3.0T scanners. For examining resolution-dependent differences, the data was acquired at several image resolutions. Using a deflection-based fiber tracking algorithm [8], we reconstructed parts of the cingulum as well as parts of the pyramidal tract for all DTI data sets [3]. A method which is capable of an automatic quantification of MR DTI parameters along arbitrarily oriented fiber bundles [5] is used for measuring the average fractional anisotropy (FA) along the fiber bundles. Moreover, we propose to determine the volume

of the sheath that encloses the single fiber tracts. By considering image noise, we derived a local relationship between DA and OU [8]. Because of this relation, a decrease of the DA implies an increase of the OU. With this observation a white matter lesion model on diffusion tensor data can be developed, where fiber bundle disturbance of arbitrary strength can be simulated at arbitrary locations. Thus, it is possible to assess existing and forthcoming FT algorithms with respect to the robust fiber bundle reconstruction in the presence of white matter lesions. Moreover, we developed a method to assess and visualize the uncertainty of fiber reconstructions based on variational complex Gaussian noise, which provides an alternative to the bootstrap method (cf. fig. 1 left). We compare fiber tracking results with and without variational noise as well as with artificially decreased image resolution and signal-to-noise [1, 2]. For quantification of DTI parameters, we introduced a method which assumes a probabilistic mixture model inside a region of interest (ROI) including the two pure tissue classes fiber and background. Since the voxel size is not negligible compared to the extension of the quantified fiber bundle, partial volume effects have to be considered. Therefore, we added a mixture or partial volume class to our model [6, 9, 10]. Our automatic quantification along bundles allows for a robust and reliable measurement of DTI parameters as outliers only have a very small influence in the results [5]. For visualization, we introduce a new color coding paradigm for DTI based fiber bundle orientation [7]. The color coding is defined with respect to an arbitrary projection plane, which can be automatically adjusted in order to minimize the local ambiguity of the encoding. Finally, our grid-based spectral fiber clustering groups anatomically or geometrically related fibers in order to improve the perception of tracking results (cf. fig. 1 center) [4].

Results. Our experiments confirm that DTI parameters like average FA, the volume of the sheath around fibers, or the number of fibers depend on the image resolution, but the amount of change also depends on the kind of fiber bundle. While the average FA value increases remarkably for the cingulum when increasing the resolution, the FA value for the pyramidal tract only slightly increases. This may be explained by the fact that the tensor field is more sensitive in areas where different fiber structures are close to each other as in the case of the cingulum. The volume of the sheath, however, differs more for the pyramidal tract. This may be explained by partial volume effects where bundles in isotropic surroundings are assessed too large whereas fibers in inhomogeneous areas are not tracked at borders. Our

proposed lesion phantom based on the relationship between OU and DA is employed to improve our deflection based FT algorithm. We applied it to synthetic fiber bundles as well as to real DTI data and demonstrated the robustness of the modified FT algorithm. Using our variational complex Gaussian noise, the uncertainty due to image noise can be measured and visualized. We found a high robustness to a decreased signal-to-noise ratio, but still, the effects of image quality on the tracking result will depend on the employed fiber tracking algorithm and must be handled with care, especially when being used for neurosurgical planning or resection guidance. Furthermore, we showed that the results of our quantification are largely independent of the ROI extension, which facilitates reproducible quantification of white matter infiltration [10]. The automatic quantification along fiber bundles drastically reduces the manual effort and hence the time for quantifying, e.g., the FA along a complete bundle. An excellent differentiation of fiber orientations is achieved by our color coding so that it directly improves in vivo brain navigation with potential application to therapy planning. Moreover, our fiber clustering automatically determines the number of clusters depending on the desired granularity and constitutes the basis for an enhanced perception and interaction. Finally, we demonstrated that the introduced methods not only allow for an early, direct, and sensitive detection of white matter infiltration (cf. fig. 1 right), but may also be employed for monitoring the therapy of ALS or MS patients, which emphasizes the clinical relevance of our results [6, 9, 10].
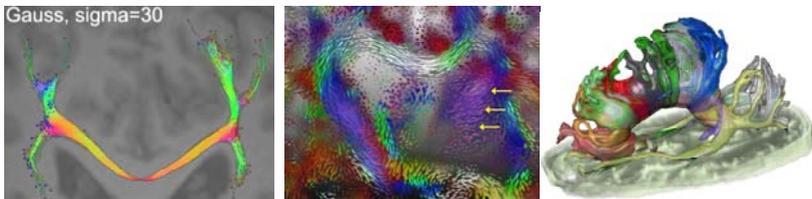
Figure 1. Left: Complex Gaussian noise used to visualize the uncertainty due to noise [2]. Center: Fiber clustering is used to improve perception and interaction [4]. Right: Colored glyph based rendering of structural changes induced by a glioblastoma [9].

Discussion. There are several reasons that have prevented DTI to become a widespread clinical diagnostic modality so far. Among these, reproducibility as well as the inherent uncertainty in the data and in the results are the most important factors. Until now, we introduced some initial techniques for

quantifying and visualizing the uncertainty of the DTI data, for developing and evaluating robust fiber tracking and quantification algorithms, and for presenting the results to the clinicians such that they are easy to use and ambiguities are reduced. In the near future, we would like to identify risk structures based on the reconstructed fiber bundles in order to further reduce the risk of specific interventions and increase patient safety. Uncertainties, which cannot be reduced, may be visualized as confidence margins.

[1]   Hahn, H.K., Klein, J., Nimsky, C., Rexilius, J., & Peitgen, H.O. (2006). Uncertainty in diffusion tensor based fibre tracking. *Acta Neurochirurgica Supplementum,* Suppl. 98, 33-41.

[2]   Klein, J., Hahn, H.K., Rexilius, J., Erhard, P., Althaus, M., Leibfritz, D., & Peitgen, H.-O. (2006). Efficient Visualization of fiber tracking uncertainty based on complex gaussian noise. *Proc. of ISMRM* 2006.

[3]   Klein, J., Erhard, P., Hermann, S., et al. (2007). Resolution-dependent differences in fiber tracking and quantification. *Proc. of ISMRM* 2007.

[4]   Klein, J., Bittihn, P., Ledochowitsch, P., Hahn, H.K., Konrad, O., Rexilius, J., & Peitgen, H.-O. (2007). Grid-based spectral fiber clustering. *Proc. of SPIE*.

[5]   Klein, J., Hermann, S., Konrad, O., Hahn, H.K., & Peitgen, H.O. (2007). Automatic quantification of DTI parameters along fiber bundles. *Proc. of BVM*. 272-76

[6]   Schimrigk, S., Bellenberg, B., Schlüter, M., et al. (2007). Fractional anisotropy quantification in the corticospinal tract of ALS patients and controls using a new probabilistic mixture model. *AJNR*, 28.

[7]   Schlüter, M., Stieltjes, B., Rexilius, J., Hahn, H.K., & Peitgen, H.-O. (2004). Unique planar color coding of fiber bundles and its application to fiber integrity quantification. *Proc. of ISBI*.

[8]   Schlüter, M., Konrad, O., Hahn, H.K., Stieltjes, B., Rexilius, J., & Peitgen, H.-O. (2005). White matter lesion phantom for diffusion tensor data and its application to the assessment of fiber tracking. *Proc. of SPIE*, 835-844.

[9]   Schlüter, M., Stieltjes, B., Hahn, H.K., Rexilius, J., Konrad, O., & Peitgen, H.-O. (2005). Detection of tumor infiltration in white matter fiber bundles using diffusion tensor imaging. *Int J Med Robot Comput Assist Surg*, 1, 80-86.

[10]   Stieltjes, B., Schlüter, M., Didinger, et al. (2006) Diffusion tensor imaging in primary brain tumors: reproducible quantitative analysis of corpus callosum infiltration as measure of contralateral involvement. *NeuroImage*, 31, 531-42.

Correspondence. Jan Klein, MeVis Research, klein(at)mevis.de

III. Monkey Neurophysiology and Functional MRI

Monkey Neurophysiology and Functional MRI

Kreiter, A.K.

Institute for Brain Research, University of Bremen, and Center for Advanced Imaging (CAI) – Bremen

Functional magnetic resonance imaging (fMRI) is a technique which allows to assess physiological states of the human brain with unprecedented spatial resolution, but there seemed to be little reason to use fMRI for investigating the macaque's brain. Modern neurophysiological techniques achieve a spatial and temporal resolution which is by a factor of thousand better than fMRI, and they measure the bioelectrical signals representing the basis of cerebral information processing directly, not its consequences for blood oxygenation. However, fMRI's lack of fine spatial resolution is complemented by an important advantage: it allows to access the entire brain within one measurement and provides therefore an overview over different brain structures likely to be involved in the specific cognitive task under investigation. Such a quick overview can hardly be achieved by other techniques available at present. Using this technique with macaque monkeys allows not only to identify efficiently the anatomical structures associated with specific functions but opens the possibility for subsequent detailed neurophysiological analysis of neuronal information processing within and between the identified anatomical structures. Furthermore, the possibility to acquire a very large number of experimental trials for individual animals allows to achieve very accurate and reliable maps for individual brains. The importance of such fMRI-based guidance of neurophysiological investigations rises with the complexity of the cognitive processes under investigation. While early investigations of the initial steps of sensory processing allowed accurate predictions of the relevant structures based on the well known neuroanatomy, predictions of the set of relevant structures involved in complex tasks including different cognitive functions are difficult and often not reliable.

A second important function of monkey-fMRI is to provide a link between the detailed neurophysiological knowledge, which can be gathered only for the monkey brain, and our knowledge on the human brain. As a technique which can be applied in both species, it is particularly well suited to identify commonalities as well as differences in the way both species process information in their brains.

The running projects with macaque monkeys described in the subsequent abstracts demonstrate that it is possible to achieve the goals described above after developing and adapting the necessary equipment and methods, which include behavioral conditioning techniques and equipment, implantation methods, and fMRI data acquisition and analysis. The work by Olmedo Babé and Freiwald on conflict resolution is a good example for the guidance function of fMRI for investigations of complex cognitive mechanisms. They successfully developed a task for testing the Stroop-, Simon-, and Eriksen flanker effect in macaque monkeys during fMRI. Their results identify cortical areas involved in the corresponding executive functions and allow for direct comparison with similar investigations in humans.

A particularly successful and advanced application of fMRI in macaque monkeys is the identification of specific face processing modules in the monkey brain. In their present work Freiwald and Tsao use this technique to localize these small and variably placed structures in the inferotemporal cortex for guiding recordings from large numbers of face cells. This allows them to identify specific functions for these modules which could not have been described by fMRI or single unit recordings alone. The present study provides also a basis for transferring the detailed neurophysiological results to the human brain in which fMRI revealed similar modules. This is also a goal of the study of Stemmann and Freiwald who identified a network of cortical areas involved in attentional control and processing of motion stimuli. These findings allow to integrate the results of their previous single unit studies with knowledge obtained from investigations in humans with similar paradigms.

Moeller and Tsao describe indicators of state dependent interactions of brain regions by means of fMRI. They find that the spatial extend of activity covariations differs clearly for anaesthetized monkeys, awake monkeys observing a blank screen, and monkeys seeing various stimuli. In a project combining neurophysiology and fMRI, Zinke and colleagues describe first results for a monkey performing a working memory task. An independent

component analysis on the data, revealed networks of functionally connected regions for different stages of the task. This study complements a companion study with humans (see Galashan et al., this reader section 7) and identifies the targets for subsequent neurophysiological investigations.

Correspondence. Andreas Kreiter, Institute for Brain, University of Bremen, Hochschulring 16a, D-28359 Bremen; kreiter(at)brain.uni-bremen.de

The Neural Machinery for Face Processing

Freiwald, W.A.[1,2] and Tsao, D.Y.[1,2]

[1]Institute for Brain Research, University of Bremen, [2]Center for Advanced Imaging (CAI) - Bremen

Introduction. FMRI has revealed several discrete regions of cortex in both human and macaque brains that show increased activation to faces compared to other visual objects. Macaque face-selective areas are arranged along the temporal lobe in a posterior to anterior manner (fig. 1). Two fundamental questions about the function of face patches are (a) whether they encode only faces or other objects as well and (b) whether each patch subserves a unique functional role in face-recognition. To address these questions, we have performed single-unit and local field potential (LFP) recordings targeted to two face-selective regions which we had identified by fMRI as being face-selective [1].

Methods. Four male rhesus macaques (M1: 7 kg, 6 years old, M2: 4 kg, 3 years old) were implanted with Ultem headposts, trained via standard operant conditioning techniques to maintain fixation on a spot for a juice reward, and then scanned in a 3 T horizontal bore magnet (Siemens Allegra®) to allow identification of face-selective regions. All four animals had prominent face-selective regions located ~ 6 mm and ~ 17 mm anterior to the ear canals (the "central face patch" and the "anterior face patch", respectively) which were targeted for single-unit and LFP recordings. FMRI data were acquired using a standard face localizer stimulus and the following imaging parameters: EPI, TR=3 sec; TE = 30 ms; 64 x 64 matrix; 1.25 x 1.25 x 1.25 mm voxels; 28 coronal slices.

Results. In the central face patch, we tested the face selectivity of 405 single units using 96 images of faces and other objects. The stimuli were presented foveally every 400 ms (200 ms on and 200 ms off), in random order for 4 to 10 repetitions, while the monkey fixated. We recorded responses from all single units encountered, regardless of visual responsiveness or face selectivity. Across the population of recorded cells, 182/241 (76%) cells in M1 and 138/164 cells (84%) in M2 gave significant responses (14) to at least

one of the 96 images and were therefore classed as visually responsive. We found that 97% of these visually responsive cells were face-selective, thereby providing evidence that this patch constitutes a face-specific cortical module (fig. 2). The LFP was also strongly face-selective, with two face-selective peaks at 130 and 200 ms. When tested with parameterized cartoon faces, 88% of cells showed significant tuning to at least one cartoon parameter, and tuning was usually ramp-shaped, e.g., cells tuned to view angle will respond maximally to leftward profile and minimally to rightward profile.
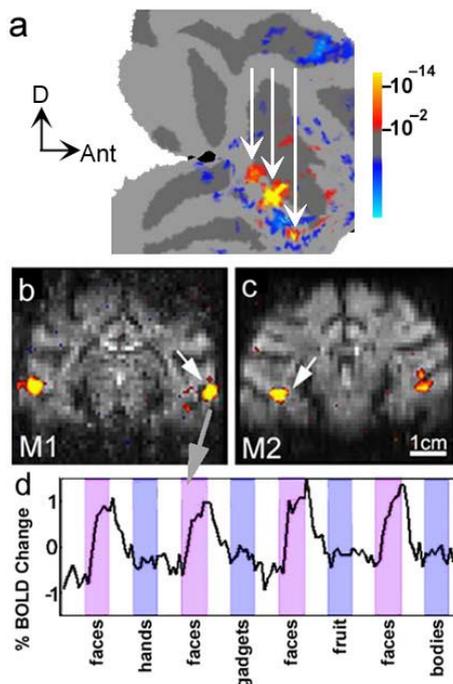
Figure 1. Face patches in the macaque. (a) Flat map of the right hemisphere visual cortex (macaque M1) showing three patches of face-selective fMRI activation spanning the anteroposterior extent of the temporal lobe. White arrows indicate the three face patches. (b) and (c) Coronal fMRI sections from monkeys M1 and M2 showing the central pair of face patches; white arrows indicate patches we have recorded from. (d) BOLD time course from the central face patch (gray arrow).
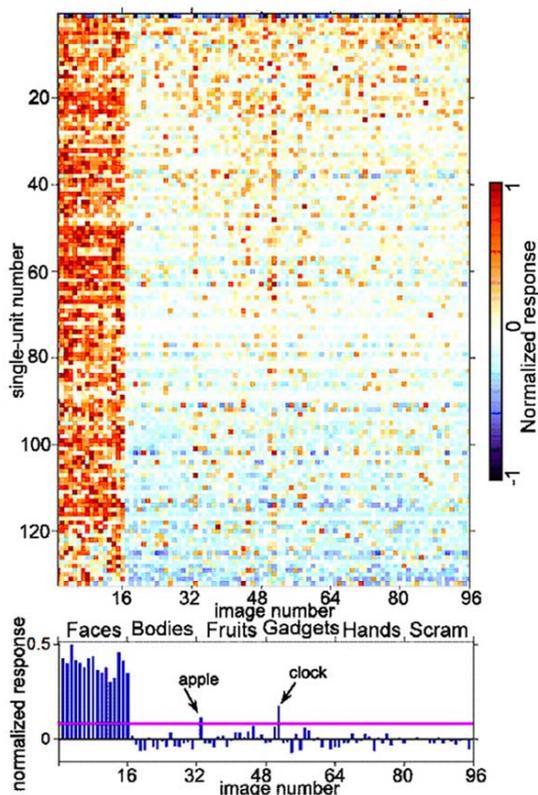
Figure 2. (top) Responses of 132 neurons from M1's central face patch to 96 images of faces and non-face objects. (bottom) Average normalized population response to each image. For each cell, responses were summed from 100 to 300 ms, averaged over all presentations, baseline subtracted, and normalized to the maximum average response. All faces produced significant population responses (>5 standard deviations, magenta line); of the other 80 images, a clock and an apple gave small but significant responses.

Recordings from a second, more anterior face-selective region (located ~A17 on the outer lip of the inferior temporal gyrus), showed that almost all cells in this region were also face-selective, responding more strongly to pictures of faces than of other objects and body shapes. However, functionally, this new anterior area differs in at least three ways from the central face patch:

First, LFPs, biphasic in shape in response to all objects, are several tens of milliseconds faster for faces than other objects. Second, single-unit responses are very strongly dependent on face view direction, and much less on face identity. Third, view-selectivity is highly symmetrical, i.e. a cell with preference for a left-ward looking profile, will respond to a right-ward looking profile view as well. We found cell-by-cell correlation coefficients as high as 0.9 for responses to mirror-symmetric view directions (averaged over identity).

Discussion. Our results provide evidence that face-recognition in macaques relies on a system of domain-specific modules, each specialized for a different computational task. Cells in the central face patch are measuring the physical properties of faces along multiple face feature dimensions. Cells in the anterior face patch appear to be computing an intermediate stage of view-invariance, namely view-specific mirror symmetry invariance.

[1]   Tsao, D.Y., Freiwald, W.A., Knutsen, T.A., Mandeville, J.B., & Tootell, R.B. (2003). Faces and objects in macaque cerebral cortex. *Nat Neurosci*, 6, 989-995.

[2]   Tsao, D.Y., Freiwald, W.A., Tootell, R.B.H., & Livingstone, M.S. (2006). A cortical region consisting entirely of face cells. *Science*, 311, 670-674.

Correspondence. Winrich Freiwald, Institute for Brain Research and Center for Advanced Imaging, University of Bremen, Grazer Strasse 6, D-28359 Bremen; winrich.freiwald(at)googlemail.com

Networks of Attention in Macaque Monkeys Performing a Motion-Tracking Task

Stemmann, H.[1,2] and Freiwald, W.A.[1,2]

[1]Brain Research Institute, Department of Theoretical Neurobiology, University of Bremen, [2]Center for Advanced Imaging (CAI) – Bremen

Introduction. Using fMRI in humans, it has been possible to identify networks of cortical areas exerting attentional control and to compare the degree of attentional modulation across sensory cortical areas and subcortical structures [1]. For the macaque monkey brain, which has been extensively studied at the single-cell level, such a large-scale picture of attentional mechanisms is still lacking. To fill this gap, we used fMRI to image brain activation in macaque monkeys performing a spatial attention task.

Methods. We devised a motion tracking task in which macaques had to pay attention to one of two random dot surfaces (RDS), positioned on the horizontal meridian at opposite positions from the central fixation spot (see fig. 1). RDSs were presented in a circular aperture 6° in diameter positioned 5° from the fixation spot on the horizontal meridian. Dot density of each surface was 5 dots per square degree of visual angle. Eye position of the animals was monitored by an optical eye measurement system (ISCAN Inc., Burlington MA, USA). After an initial fixation period, one RDS was cued as the behaviorally relevant stimulus (the target) by a small line to the side of the fixation spot, pointing to this surface. While RDSs were randomly changing translation direction every 50ms (or 60ms), monkeys had to pay attention to the target until the translation direction ceased changing for up to 800ms, to be followed again by rapid direction changes. Direction changes occurred in random multiples of 20°. The monkeys were required to keep fixation in a 2° x 2° window throughout the whole stimulation period until the occurrence of the prolonged translation motion of the target. After detection of this event monkeys had to report the direction of the prolonged motion step by a saccade to one out of 8 peripheral saccade target dots positioned 8.5° from the fixation spot. A trial was rated successful if the animal initiated a response within 800ms after the beginning of the

prolonged translation movement and reached the appropriate saccade target 500ms afterwards. Successful trials were rewarded with a drop of liquid.
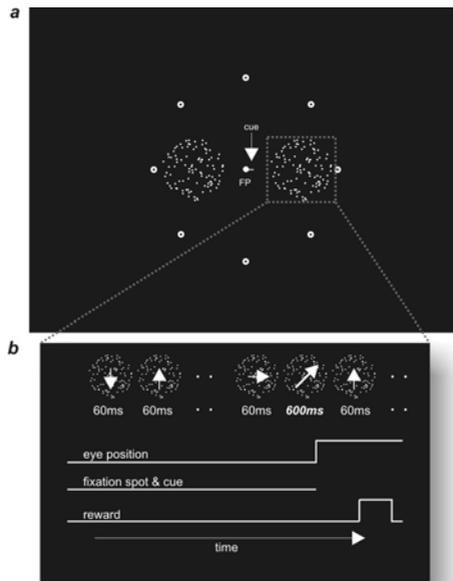
Figure 1. Visual stimuli were projected onto a translucent screen that was positioned 54cm in front of the monkey's eyes; (a) shows the stimulus configuration as seen by the subjects, and (b) depicts the behavior of the target RDS and the time courses of eye position, fixation spot and cue and reward during a successful trial.

Two monkeys were scanned inside a horizontal bore 3T head scanner (Allegra®; Siemens, Erlangen, Germany), using an EPI sequence. Functional time series consisted of gradient-echoplanar whole-brain images: TR = 1.5s; TE = 30ms, 1.56 x 1.56 x 2mm voxels (24 transversal slices). In addition, for each subject, a high-resolution anatomical image (MPRAGE) was acquired (0.5 x 0.5 x 0.5 mm voxels). A block design was used. Conditions were: (1) behaviorally relevant surface RIGHT (right > left) and (2) behaviorally relevant surface LEFT (left > right). Blocks were separated by a 5s (or 10.5s) period of passive fixation during which only a fixation spot was presented. Data were analyzed using statistical parametric mapping (SPM5). Scans which showed an unacceptable level of movement artifacts or during which performance was low were disregarded from further analysis.

Results. Monkeys' performance reached levels of 50% (compared to a chance level of 12.5%) and above in the scanner. Monkey M's mean performance for the right target was 59.9% (+- 1.95 standard error of the mean) and for the left target 48.9% (+- 2.41). Monkey Q accomplished 62.1% (+- 2.48) and 55.2% (+- 2.40) correctly, for right and left target respectively. Behavioral data from a third monkey in a valid / invalid cuing variant of the task showed that the task was attentionally demanding: with an invalid cue response times increased by 30ms and more and performance rates dropped close to chance level. We found highly significant increases of BOLD responses in several cortical areas when attention was paid to the RDS in the opposite hemifield (see fig. 2). These increases were very pronounced in motion-sensitive areas in the superior temporal sulcus (MT and FST). But we also found effects as early as in area V1 and early extrastriate areas (V2 and V3). Furthermore, we found activation in the intra-parietal sulcus (areas VIP and LIP), the frontal eye fields and the superior colliculi.

Yellow / Red :   right attend   > left attend
Blue / Green :   left attend   > right attend
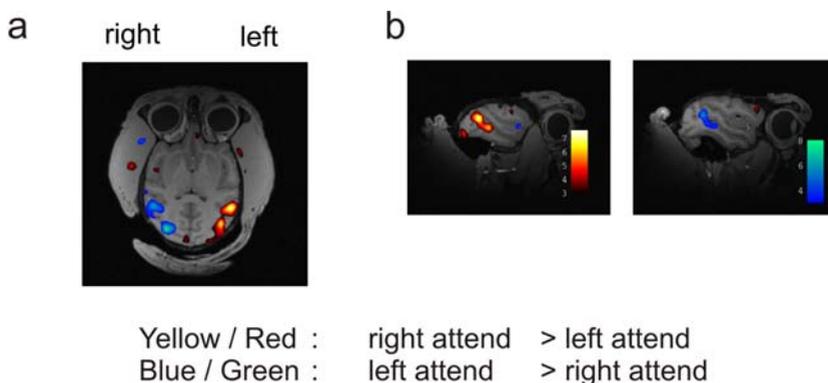
Figure 2. Attention-related modulation in areas V2 and MT is shown in monkey Q obtained from a single experimental day superimposed on (a) transverse and (b) parasagittal sections of anatomical images. Color bars indicate t-values.

Discussion. Employing an attentionally demanding motion tracking task, we have been able to describe a distributed network of cortical and subcortical activations related to the attentional state of the subjects. This network includes area MT, which in many electrophysiological studies has been shown to be modulated by attention [2, 3]. Using the exact same task

described in this abstract in previous electrophysiological recordings, we have found attention to modulate activity of individual MT neurons [4]. Thus, BOLD and single-unit activity are modulated by attention in a qualitatively similar way. This result shows that BOLD responses can be used as indicators of attentional modulation at the single cell level. Importantly, fMRI allowed us to scan the entire macaque brain at a resolution sufficient to even find activation in as small and circumscribed structures as the superior colliculus. Thus a whole network of areas included in attentional processing of dynamic motion stimuli could be imaged. This network includes the earliest visual areas, areas inside the superior temporal sulcus known to be involved in motion processing, as well as areas thought to be involved in directing attention to spatial locations [5]. This finding will allow for detailed investigations into the neural mechanisms of spatial attention.

[1] Kanwisher, N. & Wojciulik, E. (2000). Visual attention: insights from brain imaging. *Nature Reviews Neuroscience*, 1, 91-100.

[2] Treue, S. & Maunsell, J.H.R. (1996). Attentional modulation of visual motion processing in cortical areas MT and MST. *Nature,* 382, 539-541.

[3] Wegener, D., Freiwald, W.A., & Kreiter, A.K. (2004). The influence of sustained selective attention on stimulus selectivity in macaque area MT. *Journal of Neuroscience,* 24, 6106-6114.

[4] Stemmann, H. &. Freiwald, W.A. (2005). Effects of attention during rapid serial visual presentation on macaque area MT neurons, Program No. 411.7. *2005 Abstract Viewer/Itinerary Planner.* Washington, DC: Society for Neuroscience, Online.

[5] Corbetta, M., Akbudak, E., Conturo, T.E., Snyder, A.Z., Ollinger, J.M., Drury, H.A., Linenweber, M.R., Petersen, S.E., Raichle, M.E., van Essen, D.C., & Shulman, G.L. (1998). A common network of functional areas for attention and eye movements. *Neuron,* 21, 761-773.

Correspondence. Heiko Stemmann, Brain Research Institute, Department of Theoretical Neurobiology, University of Bremen, POB 330 440, D-28334 Bremen; stemmann(at)brain.uni-bremen.de

On fMRI and Cortical Networks

Moeller, S. [1,2] and Tsao, D.Y.[1,2]

[1]Institute for Brain Research, University of Bremen, [2]Center for Advanced Imaging (CAI) - Bremen

Introduction. How is brain activity organized during different stimulus and arousal states? In a typical fMRI experiment, one looks for regions of the brain that show activity magnitude changes correlated to specific stimulus changes (e.g., seeing visual motion). This approach discards all non-stimulus driven fluctuations in response (fig. 1). But a growing body of work indicates that the brain is highly active even in the absence of any external stimuli. The fact that this intrinsic activity consumes the lion's share of the brain's energy budget and moreover, is spatially organized into specific correlated networks, suggests that it is of critical functional significance [1]. How are spatially correlated activity fluctuations generated at the level of single cells and what is their function? Monkey fMRI opens a door to addressing these fundamental questions by allowing one to identify and characterize correlated networks at a coarse scale (~ 1 mm^3 resolution), which can subsequently be studied in detail through electrophysiology. Here, we used Independent Components Analysis to identify macaque brain networks showing correlated activity time courses across a wide variety of stimulus and arousal states, and then compared the spatial structure of the correlated networks across the different stimulus and arousal states.

Methods. Four male rhesus macaques were implanted with Ultem headposts, trained via standard operant conditioning techniques to maintain fixation on a spot for a juice reward, and then scanned in a 3 T horizontal bore magnet (Siemens Allegra®) during both awake and anesthetized states. Different visual stimuli were presented during the alert state; stimuli included: 1) a blank screen, 2) a clip from a James Bond film, 3) a face localizer stimulus, 4) a retinotopic localizer stimulus, 5) a disparity localizer stimulus, 6) a motion localizer stimulus, 7) a color localizer stimulus, and 8) a 3D structure-from-motion localizer stimulus. Monkeys were required to fixate during all stimuli. FMRI data were acquired using the following imaging

parameters: EPI, TR=3 or 4 sec; TE = 30 ms; 64 x 64 matrix; 1.25 x 1.25 x 1.25 mm voxels; 28 or 42 coronal slices. An automated procedure for comparing the reliability of different independent components based on bi-laterality and reproducibility across multiple scan sessions was developed. Using this procedure, we identified a set of robust correlated networks for each stimulus condition. To compare the global spatial structure of correlated networks across different stimulus conditions, we computed correlation coefficients between all possible network pairs. To compare the local spatial structure of correlated networks across different arousal states, we computed, for both alert and anesthetized states, the variance within each network as a function of pairwise voxel distance.
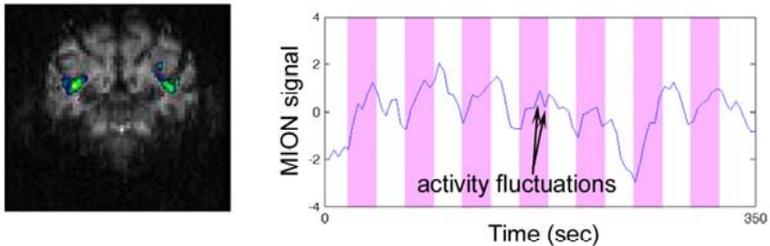
Figure 1. (Left) Area MT localized using a standard motion localizer stimulus. In this stimulus, epochs 1-4, 6, and 7 consisted of different types of motion; epoch 5 consisted of static dots. (Right) Raw time course from a single run and a single voxel to the motion localizer stimulus (voxel indicated in yellow on the functional slice). In addition to absolute magnitude changes which occur in response to changes in stimulus condition, the response level shows fluctuations within a given stimulus block. Can such fluctuations, which are normally thrown out as noise, be used to identify functionally connected areas?

Results. ICA analysis revealed ~ 30 discrete networks across the brain. Some of these networks correspond to previously known networks, thus validating the technique. Within visual cortex, these included: MT/MST/FST, CIPS, foveal retinotopic cortex, peripheral retinotopic cortex, a LIP-FEF network, and a face processing network. In addition, we identified with high reliability several new networks in temporal, prefrontal, and parietal cortex. Many networks were reproducible across different stimulus states, surprising

considering the variety of visual stimuli that were used. For example, CIPS (caudal intraparietal sulcus), a region first identified as being strongly selective for 3D structure [2], appeared as a discrete correlated network not only in experiments in which the monkey was viewing the 3D localizer stimulus, but also in experiments in which the animal was viewing a flat flickering wedge (retinotopic localizer). However, it did not appear as a correlated network when the monkey was simply fixating a blank screen; thus the activity fluctuations were not due to the monkey simply looking around the 3D environment of the scanner bore itself. We observed two large groups of networks that showed anti-correlated activity between each other, with the strongest anti-correlation occurring between visual and auditory cortex. This suggests that monkeys may also have a default network. Comparison of networks between anesthetized and alert (while fixating a blank screen) states revealed that many more correlated networks are present in the former than in the latter state. Indeed, almost the same number of correlated networks was observed in the anesthetized state as in the alert (while viewing a James Bond movie clip) state.

Discussion. Our results show that the brain, when activated by a stimulus, responds not only by an increase in activation within the area(s) dedicated to coding that stimulus, but also, by increases in spontaneous activity fluctuations in multiple additional areas, some of which may show almost no change in mean response magnitude to the stimulus. The spontaneous activity fluctuations are spatially organized to respect area borders. These discrete correlated networks can be identified in a straightforward manner using Independent Components Analysis. The networks are highly reproducible across different scan sessions using the same stimulus, and surprisingly, are often reproducible even when using different stimuli. The networks seem to be broadly organized into 2 anti-correlated sets of networks, suggesting the possibility that the macaque brain contains a homolog of the human "default" network [1]. The fact that many correlated networks were apparent during anesthesia indicates that the anesthetized brain is hardly at rest, but is experiencing multiple spontaneous activity fluctuations which are coherent within (but not across) areas. Our work paves the way for future electrophysiological experiments to study the neuronal basis for large scale coherent spontaneous activity fluctuations.

[1] Raichle, M.E. & Mintun, M.A. (2006). Brain work and brain imaging. *Annual Review of Neurosci*, 29, 449-476.

[2] Tsao, D.Y., Vanduffel, W., Sasaki, Y., Fize, D., Knutsen, T.A., Mandeville, J.B., Wald, L.L., Dale, A.M., Rosen, B.R., Van Essen, D.C., Livingstone, M.S., Orban, G.A., & Tootell, R. (2003). Stereopsis activates V3A and caudal intraparietal areas in macaques and humans. *Neuron*, 39, 555-568.

Correspondence. Doris Tsao, Institute for Brain Research and Center for Advanced Imaging, University of Bremen, Hochschulring 16a, D-28359 Bremen; doris(at)nmr.mgh.harvard.edu

Conflict Resolution in Macaques: Behavioral and fMRI Evidence

Olmedo Babé, M.O.[1,2] and Freiwald, W.A.[1,2]

[1]Brain Research Institute, Department of Theoretical Neurobiology, University of Bremen, [2]Center for Advanced Imaging (CAI) – Bremen

Introduction. Conflict or interference resolution is a cognitive control mechanism, whose neural mechanisms have been widely researched in the human brain. Cognitive control refers to a set of executive functions which serve to configure cognitive control for task performance, especially in challenging and non-standard conditions. It has been proposed that conflicts or interferences in information processing need to be monitored in order to allow for subsequent adjustments of cognitive control resources [1]. Tasks have been devised to generate different kinds of interference. In the classical Stroop task, subjects are asked to name the font color of a written word. When the color of the letters does not match the meaning of the word (for example, "green" written in blue letters), responses slow down and error rates increase significantly [2]. These effects are attributed to a conflict between an over-learned stimulus-response association (reading) and another stimulus-response association demanded by the task (color naming). The Simon effect describes the occurrence of a conflict between the spatial position of the stimulus and the required response, for example, when a stimulus which requires a response to the right is placed on the left [3]. In the Eriksen flanker task, a conflict is produced by distracter stimuli in close spatial proximity to a central target stimulus, other stimuli with incongruent information [4]. Conflict conditions in these three tasks are reflected in increases of reaction times (RTs) and error rates. We have adapted these tasks for use in macaque monkeys. Our goals were first to establish that these paradigms induce conflict conditions and, second, by imaging the brains of macaque monkeys which perform conflict-resolution tasks to identify areas more active during conflict conditions than non-conflict conditions. Using both tasks and imaging technologies as in humans aids in comparing the underlying neural mechanisms more directly and in avoiding interpretative difficulties which have arisen in the past [5].

Methods. We over-trained (~5 months per task) two monkeys (macaca mulatta) on stimulus-response association tasks defined in two feature domains. In the motion task, monkeys had to indicate the motion direction of a foveally presented random dot surface (RDSs) with a saccade in the corresponding direction (left or right) or maintain fixation in the absence of a coherent motion signal. Subsequently, monkeys were trained on a color task, which required them to saccade to the left or right or not to generate a saccade depending on the color of a centrally presented surface. Once monkeys solved these tasks reliably (performance levels above 95%), they were exposed to colored RDSs and had to perform the color discrimination task as before, while ignoring motion. We will refer to this task as the Stroop task (fig. 1). A task condition is said to be congruent when color and motion indicate the same direction of saccade movement, incongruent when color and motion are associated with opposite saccade directions, and neutral when motion is incoherent. In a variant of the task, which we will refer to as the Simon task, the surface was placed at an eccentric position, to the upper right or left of the fixation spot. In the Flanker task the colored RDS was surrounded by a colored random dot ring.

Figure 1. Schematic of colored RDS (motion direction indicated by arrow) with central fixation spot, two saccade targets (top) and sequence of a trial (bottom).
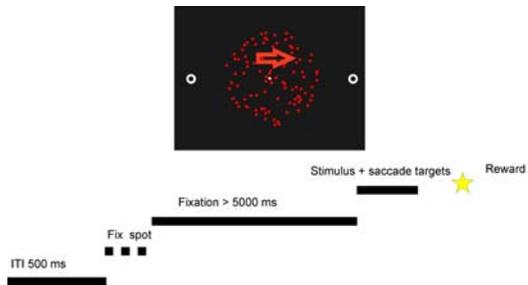
Both monkeys (D and L) were scanned inside a horizontal bore 3T head scanner (Allegra; Siemens, Erlangen, Germany), using an EPI sequence. Functional time series consisted of gradient-echoplanar whole-brain images; TR: 1.5s; TE: 30ms, 1.56 x 1.56 x 2mm voxels (24 horizontal slices). For each subject, a high-resolution anatomical image (magnetization prepared rapid acquisition gradient echo) was acquired (0.5 x 0.5 x 0.5 mm voxels).

Results. Behavioral results show that both monkeys experienced conflict in all three task conditions. Reaction times and error rates in the Stroop task are shown in table 1.

Task Condition	Neutral	Incongruent	Congruent
Monkey D	354ms / 3%	351ms / 10%	326ms / 1%
Monkey L	402ms / 4%	420ms / 29%	375ms / 2%

Table 1. Behavioral data.

Differences in both behavioral measures were significantly different for the incongruent and congruent conditions (p=0.001, Tukey's B, see [6] for details). The same pattern of results was found in the Simon and Flanker task as well: reaction times in congruent conditions were much faster than in incongruent ones, and error rates were higher in incongruent than in congruent conditions. All pair-wise differences were highly significant at p=0.001. In addition to this basic pattern, other significant task- and monkey-specific behavioral differences were observed. E.g., monkey D responded more slowly in the neutral Stroop condition than in the congruent Stroop condition, and responded faster in the flanker condition when the ring was of the identical color as the central RDS (super-congruent condition) compared to when they were of different, but congruent colors. All these behavioral differences occurred inside and outside the scanner. We found conflict-dependent differences of BOLD activation in dorso-medial areas 9 and 10, caudate nucleus and dysgranular insula (fig. 2), but not in the anterior cingulate cortex.
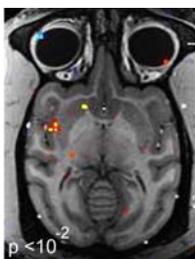
Figure 2. Activation map (51 runs, contrast incongruent vs. super-congruent, flanker task) and corresponding time courses of four behavioral conditions from insular "hot-spot".

Discussion. Macaque monkeys experience conflict in three different tasks. This is reflected in increases in response delay and error rates. "Neutral" Stroop-like conditions with random motion seem to evoke a mild form of conflict, because the lack of a motion signal had been associated with a no-go response during training. Using functional MRI inside the scanner while

monkeys are performing the task has identified three regions to be more active during conflict than no-conflict conditions. These regions have also been found in earlier human studies. However, we have, to our surprise, not found conflict-related activation of the anterior cingulated region, which has been suggested as the main cortical structure to monitor conflict [1]. Imaging results cannot easily differentiate between conflict monitoring and conflict resolution mechanisms. But electrophysiological recordings have the temporal resolution necessary to differentiate between these two options. These recordings shall be performed in a follow-up study in the areas identified here.

[1]   Carter, C.S., Braver, T.S., Barch, D.M., Botvinick, M., Noll, D., & Cohen, J.D. (1998). Anterior cingulate cortex, error detection, and the online monitoring of performance. *Science,* 280, 747-749.

[2]   Stroop, J. (1935) Studies of interference in serial verbal reactions. *Journal of Experimental Psychology*, 18, 643-662.

[3]   Simon, J.R. & Small A. M. (1969) Processing auditory information: interference from an irrelevant cue. *Journal of Applied Psychology*, 53, 433-435.

[4]   Eriksen, B.A. & Eriksen, C.W. (1974). Effects of noise letters upon the identification of a target letter in a nonsearch task. *Perception & Psychophysics* 16, 143-149.

[5]   Ito, S., Stuphorn, V., Brown, J.W., & Schall, .D. (2003). Performance monitoring by the anterior cingulate cortex during saccade countermanding. *Science,* 302, 120-122.

[6]   Olmedo-Babe, M., Küstermann, E., Erhard, P., & Freiwald, W.A. (2006) Stroop-like interference in macaque monkeys: behavioral and fMRI evidence. *Soc.Neurosci.Abstr.,* 32 [63.5].

Correspondence. Winrich Freiwald, Institute for Brain Research and Center for Advanced Imaging, University of Bremen, Hochschulring 16a, D-28359 Bremen; winrich.freiwald(at)googlemail.com

IV. Functional MRI in Visual Psychophysics

Functional MRI in Visual Psychophysics

Fahle, M.

Department of Human-Neurobiology, University of Bremen and Center for Advanced Imaging (CAI) - Bremen

‚Psychophysics' – or "Psychophysik" as it was called by it's inventors Weber and Fechner – quantifies defined parameters of subjective sensations (that is, parameters stemming from the realm of 'psyche') by means of objective, quantitative measures as used in physics. Hence when studying human perception, psychophysics uses a so-called black-box approach that does not have to consider what happens inside this box called the human brain.

This definition of psychophysics immediately clarifies why psychophysics and functional Magnetic Resonance Imaging (fMRI) fit so well together. FMRI indeed opens up a new way to quantify subjective sensations that is more brain related than psychophysics, thus perfectly complementing the black box approach used by psychophysics.

Before the advent of fMRI, it was possible to measure detection and discrimination thresholds of human subjects, by expressing them in terms of units defined by physics. Hence, psychophysicists were able to precisely measure the input-output relations for different types of stimuli in human subjects - and some animals - but without much hope of disentangling the neuronal mechanisms underlying these input-output relations. Sum-potential recordings based on the electro-encephalogram (EEG) were able to give some hints regarding the location and especially regarding the time course of brain activation evoked by the presentation of a given stimulus. But the spatial resolution even of multi-channel EEG recordings is quite poor.

FMRI now allows to quantify sensations via the strength of cortical blood flow (as an indication of neuronal activity) and, even more importantly, to correlate subjective sensations with networks of brain activations.

The complementary nature of behavioral investigations by means of psychophysical methods on one side and brain imaging by fMRI on the other

side is especially obvious in psychophysical studies of patients after cerebral infarctions. These studies are able to exactly measure - by means of psychophysical tests - the functional deficits resulting from a defect of cortical tissue. The results are complemented by determining the exact localization of the cortical lesion(s) through anatomical images obtained by MRI. The correlation of functional symptoms and structural deficits often leads to a hypothesis linking a given cortical area with a defined perceptual task.

The hypotheses gained from studying patients can subsequently lead to fMRI experiments. The underlying logic is that a functional loss associated with a circumscribed cortical defect indicates that the cortical area destroyed was important for achieving the perceptual task tested. Hence, this area should be quite active when a healthy subject performs the task that was found defective in the patient. By means of fMRI, this hypothesis can be put to the test: Is the cortical area whose defect produces deficits in a given perceptual task indeed selectively activated in normal subjects aiming to solve the same task? Often, this is indeed the case, while the failure of finding the cortical activations expected demonstrates that caution is required in interpreting both types of results.

In the context of this reader, therefore, patient data are not yet included. Instead, three contributions outline different ways how to combine psychophysical and fMRI investigations. The first contribution, by Högl, Trenner and Fahle, compares cortical activations in an fMRI study during three types of video games: a racing, a puzzle, and an arcade game. All three games produce exceedingly pronounced and widespread activations, demonstrating the strong involvement of subjects in these types of activity. The differences in the distribution of activity between the games were smaller than the authors had expected, given the widely differing requirements of the games, but were generally in line with expectations regarding which areas were activated during which of the individual games.

Spang, Fahle and Morgan were able to produce stereoscopic depth without binocular disparities, based on interocular time delays, as in the Pulfrich stereo phenomenon. A stimulus apparently rotating in depth produces highly significant activations in some early cortical areas such as V3A and the intra-parietal sulcus, but only if attention is attributed to the depth feature. Obviously, attention exerts an important influence on the strength of activities in fMRI, especially for near threshold features.

By presenting random-dot stimuli at near threshold contrast, Weerda, Thiel and Greenlee were able to compare the strength of activations in fMRI with the strength of subjective sensations as expressed by the correctness of the response of the subjects. Surprisingly, they find that already in the primary visual cortex, V1, weaker stimuli, but that were experienced as stronger ('false alarms') evoked stronger responses than physically stronger stimuli that were experienced as weak, and hence missed. This is another indication, as in the preceding contribution, that activations in the fMRI are not completely determined by bottom-up stimulus features but moreover depend on top-down influences such as attention and on variations in susceptibility over time.

Together, the three contributions to this reader mirror some of the exciting possibilities inherent in the combination of psychophysical methods with fMRI.

Correspondence. Manfred Fahle, Bremen University, Dept. of Human Neurobiology, Argonnenstr. 3, D – 28211 Bremen, Germany; mfahle(at)uni-bremen.de

FMRI Correlates of Video Game Playing

Högl, D.[1], Trenner D.[1] and Fahle M.[1,2]

[1]Department of Human-Neurobiology, University of Bremen, [2]Center for Advanced Imaging (CAI) - Bremen

Introduction. Most previous imaging studies employed rather simple visual stimuli, varying just a few specifically defined features. Our first aim was to transcend these impoverished experimental conditions and to establish what happens – and which cortical areas are activated – during a complex visual behavior like video game playing when many features have to be processed simultaneously, and subjects actively interact. The second aim was to examine whether video games of different genres yield similar activation patterns, and which video games evoke the strongest BOLD responses. Our subjects played three different video games while brain activity was recorded using functional magnetic resonance imaging (fMRI).

Methods. Six healthy subjects (aged between 22 and 30, all right-handed, 3 women) played a racing game (*Re-Volt*™), a puzzle game (*Tetris*) as well as an arcade game (NeverNoid). In a blocked design, subjects were presented with a resting or game condition in 12 alternating blocks. They performed three runs of approximately 10 min each. One run consisted of 12 game/resting epochs of approximately 50 sec duration. During the game condition subjects could move their eyes freely. The resting condition provided no visual, auditory or sensomotor stimulation. Subjects were asked to close their eyes during resting condition, indicated by the absence of sound. Images were acquired with a 3-T Magnetom Allegra® System (Siemens, Erlangen / Germany) using a $T2^*$-weighted gradient EPI sequence (TR=2510ms, TE=30 msec, field of view = 192×192 mm, matrix = 64×64 mm, voxel size = $3 \times 3 \times 2.7$ mm) consisting of 38 slices through the entire brain and oriented at -23° to the T-C plane.

Results. We obtained an exceedingly high and also widespread BOLD response for all three video games. The results show similar activity patterns for the three video games with slight differences in BOLD responses (see fig. 1). Overall, we found a small lateralization favoring the right hemisphere. The activity in visual, auditory and sensomotor regions as well as the frontal

eye fields can be clearly identified from the contrast between the two conditions. Furthermore, some cortical areas showed activations related to the particular demands that the different games placed on the player. The BOLD response was even larger during the rest periods than during playing in medial and inferior parts of the temporal lobes, the inferior parietal lobules, as well as the orbital and rectal gyri.
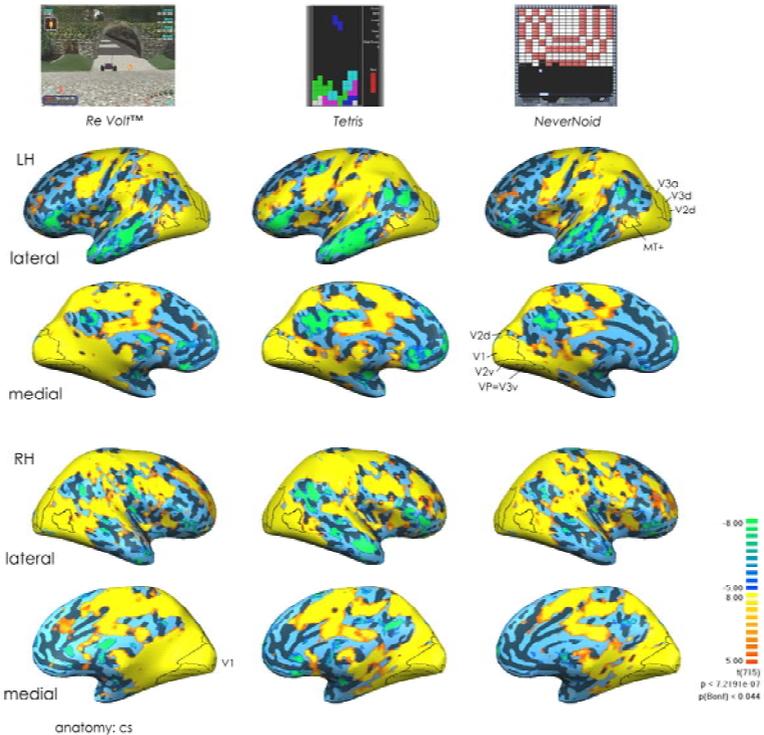
Figure 1. Results of the group study (n=6) for Re Volt™, Tetris and NeverNoid with retinotopic areas (V1, V2d, V2v, V3d, V3v=VP, V3a) and area MT+ indicated. Data are superimposed on inflated cortex representations of subject 'cs'. fMRI maps are thresholded at $p_{(Bonf)}<0.05$ (t=5.0).

Discussion. Our results agree with those of a study on human navigation within a three-dimensional, virtual-reality maze [1]. Navigation in this maze activated the medial occipital gyri, lateral and medial parietal regions,

posterior cingulate and parahippocampal gyri as well as the right hippocampus proper. The BOLD "negativity" in the inferior parietal cortex of all participants is possibly unrelated to the video games. Activation in this area may correspond to understanding numbers [2], performing calculations [3] and with inner speech. Negativity in the mid parietal precuneus was found in studies of episodic memory for either verbal or visual stimuli [4]. Groen et al. argue that medial parietal regions reflect functions of implicit (working) memory, recording data to keep track of an internal protocol of navigation [1]. The small lateralization to the right hemisphere may be attributable to the expectation that inter alia spatial abilities, which to a great extent were required for playing the video games, seem to be lateralized in the right hemisphere. Accordingly Nobre et al. [5] showed that the cortical regions involved in visuospatial attention displayed a right-hemispheric bias. In summary, this pilot-study with its exploratory nature and highly conservative structure demonstrates extremely strong BOLD activations over extended neuronal networks and some correlation to the exact game played.

[1]   Groen, G., Wunderlich, A.P., Spitzer, M., Tomczak, R., & Riepe M. (2000). Brain activation during human navigation: gender-different neural networks as substrate of performance. *Nature*, 3, 404-408.

[2]   Alonso, D. & Fuentes, L.J. (2001). Cerebral mechanisms of mathematical thinking. *Ref Neurol*, 33, 568-576.

[3]   Cohen, L., Dehaene, S., Chochon, F., Lehericy, S., & Naccache, L. (2000). Language and calculation within the parietal lobe: a combined cognitive, anatomical and fMRI study. *Neuropsychologia,* 38, 1426-1440.

[4]   Roland, P.E. & Gulyas, B. (1995). Visual memory, visual imagery, and visual recognition of large field patterns by the human brain: functional anatomy by positron emission tomography. *Cereb Cortex*, 5, 79-93.

[5]   Nobre, A.C., Sebestyen, G.N., Gitelman, D.R., Mesulam, M.M., Frackowiak R.S.J., & Frith, C.D. (1997). Functional localization of the system for visuospatial attention using positron emission tomography. *Brain*, 120, 515-533.

Correspondence. Daniela Högl, Department of Human-Neurobiology, University of Bremen, Argonnenstr. 3, D-28211 Bremen; dhoegl(at)uni-bremen.de

Stereoscopic Depth Produced by Temporal Delays Activates Early Visual Cortices

Spang, K.[1], Fahle, M.[1,2] and Morgan M.[2]

[1]Department of Human-Neurobiology, University of Bremen, [2]Henry Wellcome Centre for Applied Vision Research, City University, London

Introduction. Stereopsis has several possible functions such as distance estimation and breaking of camouflage. Different anatomical circuits may be involved in these distinct functions. Binocular disparities activate areas V3, V3A and CIPS (monkeys) and in humans V3A, V7, V4D-topo and the caudal parietal disparity region (CPDR) [1]. A puzzling finding is that the basic contrast of near/far versus zero disparity does not preferentially activate area V5/MT in monkey, and only weakly in humans. This finding contrasts with the clear single-unit recording evidence that cells in MT/V5 are organized in "near" and "far" disparity-tuned columns [2]. In our fMRI study we used the generalised Pulfrich stereophenomenon, where motion and disparity are inextricably entwined as a possible stimulus to activate V5/MT.
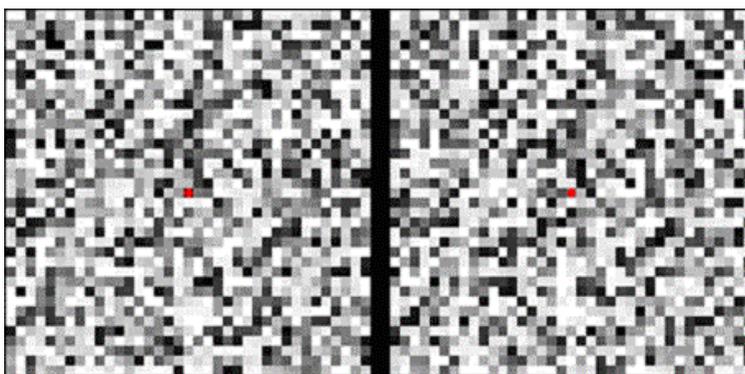
Figure 1. A pair of stimuli, presented to the two eyes.

Methods. Stimuli: the stimuli consisted of an array of 41 x 41 square elements with a side length of 15 arcmin. To induce a stereo effect, this array was shown pairwise to the observers, divided by a partition wall, so that their

left eye saw the left half of the image and their right eye saw the right half only. There were four stimulus conditions. In the first condition, the stimuli for both eyes were stationary (fig. 1). In the second condition, the luminances of all elements were modulated sinusoidally over time at 1 Hz, in phase in both eyes [3]. Subjectively the stimulus appears as a randomly flickering dynamic version of Figure 1. In the third condition, the phase of each individual element in the left eye lagged behind the corresponding element in the other eye ($0.1\pi = 18° = 50$ ms). This stimulus appears to rotate in depth around a vertical axis like a transparent rotating cylinder. We used the following protocol. Each run consisted of 19 epochs of about 37.5 seconds each (15 volumes). The 19 epochs comprised 3 epochs with the stationary stimulus (control condition), and 8 epochs with delays ("depth condition") as well as 8 epochs without delay ("flat condition"). We conducted two different versions of the basic experiment. In the first version ('attend to fixation') observers were merely asked to fixate the central dot, without special instructions to attend to the depth. In the second version ('attend to depth') observers were instructed to attend to the depth structure of the stimulus. Seven observers, aged between 22 and 30 years (3 males, 4 females) and two of the authors (KS 43, MF 54) participated in the experiments.

FMRI measurements and data analysis: scanning was performed on a 3 tesla head scanner (Siemens Allegra). Functional scans were collected using a gradient EPI sequence (T2*, TR/TE – 2510/30 ms, field of view 192x192 mm, 64x64 matrix, voxel size 3x3x2.7 mm, gap 0.3 mm, 38 slices). Sagittal anatomical scans were aquired before functional scanning (T1-weighted 3D MPRAGE). Analysis of functional and anatomical data was perfomed using Brain Voyager™ QX software, including preprocessing steps. For statistical analysis of group results we delineated regions of interest (ROI`s) in visual areas (V1, V2 , V3/VP, V3A, V4, MT/V5) for each subject taking into account the mapping procedures performed in separate experiments. We delineated two supplementary ROI's on the ascending branch of the intraparietal sulcus, naming the caudal part cIPS and the rostral part rIPS. Area cIPS includes the area adjacent to V3A and hence includes regions V7 and CPDR. Corresponding regions of all subjects were pooled for the group results. The time courses of all voxels of each region were averaged. The calculated beta values and contrasts between conditions of the GLM correspond to percent signal change.

Results. In the first version of the experiment ('attend to fixation'), subjects fixated a central fixation point in the middle of the screen without performing any perceptual task. The results differed widely between observers, probably due to differences in attention attributed to the stereoscopic feature by different observers. In spite of this strong inter-individual variation, there is some indication that the 'depth' condition evokes a stronger responses in higher visual areas, namely V3A, cIPS and rIPS and in MT, where 5 observers showed a strong (>0.2%) positive change and none showed more than a small (< 0.005%) negative change (not shown). Hence in the second run of the experiment ('attend to depth'), we instructed all observers to attend to the amount of depth present in each block. This procedure led to far less inter-observer variance than during the first experiment and to considerably stronger and more extensive BOLD signals in large parts of the occipital cortex including area MT/V5 as well as in the ventral and dorsal streams during the depth conditions as compared to the flat condition. The BOLD response was stronger in all areas for all but one observer, for whom the activation was negative in areas V1-V4 (not shown). For the group results the difference was far more pronounced and significant for all areas except V1 and V2, especially in areas V3A, cIPS, rIPS and MT.
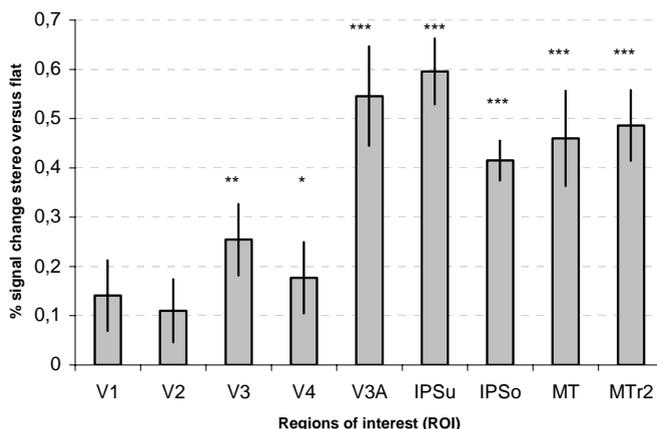
Figure 2. BOLD signal change for the group results (n=9) for visual areas: differential contrast of the stereo condition versus the "flat" condition of the experiment version 'attend to depth'. Error bars plot ± SEM. * show significant difference from zero; * p<0.05; ** p<0.01; *** p< 0.001.

Discussion. We tested the BOLD response to stimuli containing more than one plane ("depth") versus one depth plane ("flat"). Stimuli to both eyes were spatially identical, even lacking stereoscopic disparities, but a depth impression was based on temporal delays in the millisecond range between the presentations to both eyes. The absolute identitiy of spatial characteristics of the stimuli presented represents a very clean type of stimulus for testing the neuronal correlates of depth processing, without any cues for binocular rivalry and even without disparity. Here, the cortex must first compute apparent motion signals and subsequently compute depth from temporal delays between apparently corresponding motion vectors in both eyes. We demonstrate here that neuronal mechanisms in the human cortex underlying the perception of stereoscopic depth from temporal delays as in the Pulfrich phenomenon are located at similar cortical locations as those underlying the perception of binocular disparities. It is telling for the precision of the underlying neuronal mechanism that even minute temporal delays between the stimulation of the two eyes are sufficient to produce significant cortical activation, if observers attend to the depth cue. Our results moreover demonstrate that even homogenous stimuli without contours defined by stereoscopic depth as used in earlier studies specifically activate some cortical structures. This to say that these structures are more strongly activated in the presence of more than one depth level than by a single depth level, i.e. by a purely three dimensional difference in the stimuli.

[1]   Tsao, D.Y., Vanduffel, W., Sasaki, Y., Fize, D., Knutsen, T.A., Mandeville, J.B., Wald, L.L., Dale, A.M., Rosen, B.R., Van Essen, D.C., Livingstone, M.S., Orban, G.A., & Tootell, R.B.H. (2003). Stereopsis activates V3A and caudal intraparietal areas in macaques and humans. *Neuron*, 39, 555-568.

[2]   DeAngelis, G.C. & Newsome, W.T. (1999). Organization of disparity-selective neurons in macaque area MT. *J Neurosci,* 19, 1398-1415.

[3]   Morgan, M.J. & Fahle, M. (2000). Motion-stereo mechanisms sensitive to inter-ocular phase. *Vision Res*, 40, 1667-1675.

Correspondence. Karoline Spang, Department of Human-Neurobiology, University of Bremen, Argonnenstr. 3, D-28211 Bremen; kspang(at)uni-bremen.de

The Role of the Human Primary Visual Cortex in Visual Perception and Visual Search

Weerda, R.K.[1], Thiel, C.M.[1] and Greenlee, M.W.[2]

[1]Cognitive Neurobiology Group, Department of Biology and Environmental Sciences, Carl von Ossietzky University Oldenburg, [2]Department of Experimental Psychology, University of Regensburg

Introduction. It is a long debated question, whether the human primary visual cortex (V1) is part of the neuronal correlate of perceptual awareness [1, 2]. Related to this is the question if the activity of V1 neurons only represents the physical or also the perceived stimulus intensity per se. To test this, we employed a spatial uncertainty paradigm in order to dissociate sensory from perceptual processes. Subjects performed a luminance contrast discrimination task while the activity in V1 was measured with event-related fMRI.

Methods. During the luminance contrast discrimination task, four random block patterns were presented simultaneously for 200 ms against a uniform gray background on a 6° radius around the central fixation cross (fig. 1). The stimuli were identical in size and mean luminance, but one of them had a stronger luminance contrast than the other three. On each trial, the subjects' task was to fixate the fixation cross and determine via button press which one of the four stimuli was the intenser one (four-alternatives-forced-choice design). The three distractors had a contrast of 10%, whereas the contrast of the target stimulus was adjusted to the subjects' individual discrimination thresholds within this stimulus context, which were determined prior to the main experiment after extensive training on the task. For each subject, two target stimulus intensities were determined, yielding detection probabilities of 0.6 (ca. 12.5% contrast) and 0.8 (ca. 14.5% contrast), respectively. The intertrial-interval ranged from two to four seconds. While the subjects performed the task, the activity in V1 was measured with event-related fMRI (Siemens Magnetom Sonata®; 1.5 T; TR = 2 s; TE = 54 ms; α = 90°, 16 contiguous slices orthogonal to calcarine fissure; voxel size = 3 x 3 x 3 mm³). By means of a standard functional ROI definition, we were able to

analyze the retinotopic neuronal responses within V1 separately for each of the four stimulus locations and classify them a posteriori as hits, false alarms, misses and correct rejections (fig. 1). Since the BOLD-signal in V1 generally increases with increasing luminance contrast [3, 4], this enabled us to determine whether the activity in V1 ranks either

hits ≈ misses > false alarms ≈ correct rejections

or

hits ≈ false alarms > misses ≈ correct rejections.

The first outcome would be a support for the notion that activity in V1 only encodes the physical stimulus intensity, while the second would give evidence for a representation of the perceived stimulus intensity in V1. In the statistical analyses, which were performed with SPM2 [5], the measured signal during correct rejections served as baseline against which all other signals were compared.
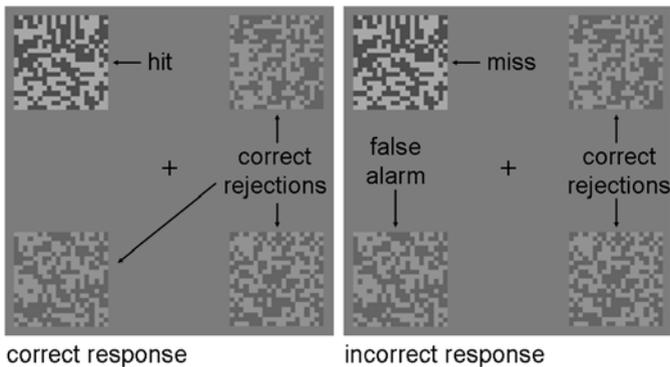
Figure 1. Stimuli and response categories for correct (left) and incorrect (right) responses.

Results. The preliminary results of six subjects (three female, mean age 24.2 yrs.) show that the mean event-related retinotopic BOLD-signal in V1 during false alarms is comparable to that one during hits and stronger than that during misses and correct rejections. Fig. 2a shows exemplary results of one subject. This effect is modulated by the luminance contrast intensity of the target stimulus. As can be seen in fig. 2b, the stronger the intensity of the

target stimulus, the stronger the retinotopic BOLD-signal during hits and false alarms and the weaker during misses, respectively.
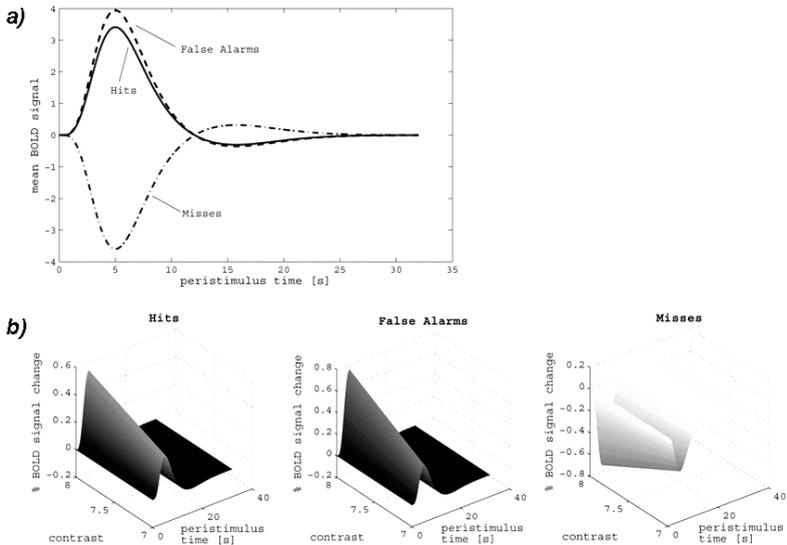
Figure 2. (a) Hemodynamic response functions fitted to the mean event-related responses during hits, false alarms and misses (correct rejections = baseline). (b) Parametric modulation of the retinotopic BOLD-signals during hits, false alarms and misses by the luminance contrast intensity of the target stimulus.

Discussion. These preliminary results show that the retinotopic activity in V1 strongly correlates with the perceived intensity of a stimulus irrespective of its physical intensity. This finding can not be explained by the effect of a simple attentional bias, since attention-related BOLD-signals in early visual areas have been shown to be correlated with performance accuracy [6], so that the average signal should be stronger during correct rejections than during false alarms, which is not the case. In an earlier study, Ress and Heeger [7] found similar results. However, since they used very small stimulus intensity differences that are near-threshold even under optimal viewing conditions, they were not able to dissociate sensory from perceptual processes. Our results point towards a representation of the perceived stimulus intensity per se in V1 and are a clear support for the notion that V1 participates in the neuronal calculations underlying perceptual awareness.

[1]   Tong, F. (2003). Primary visual cortex and visual awareness. *Nature Reviews Neuroscience*, 4, 219-229.

[2]   Rees, G., Kreiman, G., & Koch, C. (2002). Neural correlates of consciousness in humans. *Nature Reviews Neuroscience*, 3, 261-270.

[3]   Goodyear, B.G. & Menon, R.S. (1998). Effect of luminance contrast on BOLD fMRI response in human primary visual areas. *Journal of Neurophysiology*, 79, 2204-2207.

[4]   Wandell, B.A., Poirson, A.B., Newsome, W.T., Baseler, H.A., Boynton, G.M., Huk, A., Gandhi, S., & Sharpe, L.T. (1999). Color signals in human motion-selective cortex. *Neuron*, 24, 901-909.

[5]   http://www.fil.ion.ucl.ac.uk/spm/

[6]   Ress, D., Backus, B.T., & Heeger, D.J. (2000). Activity in primary visual cortex predicts performance in a visual detection task. *Nature Neuroscience*, 3, 940-945.

[7]   Ress, D. & Heeger, D.J. (2003). Neuronal correlates of perception in early visual cortex. *Nature Neuroscience*, 6, 414-420.

Correspondence. Riklef Weerda, Cognitive Neurobiology Group, Department of Biology and Environmental Sciences, Faculty V, Carl von Ossietzky University Oldenburg, D-26111 Oldenburg; r.weerda(at)uni-oldenburg.de

V.   Functional MRI in Auditory Processing

Functional MRI in Auditory Processing

Uppenkamp, S.

Medizinische Physik, Universität Oldenburg, Germany

There are several problems with functional MRI for auditory experiments. Switching of the gradient coils in the strong external magnetic field results in very loud noises due to mechanical vibrations caused by Lorentz forces acting on the coils. Precautions have to be introduced (1) to avoid damage to the subject's ears, and (2) to ensure that the recorded brain activity is caused by the actual stimulus, that has been played to the listeners, and not by the scanner noise itself. An interaction of the scanner noise with presented acoustic stimuli might have an effect on the recorded activation across auditory cortex. In recent years, big progress has been made in utilizing fMRI for auditory investigations. There are now MR compatible, high-fidelity headphones available that have been fitted into conventional ear defenders, giving an attenuation of external noise between 15 and 40 dB. Additional damping of scanner noise can be achieved by sound absorbing material around the subject's head and also inside the walls of the scanner bore. In addition to these passive measures, active noise cancellation (ANC) has been utilized to compensate for the scanner noise (e.g. [1]). By means of ANC, an additional reduction of the perceived scanner noise of 10-15 dB could be achieved so far.

The fact that the observed BOLD signal change in fMRI has a comparatively long latency of several seconds relative to stimulus onset can be turned into an advantage for auditory fMRI by introduction of the paradigm of "sparse temporal sampling". It allows for a separation of the activation due to scanner noise from the one due to the actual stimulus of interest. Instead of continuous data acquisition during epochs of stimulus and epochs of rest, stimulation and data acquisition are separated in time, with periods of several seconds of stimulus presentation without any scanning [2, 3]. A combination of sparse temporal sampling and cardiac gating, that is synchronization of the MR image acquisition with the cardiac cycle, has been shown to allow for imaging not only of the auditory cortex, but even brainstem and thalamic

structures with fMRI [4]. Still, temporal resolution of fMRI is far away from the one that can be achieved by electrophysiological methods, like EEG and MEG. In future studies, a combination of fMRI and EEG techniques will be the way to get a complete picture of auditory processing along the human auditory pathway.

The three reports in this section should give an idea of what fMRI is currently used for in auditory neuroscience. The activation studies by Uppenkamp and Ernst and Uppenkamp are aimed at finding physiological correlates of basic psychoacoustic performance, i.e., the perception of periodicity and the perception of sound intensity. The third study by Escera *et al.* is a good example for the complementary inferences that can be drawn from EEG and fMRI studies, when combining both methods utilizing the same task for the test persons.

[1]   Goldmann, A.M., Gossmann, W.E., & Friedlander, P.C. (1989). Reduction of sound levels with antinoise in MR imaging. *Radiology,* 173, 519-550.

[2]   Edmister, W.B., Talavage, T.M., Ledden, P.J., & Weisskoff, R.M. (1999). Improved auditory cortex imaging using clustered volume acquisitions. *Hum Brain Mapp,* 7, 89-97.

[3]   Hall, D.A., Haggard, M.P., Akeroyd, M.A., Palmer, A.R., Summerfield, A.Q., Elliott, M.R., Gurney, E.M., & Bowtel, R.W. (1999). "Sparse" temporal sampling in auditory fMRI. *Hum Brain Mapp*, 7, 213-223.

[4]   Griffiths, T.D., Uppenkamp, S., Johnsrude, I., Josephs, O., & Patterson, R.D. (2001). Encoding of the temporal regularity of sound in the human brainstem. *Nature Neurosci*, 4, 633-637.

Correspondence. stefan.uppenkamp(at)uni-oldenburg.de

Functional MR Imaging of Pitch Processing*

Uppenkamp, S.

Medizinische Physik, Universität Oldenburg, Germany

Introduction. Regular interval sounds and functional magnetic resonance imaging (fMRI) had previously been used to demonstrate a hierarchy of the processing of temporal pitch in human auditory cortex [1, 2]. With diotic stimulus presentation, most subjects had shown a bilateral, pitch-specific activation in the lateral edge of the transverse temporal gyrus (Heschl), outside primary auditory cortex. A specific activation in response to changes of the pitch, like in melodies, was located outside of Heschl's gyrus in adjacent cortical areas, mainly in superior temporal gyrus and sulcus. The melody-specific processing appeared to be asymmetric between hemispheres, with more activation in the right hemisphere for most listeners in that study. The anatomy of the auditory system is characterized by crossed pathways between the two ears and the two sides of the brain, with the main projections leading to the respective contralateral hemispheres. The recoding of temporal patterns begins as early as cochlear nucleus and is carried forward along the pathway through inferior colliculus and thalamus to cortex [2]. The symmetry between hemispheres of the cortical activation maps in response to diotic stimulation with fixed pitch indicates a symmetry in the neural structures for temporal processing. The extraction of temporal pitch appears to be reflected mainly by sensory coding in these structures. In contrast, the reported asymmetry between left and right hemispheres for the melody specific processing even in the case of diotic stimulation suggests a process that is higher up in the hierarchy, which not only reflects stimulus driven neural excitation but also the way we are listening to melodies. In the current study, fMRI was used to explore the influence of monaural stimulus presentation on the reported hemispheric asymmetry for the processing of sequences of notes with changing pitch.

Methods. Regular interval sounds (RIS) were used throughout the experiments. They are created by delaying a copy of random noise and adding it back to the original. The result has some of the hiss of the original

noise, but it also has a pitch corresponding to the inverse of the delay [4]. The pitch strength increases when the delay-and-add process is repeated. When the pitch is less then about 125 Hz and the stimuli are high-pass filtered at about 500 Hz, the RIS effectively excites all channels in the same way as random noise, with no resolved spectral peaks. The perception of RIS pitch is probably based on extracting time-intervals from the signal rather than spectral peaks. The different stimulus conditions in this experiment included melodies and sequences of fixed-pitch notes, with stimulation of both ears and monaural stimulation to the left and to the right ear only. Diotic presentation of random noise (no pitch) and silence were included as controls, giving a total of eight conditions. The sounds were played as sequences of 32 notes at a rate of four notes/sec. The pitch range for the melodies was 50 to 110 Hz. All stimuli were bandpass filtered between 500 Hz and 4 kHz and presented to the subjects at a level of 70 dB SPL via MR-compatible, dynamic headphones (MR confon, Magdeburg). Sparse temporal sampling was used to separate the scanner noise and the experimental sounds in time [4]. BOLD-contrast image volumes were acquired every 10 s, using a 1.5-T MRI scanner (Siemens SONATA) with gradient-echo-planar imaging. Twenty-one axial slices were acquired covering the whole of the temporal lobes. Eight normal-hearing listeners volunteered as subjects. None of them had a history of hearing or neurological disorders. A T1-weighted high-resolution anatomical image was also collected for each subject. Anatomical and functional data were analysed using SPM99. After preprocesing of the BOLD images a fixed-effects analysis was conducted across the whole group of eight subjects (total of 2048 scans), and also for each individual listener (256 scans), using the general linear model.

Results. Figure 1 A gives a summary of the results for the whole group of subjects during diotic stimulation with sequences of noise bursts, fixed pitch notes, and melodies. The activation maps were superimposed on the mean of the normalized anatomical images from all eight listeners. While the general activation in response to sound (blue) covers all of the surface of the temporal lobes including Heschl's gyrus and part of the temporal plane in both hemispheres, the pitch specific activation (in red) is largely restricted to the lateral edge of Heschl's gyrus bilaterally. This result is in good agreement with the previous study [1]. Melody specific activation (in green) appears somewhat distributed over several structures adjacent to Heschl,
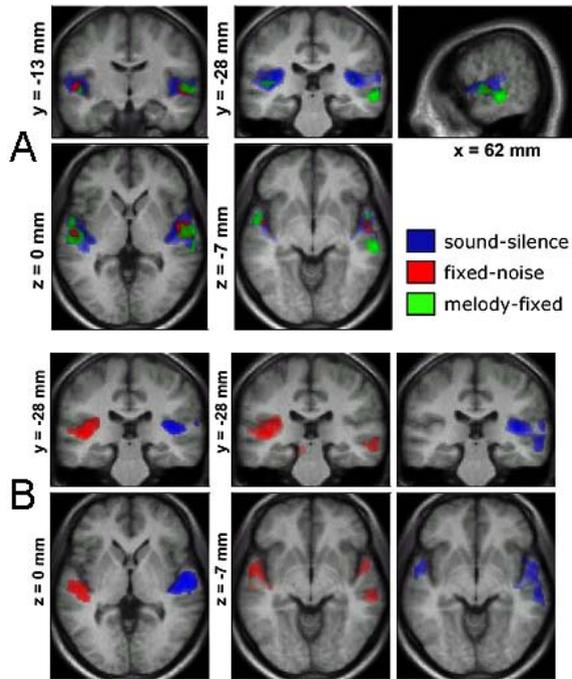
Figure 1: (A) Activation maps for a group of eight listeners for the main contrasts sound vs. silence, fixed pitch vs. noise, and melody vs. fixed pitch, diotic stimulus presentation. Threshold for significance was *t*=5.13 (*p*<0.05, corrected for multiple comparisons across the whole brain volume). (B) Activation maps for the group of eight listeners, for contrasts between sound to the left ear and sound to the right ear. Left column, red: sound right – sound left; blue: sound left – sound right. Middle column: melody right – fixed pitch left. Right column: melody left – fixed pitch right. Note the additional activity spots for the melody vs. fixed pitch comparisons, that appear to be independent of ear of entry.

including areas on the temporal plane next to the presumed pitch center (symmetric, see left of Figure 1), and areas in right superior temporal sulcus (STS) and superior temporal gyrus (STG) on both sides. Inspection of individual results revealed large differences between subjects for the melody specific activation. Four out of the eight listeners showed preferential activation in the right hemisphere, while two showed bilateral activation and two other had the main activation clusters for melodies in the left hemisphere. Figure 1 B shows the effect of monaural stimulus presentation.

A contrast between monaural sound in general and silence shows preferential activation of the respective contralateral hemispheres, as expected. A contrast between the conditions with sound either to the left or to the right ear results in complete lateralization of the respective activation maps (left part of figure). The middle and right columns of Figure 1 B show the contrasts between the conditions with melodies to one ear and sequences of fixed-pitch notes to the other. Activation around the surface of the temporal lobes, mainly in Heschl's gyrus (see coronal slices, top), is completely lateralized, as before, reflecting the crossed projections from the brainstem to primary auditory cortical areas. However, the melody specific areas outside Heschl's gyrus (the "green areas" from Fig. 1 A) are always activated in both hemispheres, irrespective of the ear of entry.

Discussion. The results for diotic stimulus presentation can be interpreted as further evidence for the hierarchical organization of temporal pitch processing. The findings for monaural stimulus presentation suggest that the regions specifically responsive to changes of the pitch reflect a higher processing stage, that integrates input from all pitch sensitive areas in the brain, irrespective of the particular ear of entry for the sound. The melody-specific activation seems to reflect the process of feature extraction from a highly processed, recoded sound representation. In conclusion, it can be interpreted as a representation of a cognitive process beyond a purely sensory coding of stimulus properties, probably involving attention and individual musical aptitude.

[1]   Patterson, R.D., Uppenkamp, S., Johnsrude, I.S., & Griffiths, T.D. (2002). *Neuron,* 36, 767-776.

[2]   Griffiths, T.D., Uppenkamp, S., Johnsrude, I.S.,. Josephs, O., & Patterson, R.D. (2002). *Nature Neurosci*, 4, 633-637.

[3]   Yost, W.A. (1996). *J Acoust Soc Am*, 100, 511-518.

[4]   Hall, D.A., Haggard, M.P., Akeroyd, M.A., Palmer, A.R., Summerfield, A.Q., Elliott, M.R., Gurney, E.M., & Bowtell, R.W. (1999). *Hum Brain Mapp,* 7, 213-223.

[5]   Uppenkamp, S. & Rupp, A. (2005). in *Fortschritte der Akustik - DAGA 2005*, Fastl, H. & Fruhmann, M. pp. 471-2. Dtsch. Gesell. f. Akustik e.V., Berlin.

Correspondence. stefan.uppenkamp(at)uni-oldenburg.de

FMRI Evidence for Spatial Dissociation of Changes of Overall Level and Signal-to-Noise Ratio in Auditory Cortex for Tones in Noise Maskers*

Ernst, S.M.A. and Uppenkamp, S.

Institut für Physik, Carl von Ossietzky University, Oldenburg, Germany

Introduction. The phenomenon of masking has been widely used in auditory research to study both peripheral and central auditory processing in human listeners. Masked thresholds are often expressed as a ratio of signal intensity and masker intensity indicating the importance of the sensation correlated to sound intensity. It is, however, still not completely understood how exactly the physical parameter sound intensity is transformed into the sensation which is usually referred to as loudness and the partial loudness/audibility of a signal in the presence of a masker. In the present study we used functional MRI to investigate the representation of changes of level and signal-to-noise ratio (S/N) in human auditory cortex.

Methods. Five-note melodies with four randomly chosen predefined frequencies from 440 to 587 Hz were presented in a masking noise with S/N from –18 dB to +24 dB in 6 dB-steps. The noise was white noise, bandpass filtered between 250 Hz and 4 kHz. The notes were sinusoids of 750 ms duration. The level of the masking noise was 60 dB HL. For small S/N (-18, -12, -6 dB) the overall level, i.e. the root-mean-square (RMS), of the sound is nearly constant, but the audibility of the tone varies with S/N. For S/N of 0 dB and above, the tone is always clearly audible, and the perceived change is mainly the increase of overall level. In addition to these eight stimulus conditions, noise only and silence were run as control conditions. Stimulus conditions changed randomly from trial to trial. All stimuli were presented diotically via MR-compatible, dynamic headphones mounted into ear defenders (MR confon, Magdeburg). Twelve listeners between 22 and 28 years of age (mean 23.9 a, standard deviation 1.7 a) were scanned (6 male, 6 female, all but one were right-handed). None of the volunteers had a history of hearing impairment or head injury. Functional MRI data were acquired using a Siemens Sonata 1.5 Tesla MRI system. In total, 320 echo-

planar imaging (EPI) volumes were acquired over four sessions (80 volumes per session). A T1-weighted high-resolution anatomical image was collected for each subject. For functional data, twenty-one axial slices (resolution 1.95 x 1.95 x 5 mm; echo time TE = 63 ms) were acquired covering most of the cortex, including the whole temporal lobes. Sparse imaging with clustered volume acquisition (acquisition time TA = 2.5 sec) was used. On each trial, there was a 5.2 s stimulus interval followed by a 2.5 s scanning interval, making a total repetition time of TR = 7.7 s. Anatomical and functional data were analyzed using SPM99. The preprocessing of the BOLD images included realignment of subject motion, normalization of individual scans to a standard EPI template, and smoothing with a Gaussian filter of 5 mm full width at half maximum. Fixed-effects analysis was conducted across the whole group of twelve subjects (3840 scans) and for each individual listener (320 scans, i.e. 32 repetitions for each stimulus condition), using the general linear model.

Results. The aim of the present study was to identify brain regions which are sensitive to changes in the signal-to-noise ratio (S/N) for a sinusoid in a masking noise. The clear perceptual separation of changes of overall level and changes of the audibility of the sinusoids in noise is reflected by a spatial dissociation of the respective activation in auditory cortex.
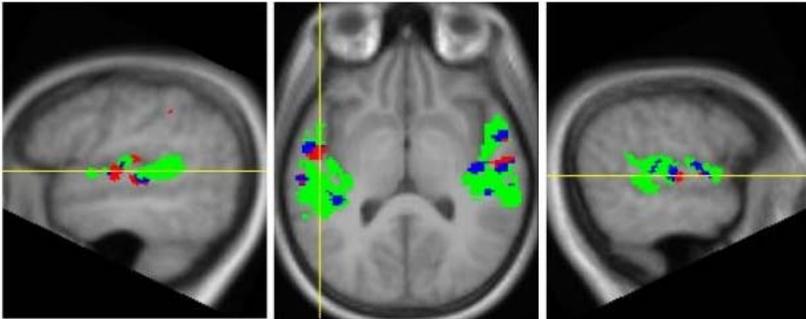
Figure 1. Group activation for three conditions, rendered onto the average structural image of the group. Green: regions with monotonic increase of activation (as measured by voxel intensity) for stimuli with increasing overall level. Red: regions with monotonic increase of activation (as measured by voxel intensity) for stimuli with increasing S/N and nearly constant overall level. Blue: regions with monotonic increase of activation over all S/N condition.

Brain regions sensitive to level changes (RMS-only voxels, green region in fig. 1) were mainly found in Planum temporale, while those regions sensitive to S/N changes (SNR-only voxels, red regions in fig. 1) were mainly located in the lateral edge of Gyrus temporalis transversus (Heschl). There is little overlap between the two activated regions. These data indicate a different coding mechanism for overall loudness and audibility of periodic signals.
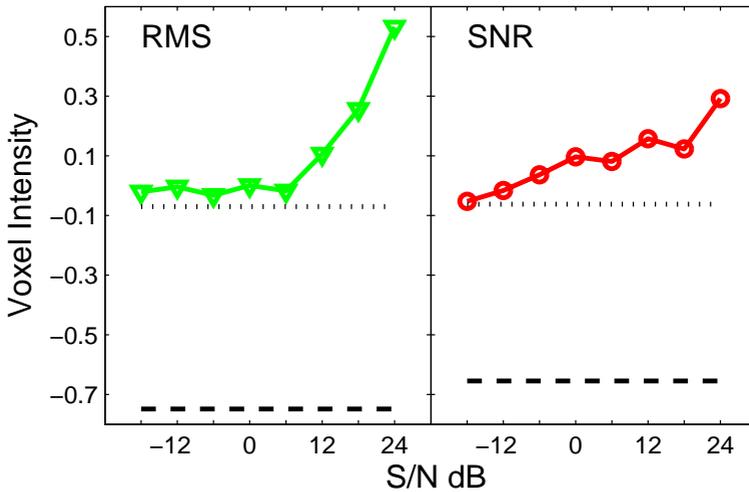
Figure 2. Voxel intensity as a function of S/N. The intensity functions for voxels that fulfill the conditions for RMS-only (green) and for SNR-only (red) are shown. The horizontal lines represent the voxel intensity in the control conditions (masker-alone: dotted; silence: dashed).

Discussion. There have been a number of studies investigating the level dependent representation of sounds in human cortex with fMRI. In agreement with the present study, they generally showed an increase in activation with increasing sound level (see fig. 2, left panel). However, only a few studies (e.g. [1, 2, 3]) investigated the topographic location of this increased activation. Supporting the present study, they reported a parametric change of activation with sound level in primary auditory areas (Heschl's gyrus) and also non-primary areas (e.g. planum temporale). Our findings in this study are in good agreement with the MEG study by Gutschalk et al. [4], if we assume that an increase in audibility is closely related to increasing

pitch strength. In that study, a separation of level and pitch representation could be demonstrated by describing these aspects in the sustained field by two spatially separate equivalent dipole sources in each hemisphere. One dipole in lateral Heschl's gyrus was particularly sensitive to changes in pitch, while the other one in Planum temporale, just posterior to the first, was particularly sensitive to changes in sound level.

[1]   Brechmann, A., Baumgart, F., & Scheich, H. (2002). Sound-level-dependent representation of frequency modulations in human auditory cortex: a low-noise fMRI study. *J Neurophysiol,* 87, 423-433.

[2]   Sigalovsky, I.S. & Melcher, J.R. (2006). Effects of sound level on fMRI activation in human brainstem, thalamic and cortical centers. *Hear Res*, 215, 67-76.

[3]   Hart, H.C., Palmer, A.R., & Hall, D.A (2002). Heschl's gyrus is more sensitive to tone level than non-primary auditory cortex. *Hear. Res*, 171, 177–190.

[4]   Gutschalk, A., Patterson, R.D., Rupp, A., Uppenkamp, S., & Scherg, M. (2002). Sustained magnetic fields reveal separate sites for sound level and temporal regularity in human auditory cortex. *NeuroImage,* 15, 207-216.

Correspondence. Stephan Ernst, Neurosensory Science, Institute for Physics, Carl von Ossietzky Universität, 26111 Oldenburg; stephan.ernst(at)mail.uni-oldenburg.de

Spatiotemporal Brain Imaging During Involuntary Attention Switching: A Combined fMRI-ERP-Study

Escera, C.[1,2], Domínguez-Borràs, J.[1], Schardt, D.[3], Fehr, T.[3,4], Erhard, P.[4] and Herrmann, M.[3,4]

[1]Cognitive Neuroscience Research Group, Department of Psychiatry and Clinical Psychobiology, Faculty of Psychology, University of Barcelona (Catalonia-Spain), [2]Hanse Wissenschaftskolleg – Delmenhorst, [3]Department of Neuropsychology and Behavioral Neurobiology, University of Bremen, [4]Center for Advanced Imaging (CAI) - Bremen

Introduction. A large body of evidence indicates that the unexpected occurrence of an auditory novel event engages attention involuntarily to lead to behavioral distraction, a phenomenon of an obvious evolutionary advantage [1, 2]. The concomitant recording of electric brain responses (ERPs) to the occurrence of these novel sounds discloses that involuntary attention to sound takes place in three successive processing stages, each associated to a particular neural event, namely the mismatch negativity (MMN), the novelty-P3, and the reorienting negativity (RON), respectively [3]. However, the anatomical underpinning of these neural events during involuntary attention is less understood. The present study aimed at identifying such neural networks by using fMRI, which is superior in spatial resolution to EEG.

Methods. Sixteen healthy, right-handed volunteers (four males, mean age 25.7 yrs., SD 6.8) with no history of neurologic, psychiatric or auditory/ visual disorders were examined. Subjects underwent two experimental sessions during which they performed the same task, one during EEG recording, the other during fMRI scanning. Half of the subjects started with the EEG session, whereas the other half had the scanning session first. Subjects were presented with auditory-visual stimulus pairs consisting of a 200 ms sound followed after 300 ms by a digit (2 to 9) lasting 200 ms on the screen. The sounds were either a standard tone (600 Hz; $p = 0.8$), a deviant tone (700 Hz; $p = 0.1$) or an environmental unique novel sound ($p = 0.1$). The order of the pairs was randomized, and the subjects were instructed to

press a response button to odd digits and another one to even digits, as fast and accurate as possible, and to ignore the auditory stimulation. EEG was recorded from 29 Ag/agCl electrodes placed on the scalp according to the extended 10-20 system. Imaging was performed on a 3-T Magnetom Allegra™ System (Siemens, Erlangen / Germany) using a T2*-weighted EPI sequence with a TR 2500 ms, and the following parameters: TE 30 ms, flip angle 90º, 64 x 64 matrix, FOV 192 x 192.

Results. Overall hit rate across sessions and trials was 91.4 percent, with no significant differences between trials or sessions. However, response times (RT) were shorter in the EEG session compared to the fMRI one ($F_{[1, 14]} = 6.19$; $p < 0.05$). As expected, distracting trials increased RT ($F_{[1.39, 19.44]} = 10.98$; $p < 0.01$), with the novel RT being longer than both the standard (LSD $p < 0.05$) and deviant ($p < 0.01$) RTs.

The ERPs elicited by the auditory-visual stimulus pairs showed the characteristic three-phasic waveform including MMN/N1, P3a/novelty-P3 and RON components for both deviant and novel trials, with respective peak latencies of about 145, 265 and 415 ms after auditory-stimulus onset.

As for fMRI, brain regions activated following deviant trials showed significantly greater responses versus standard trials in bilateral temporal cortical regions. These regions of the right temporal cortex included four clusters in the superior temporal gyrus (i) 55, -2, 0; ii) 63, -21, 7; iii) -53, 4, -7 – BA 38; iv) -48, -4, -10) as well as a maximum activation in the middle temporal gyrus (59, 7, -12 – BA 21). In overall, deviant-related activation was stronger in the right hemisphere. The activation pattern following novel trials encompassed multiple cortical and subcortical regions compared to standard trials. Similar to deviant trials, novel trials activated four clusters in the right superior temporal gyrus (i) 55, -21, -1; ii) 65, -29, 7 – BA 42; iii) 50, 5, -9; iv) -59, -42, 15) and left middle temporal gyrus (-55, 5, -15), although these areas were much smaller than the ones activated by deviant trials. In contrast to the activation to deviants, novel trial-related activation extended further to adjacent regions in the right inferior frontal gyrus (2 clusters: 44, 18, 10 – BA 45; 51, 22, 15), right postcentral gyrus (67, -19, 14 – BA 40) as well as subcortically to the right insular cortex (46, -6, -1). Another area showing activation following novel trials were four clusters in the left inferior frontal gyrus (i) -53, 30, 13; ii) -48, 25, 4; iii) -53, 31, 2; iv) -59, -42, 15), where the maximum activation in this second contrast of interest was found.
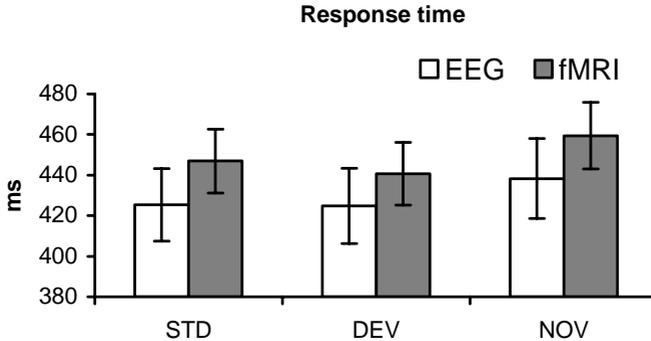
Response time

Figure 1. Response times obtained in the auditory-visual distraction task, in the two experimental settings (EEG, white bars, and fMRI, grey bars), and for the three types of trials (STD, standard; DEV, deviant; NOV, novel). Notice that subjects were slower in the scanner than in the EEG lab, and also in novel trials.

Discussion. The results obtained in the present experiments confirm previous results showing that the unexpected occurrence of a deviant or novel auditory event impoverish current task performance, as indicated by the enlargement of the corresponding RT compared to that of the standard trials. Moreover, these results extend previous findings by showing that these effects can also be obtained during fMRI scanning, even when the distracting sound occur along with the scanning noise produced by the magnet coils. It should be noted that the scanning noise did, however, affect overall task performance, as the subjects were slower in the fMRI session than in the EEG session. These two latter observations are in agreement with those of Novitski et al. [5], who reported that the magnetic noise affected (auditory) stimulus processing whilst preserving deviance-related processing, as revealed by ERPs.

The results obtained here also allow confirming the characteristic waveform structure of the distraction potential [3], composed of the MMN/N1, the P3a/Novelty-P3, and RON elicited to the distracting sounds.

The novel results of the present study are those disclosing that both deviant and novel auditory events activated a distributed and partially overlapping cerebral network. Specifically, both deviant tones and novel sound activated the bilateral superior and middle temporal gyrus, with the deviant tones

engaging more extensive regions, particularly over the right hemisphere. In turn, novel sounds engaged less extensive regions of the superior temporal
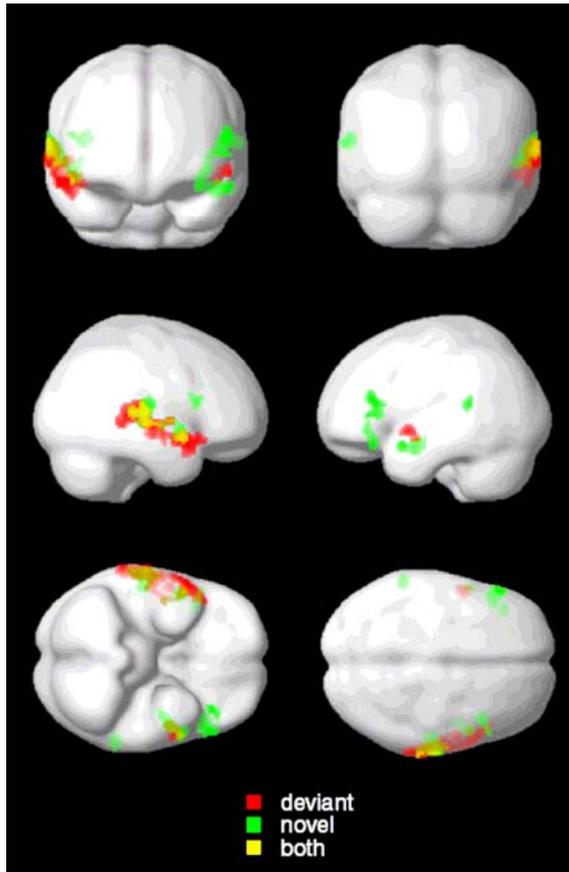
Figure 2. Superimposed maps of BOLD signal increases for both the deviant-standard and novel-standard contrasts rendered on a smooth standard reference brain. Regions in red were activated by deviant tones, regions in green by novel sounds, and regions in yellow by both. The figure shows the partially overlapping (over the right hemisphere) but still distinct neural networks activated by the two types of distracting events.

gyrus, but they did activated a more posterior region of this gyrus, possibly encompassing part of the Wernicke's area, and also the left inferior frontal gyrus. These later results may arisen from the novel sound involving the neural circuitry for semantic analysis, as these sounds were selected from a larger data base based on their familiarity and meaning [4].

[1]   Escera, C., Alho, K., Winkler, I., & Näätänen, R. (1998). Neural mechanisms of involuntary attention to acoustic novelty and change. *Journal of Cognitive Neuroscience, 10*, 590-604.

[2]   Escera, C., Alho, K., Schröger, E., & Winkler, I. (2000). Involuntary attention and distractibility as evaluated with event-related brain potentials. *Audiology & Neuro-Otology*, 5, 151-166.

[3]   Escera, C. & Corral, M.J. (2003). The distraction potential (DP), an electrophysiological tracer of involuntary attention control and its dysfunction. In I. Reinvang, M.W. Greenlee, & M. Herrmann (Eds.), *The Cognitive Neuroscience of Individual Differences* (pp. 63-76). Oldenburg: BIS-Verlag.

[4]   Escera, C., Yago, E., Corral, M.J., Corbera, S., & Nuñez, M.I. (2003). Attention capture by auditory significant stimuli: semantic analysis follows attention switching. *European Journal of Neuroscience*, 18, 2408-2412.

[5]   Novitski, N., Alho, K., Korzyukov, O., Carlson, S., Martinkauppi, S., Escera, C., Rinne, T., Aronen, H.J., & Näätänen, R. (2001). Effects of acoustic noise of functional magnetic resonance imaging on the processing of auditory stimuli and change as reflected by event-related brain potentials. *NeuroImage*, 14, 244-251.

Correspondence. Carles Escera, Department of Psychiatry and Clinical Psychobiology, University of Barcelona. P. Vall d'Hebron 171. 08035-Barcelona, Catalonia-Spain; cescera(at)ub.edu

VI. Neurochemical Modulation of Cognitive Functions - Pharmaco-fMRI

Neurochemical Modulation of Cognitive Functions - Pharmaco-fMRI

Thiel, C.M.

Institute of Biology and Environmental Sciences, Cognitive Neurobiology, Carl von Ossietzky University Oldenburg

The advent of neuroimaging methods such as functional magnetic resonance imaging (fMRI) and positron emission tomography (PET) has provided investigators with tools to study neural processes involved in cognitive functions in humans. Recent years have seen an increasing amount of studies which mapped higher cognitive functions to specific brain regions. These studies have had a great impact on our understanding of neuroanatomical correlates of cognitive functions in the living human brain. A particular cognitive process may however not only be linked to a certain network of brain areas, but also to a particular neurochemical system. Through the combination of neuroimaging with psychopharmacology (often called "pharmacological fMRI") it has become possible to investigate the neurochemistry of cognitive functions and to localize drug effects in the human brain [1].

Recent years have seen an increase in pharmacological neuroimaging studies [2]. Combining fMRI with psychopharmacology basically involves the administration of a drug or a respective placebo before volunteers undergo a cognitive task inside the scanner. A comparison between drug and placebo then reveals the drug's action on task-related brain activity. Note that the findings of such studies identify neurochemical modulation of brain activity that is induced by a specific task rather than excitation or inhibition of brain regions per se (for the latter approach see [3]). Pharmacological MRI studies are not only informative with regard to neurochemical modulation of cognitive functions in healthy brains but also for understanding neurotransmitter changes and treatment effects in neurological or psychiatric disease.

The present chapter presents several approaches on studying the neurochemistry of cognitive functions by means of neuroimaging methods. The papers selected focus on cholinergic modulation of visuospatial attention. Thiel presents two fMRI and one ERP study investigating the role of the cholinergic agonist nicotine on visuospatial attention in cued target detection tasks. These studies show that nicotine speeds reorienting of visuospatial attention and reduces neural activity in the posterior parietal cortex. Additional ERP and fMRI evidence further suggests that the effects of the drug are not on an early perceptual level but on later processing stages. Vossel and colleagues add clinical evidence to these findings in showing that patients with hemispatial neglect may benefit from nicotine in cued target detection tasks, however only if the parietal cortex is spared. The data presented by Giessing and colleagues focuses on the question whether fMRI is capable to add to the prediction of drug effects. They used multivariate analysis techniques to show that individual differences in brain activity under placebo can contribute to the prediction of the behavioral effects of nicotine. This new approach might contribute to a new clinical application of fMRI, i.e., the discovery of reliable markers of individual drug effects. Finally, the paper by Neber and colleagues combines fMRI and genetics, another recent development in neuroimaging research [4], in order to investigate the effects of a single nucleotide polymorphism of the nicotinic receptor gene CHRNA4 on neural correlates of visuospatial attention.

[1]   Coull, J.T. & Thiel, C.M. (2004). Functional Imaging of Cognitive Psychopharmacology. In: *Human Brain Function* (Frackowiak R, Friston KJ, Frith CD, Dolan RJ, Price CJ, Ashburner J, Penny W, Zeki S, eds), pp 303-327. Elsevier.

[2]   Honey, G. & Bullmore, E. (2004). Human pharmacological MRI. *Trends Pharmacol Sci*, 25, 366-374.

[3]   Salmeron, B.J. & Stein, E.A. (2002). Pharmacological applications of magnetic resonance imaging. *Psychopharmacol Bull*, 36, 102-129.

[4]   Hariri, A.R. & Weinberger, D.R. (2003). Imaging genomics. *Br Med Bull*, 65, 259-270.

Correspondence. christiane.thiel(at)uni-oldenburg.de

Cholinergic Modulation of Visuospatial Attention in the Human Brain

Thiel, C.M.

Institute of Biology and Environmental Sciences, Cognitive Neurobiology, Carl von Ossietzky University Oldenburg

Introduction. The neurochemical modulation of attention has been investigated both in animal and man. Several lines of evidence suggest that the neurotransmitter acetylcholine (ACh) is involved in selective attention, specifically in reorienting visuospatial attention (e.g. [1]). Cued target detection tasks have been often used to study selective visuospatial attention [2]). In these tasks visual cues either validly or invalidly indicate the location of an upcoming target. Misleading advance information delays target detection. The difference in reaction times to validly and invalidly cued stimuli is often referred to as 'validity effect' and regarded as an indicator for reorienting of attention. Behaviourally, it has been shown that nicotine reduces the validity effect [1]. The advent of functional neuroimaging techniques, such as fMRI, has enabled us to study cognitive processes in the living human brain. "Pharmacological fMRI" involves the manipulation of neurotransmitter systems in combination with functional neuroimaging and has led to important insights into the *neural correlates* of neurochemical modulation of attention [3]. Here I will present fMRI and EEG evidence investigating the effects of nicotine on visuospatial attention. Study 1 investigates whether the posterior parietal cortex, which is involved in visuospatial attention, is modulated by nicotine during attentional reorienting. Study 2 investigates whether the results obtained in study 1 are due to a broader focus of attention under nicotine. Study 3 investigates with ERPs the processing stage at which nicotine deploys its effects.

Methods. Study 1: In a within subjects design, 15 non-smoking volunteers were given either placebo or nicotine (NICORETTE® polacrilex gum 1 mg and 2 mg) prior to performing a cued target detection task inside the scanner (Siemens SONATA MRI scanner, 1.5T). Valid (80%) and invalid (20%)

trials were randomly intermixed. Reorienting-related brain activity was isolated by contrasting invalidly with validly cued trials and comparing these activations between placebo and nicotine.

Study 2: Fourteen non-smoking volunteers were given either placebo or nicotine (2 mg) prior to performing a cued target detection task. Attention was either validly (80%) or invalidly (20%) cued to the right or left visual field. In contrast to study 1, targets always appeared simultaneously with a similar non-target on the opposite side. We investigated reorienting-related brain activity and the effects of orienting attention to the right or left side of space under placebo and nicotine.

Study 3: Sixteen non-smoking volunteers were given either placebo or nicotine (2 mg). Event-related potentials were recorded while subjects were performing a cued target discrimination task with valid (80%) and invalid (20%) trials. EEG was recorded using a high impedance 64 channel Net Amps 200 system. We analyzed the effects of nicotine on early attention-related components of the ERP, P1 and N1.

Results and Discussion. Study 1: Nicotine showed a tendency to speed reaction times in invalidly cued trials as compared to validly cued trials. On the neural level, the effects of nicotine were mainly evident in the left intraparietal sulcus and precuneus and due to a reduction of neural activity in invalidly cued trials (see fig. 1A). We conclude, that nicotine enhances reorienting of attention in visuospatial tasks and that one behavioural correlate of speeded reaction times is reduced posterior parietal activity(see [4] for details).

Study 2: Nicotine reduced neural activity in the right posterior parietal cortex in invalid as compared to valid trials. We thus were able to replicate the findings obtained in study 1. Directing attention to either the right or left side of space increased neural activity in left and right extrastriate areas to a similar extent under placebo and nicotine. Our results thus speak against the hypothesis that nicotine broadens the focus of attention.

Study 3: Nicotine reduced the validity effect by decreasing reaction times to invalidly cued targets. The early attention-related components of the ERP, P1 and N1, were however not modulated by nicotine, suggesting that the effect does not occur at an early visual level (fig. 1B). Nicotine however enhanced the amplitude of the P3a component to invalidly cued targets, a
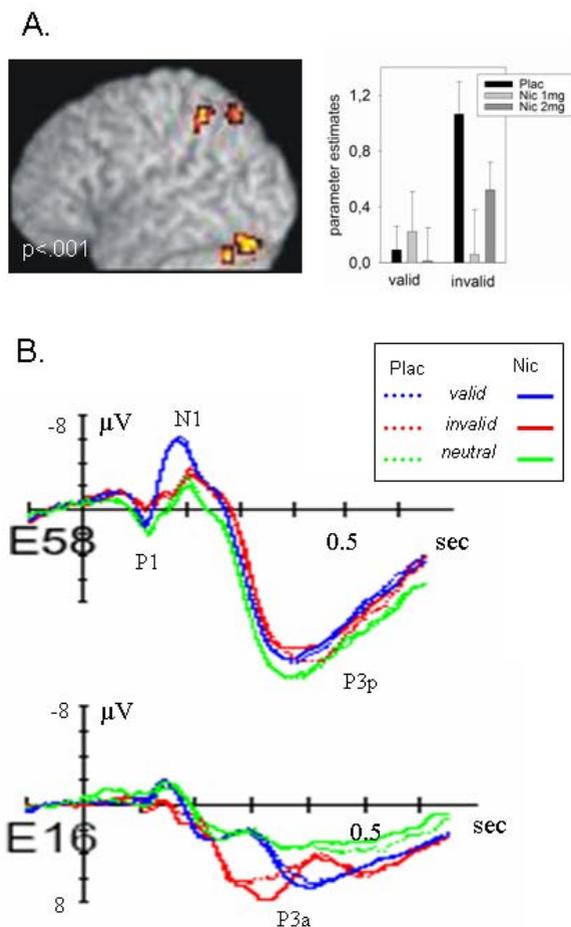
Figure 1. (A) Brain regions showing greater neural activity during reorienting of attention under placebo as compared to nicotine and neural activity in posterior parietal cortex as a function of drug and cue condition. (B) Grand mean averages at an occipital (top) and frontal electrode (bottom) as a function of drug and cue condition.

component often associated with involuntary shifting of attention. The results therefore indicate that the nicotine-induced reduction of the validity effect is not due to a modulation of sensory-perceptual processing of invalidly cued targets but rather to an alteration of evaluation and decision processes (see [5] for details).

[1] Witte, E.A., Davidson, M.C., & Marrocco, R.T. (1997). Effects of altering brain cholinergic activity on covert orienting of attention: comparison of monkey and human performance. *Psychopharmacology*, 132, 324-334.

[2] Posner, M.I. (1980). Orienting of attention. *Q J Exp Psychol [A]*, 32, 3-25.

[3] Thiel, C.M. (2003). Cholinergic modulation of learning and memory in the human brain as detected with functional neuroimaging. *Neurobiol Learn Mem,* 80, 234-244.

[4] Thiel, C.M., Zilles, K., & Fink, G.R. (2005). Nicotine modulates reorienting of visuospatial attention and neural activity in human parietal cortex. *Neuropsychopharm*, 30, 810-820.

[5] Meinke, A., Thiel, C.M., & Fink, G.R. (2006). Effects of nicotine on visuo-spatial selective attention as indexed by event-related potentials. *Neurosci,* 141, 201-212.

Correspondence. Christiane Thiel, Institute of Biology and Environmental Sciences, Cognitive Neurobiology, Carl von Ossietzky University Oldenburg, 26111 Oldenburg; christiane.thiel(at)uni-oldenburg.de

Influences of Nicotine on Neural Correlates of Visuospatial Attention: General Effects and Interindividual Differences

Gießing, C.[1], Fink, G.R.[2] and Thiel, C.M.[1]

[1]Institute of Biology and Environmental Sciences, Cognitive Neurobiology, Carl von Ossietzky University Oldenburg, [2]Institute of Neuroscience and Biophysics, Department of Medicine, Research Centre Jülich

Introduction. The studies presented deal with the question whether the cholinergic stimulant nicotine influences a fundamental cognitive requirement: The ability to detect behaviorally relevant visual events that occur outside the current focus of attention. Nicotine absorption in the form of tobacco consumption is a risk factor for several diseases like e.g., lung cancer or myocardial infarction. In contrast, recent studies suggest that nicotine in its pure form is also a valuable pharmaceutical agent and might improve cognitive and behavioral impairments of patients with Alzheimer's disease, or attention-deficit hyperactivity disorder [1]. However, the cognitive and neural mechanisms underlying these nicotine-induced cognitive enhancements are still unclear. The detection of visual events that occur outside the current focus of attention has been investigated in cued target detection tasks using validly and invalidly cued trials. To understand nicotine's neurobiological and cognitive effects three studies with "normal", healthy subjects have been conducted. Within the first study (study I) we investigated the neural network involved in reorienting visuospatial attention towards visual events that occur outside the current focus of attention. Two further studies were conducted to investigate the effects of nicotine on reorienting visuospatial attention. One study (study II) dealt with *common* effects of nicotine on this reorienting-related neural network activity. In contrast, the third study (study III) analyzed the *individual* differences in the behavioral effects of nicotine and tested whether individual behavioral nicotine effects are related to interindividual differences in neural network activity before drug exposure.

Results. Study I: In the first fMRI study we investigated which brain areas are generally involved in the detection of unattended visual events.

Therefore, we compared invalid and valid trials within a Posner paradigm in which the trials were presented intermingled in different blocks containing either 50%, 75% or 100% valid trials. Significantly different activations to invalid as compared to valid trials (i.e. reorienting-related activity) were found in the right and left intraparietal sulcus (see fig. 1A) and the right superior parietal cortex.

Study II: In study II we analyzed the modulatory effects of nicotine on the neural network involved in reorienting attention. Using a similar paradigm as above subjects were studied under placebo and nicotine (Nicorette® polacrilex gum 1 and 2 mg). Nicotine did not affect behavioral performance. However, within the 2 mg condition nicotine reduced the difference in the blood oxygenation level dependent signal between invalid and valid trials (i.e., the validity effect) by reducing the neural activity during invalid trials (see fig. 1A and B). Under placebo, reorienting-related neural activity in the right intraparietal cortex was dependent on the block context in that activity was stronger in the moderate cue reliability condition (blocks with 64% valid trials) than in the low cue reliability condition (blocks with 50% valid trials). The context dependent differences in parietal activity between invalid and valid trials were reduced by nicotine in the 2 mg nicotine condition.

Study III: While the previous studies analyzed the averaged nicotine effects over all subjects, study III investigated the individual differences in behavioral effects of nicotine. Several studies suggest that the behavioral effects of nicotine differ strongly between subjects (e.g. [2]). We therefore investigated whether individual differences in reorienting-related neural activity under placebo may be used to predict individual behavioral effects of nicotine. To increase our sensitivity and to account for the network structure of the brain we used a parietal least square (PLS) approach. The results of the PLS analysis suggest that neural data under placebo can be used to predict individual behavioral effects of nicotine. Neural activity in the left posterior cingulate cortex, extending to the precuneus and the right superior parietal cortex, the right dorsal medial prefrontal cortex and the left ventral medial prefrontal cortex significantly contributes to that prediction (see fig. 1C). The PLS analysis revealed that the inter-subject variability of neural activation within these brain areas is reliably related to interindividual behavioral nicotine effects.
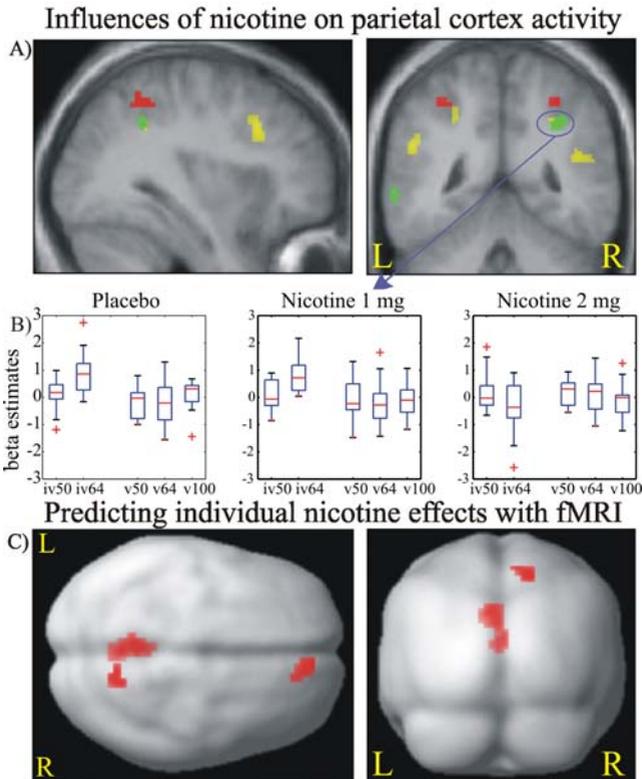
Figure 1. Nicotine and its neural effects on reorienting visuospatial attention. (A) Within the right and left intraparietal sulcus (IPS) study I and II consistently revealed significant differential activations in invalid as compared to valid trials (red: validity effect in study I; yellow: validity effect in study II; t-contrasts, p<0.001, uncorrected, only clusters bigger than 200 mm3 are presented). (A) and (B): Neural activation within the right IPS depends on block context / cue reliability condition and is reduced by 2 mg nicotine (fig. 2A, green color: validity by 2 mg nicotine interaction; fig. 2B: box and whisker plot of parameter estimates/activation strength within the right IPS; v50/v64/v100: valid trials in 50, 64 or 100 percent cue reliability condition, iv50/iv64: invalid trials in 50 or 64 percent cue reliability condition). (C) Brain regions which reliably contribute to the prediction of individual behavioral nicotine effects (study III).

Conclusion. Using fMRI in combination with a pharmacological challenge our studies revealed that nicotine reduces parietal cortex activity related to reorienting visuospatial attention. Furthermore, in study III we demonstrated a new approach predicting drug effects with fMRI. Our results show that differential neural activity in brain regions involved in focusing and reorienting visuospatial attention are correlated with individual behavioral effects of nicotine. In medical practice, functional MRI has been applied as a diagnostic tool, e.g., for pre-surgical planning in patients with epilepsy [3]. However, despite the successful use of fMRI in research, clinical applications of functional MRI are still limited. In the long run, our work (study III) might contribute to a new clinical application, i.e., the discovery of reliable markers of individual drug effects. A multivariate pattern analysis which accumulates information of different brain regions seems to be the most promising approach to develop these neural markers.

[1]   Levin, E.D., McClernon, F.J., & Rezvani, A.H. (2006). Nicotinic effects on cognitive function: behavioral characterization, pharmacological specification, and anatomic localization. *Psychopharmacology,* 184, 523-539.

[2]   Perkins, K.A. (1999). Baseline-dependency of nicotine effects: a review.. *Behavioural Pharmacology,* 10, 597-615.

[3]   Bookheimer, S.Y. (1996). Functional MRI applications in clinical epilepsy. *NeuroImage,* 4, 139-146.

Correspondence. Carsten Giessing, Institute of Biology and Environmental Sciences, Cognitive Neurobiology, Carl von Ossietzky University Oldenburg, 26111 Oldenburg; c.giessing(at)uni-oldenburg.de

Nicotinic Modulation of Visuospatial Attention in Healthy Volunteers and Patients with Chronic Spatial Neglect

Vossel, S.[1,2,3], Thiel, C.M.[3] and Fink, G.R.[1,2,4]

[1]Institute of Neuroscience & Biophysics – Medicine, Research Centre Jülich, [2]Brain Imaging Centre West, [3]Institute of Biology & Environmental Sciences, University of Oldenburg, [4]Department of Neurology, University Hospital Cologne

Introduction. The cholinergic neurotransmitter system has been proposed to be involved in attentional processes on the basis of animal as well as human studies [1]. Thus, it has been shown, for example, that the cholinergic agonist nicotine speeds up reaction times (RTs) when misleading spatial information is provided by invalid cues in the location-cueing paradigm. In particular, nicotinic stimulation decreases the difference in RTs between invalidly and validly cued targets (i.e., the 'validity effect') indicating facilitated attentional reorienting (e.g., [2, 3]). Pharmacological functional magnetic resonance imaging (fMRI) studies have revealed that a neural correlate of this effect is a reduction of activity in parietal cortex [4, 5]. It has been suggested that the effect of nicotine depends on baseline performance, i.e., on the size of the validity effect under placebo [4]. As the size of the validity effect varies as a function of cue validity (i.e., the ratio between valid and invalid trials), we tested this assumption in a location-cueing paradigm with two different cue types (90% and 60% cue validity) in healthy subjects in an fMRI study [6]. We hypothesized that the nicotinic reduction of the validity effect and parietal cortex activity would particularly be observed in the high cue validity condition. Spatial neglect is a neurological syndrome which is frequently observed after stroke, in particular after damage to the right hemisphere. Neglect patients are characterized by a reduced awareness and impaired responses to stimuli occurring in the side of space contralateral to the lesion [7]. It has been suggested that a lateralized deficit in attentional reorienting considerably contributes to the neglect syndrome: in the location-cueing paradigm many patients show disproportionate slow RTs when contralesional targets are preceded by invalid cues [8]. Consequently, neglect patients show a bigger validity effect

for contralesional than for ipsilesional targets indicating impaired reorienting towards contralesional events. Hence, we tested in a second study whether this reorienting deficit can be ameliorated by an acute cholinergic stimulation via nicotine.

Methods. In study 1 (fMRI study in healthy subjects) we investigated 24 participants in a double-blind placebo-controlled between-subject design. We used a location-cueing paradigm with valid and invalid trials employing two differently coloured cues (green, blue) with different cue validity (90%, 60%). Echoplanar images (EPI) with blood oxygen level-dependent contrast were obtained using a 1.5 T Sonata MRI system (Siemens). Data were analysed with Statistic Parametric Mapping software (SPM2) and are reported at $p<.001$ uncorrected.

In study 2 (behavioural study in neglect patients) we tested 8 patients with right-hemispheric lesions and chronic spatial neglect as indexed by standard neuropsychological tests. We employed a within-subject cross-over design and used a location-cueing paradigm with valid, invalid, neutral and 'no cue' trials. Lesion analyses were performed with SPM2 and MRIcro software.

In both studies the subjects received either a nicotine polacrilex gum (Nicorette®, 2mg, Pharmacia/Pfizer) or a taste-matched placebo gum (Pharmacia/Pfizer) prior to performing the experimental tasks.

Results. Study 1 confirmed that the validity effect is significantly bigger in a high (90%) than in a low (60%) cue validity condition. Moreover, cue validity modulated reorienting-related neural activity in a right-hemispheric fronto-parietal network (see figure 1). Importantly, nicotine reduced the validity effect in the high cue validity condition only. Brain areas contributing to this interaction effect of the cognitive and the pharmacological modulation were located in right fronto-parietal as well as left anterior cingulate cortex.

Study 2 showed that the effects of nicotine in patients with spatial neglect are highly variable in that a nicotinic reduction of the validity effect for contralesional targets was observed in four of the eight patients only. Lesion analyses suggested a dependency of the pharmacological effect on the site of brain injury: those patients who did not show a smaller validity effect for left targets under nicotine had extensive damage to parietal and temporo-parietal brain regions.
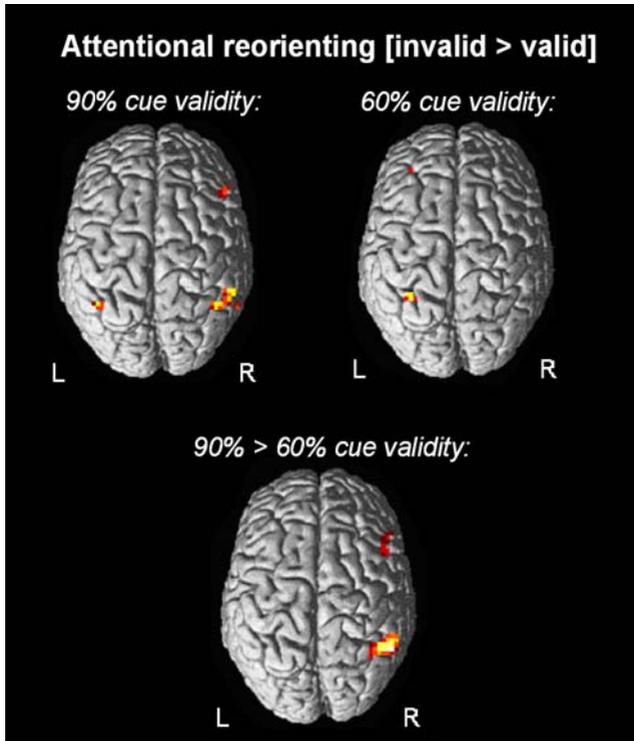
Figure 1. Brain areas related to attentional reorienting in the high (90%) and the low (60%) cue validity condition.

Discussion. The size of the validity effect depends on cue validity (i.e., on the amount of top-down information provided by the spatial cues) in healthy subjects. A neural correlate of lower validity effects (i.e., facilitated reorienting) is reduced neural activity in the right parietal and frontal cortex. Nicotine facilitates attentional reorienting in the context of high cue validity only. In the right superior parietal cortex and near the right temporo-parietal junction nicotine reduces reorienting-related neural activity particularly in invalid trials in the context of high cue validity.

In patients suffering from chronic neglect a reduction of the validity effect for contralesional targets under nicotine is observed in a subgroup of patients only. The data suggest a dependency of the nicotinic effect on the lesion site

of the patients. In particular, the nicotine-induced reduction of the validity effect depends on the integrity of those brain areas (or at least parts thereof) where nicotine has been shown to modulate neural activity related to attentional reorienting in healthy subjects in study 1 and prior fMRI studies.

[1]   Posner, M.I., & Fan J. (2004). Attention as an organ system. In: J.R. Pomerantz & M.C. Crair (Eds.). *Topics in Integrative Neuroscience: From Cells to Cognition*. Cambridge: Cambridge University Press.

[2]   Witte, E.A., Davidson, M.C., & Marrocco, R.T. (1997). Effects of altering brain cholinergic activity on covert orienting of attention: comparison of monkey and human performance. *Psychopharmacology*, 132, 324-334.

[3]   Murphy, F.C., & Klein, R.M. (1998). The effects of nicotine on spatial and non-spatial expectancies in a covert orienting task. *Neuropsychologia*, 36, 1103-1114.

[4]   Thiel, C.M., Zilles, K., & Fink, G.R. (2005). Nicotine modulates reorienting of visuospatial attention and neural activity in human parietal cortex. *Neuropsychopharmacology*, 30, 810-820.

[5]   Giessing, C., Thiel, C.M., Rösler, F., & Fink, G.R. (2006). The modulatory effects of nicotine on parietal cortex depend on cue reliability. *Neuroscience*, 137, 853-864.

[6]   Vossel, S., Thiel, C.M.,& Fink, G.R. (2006). Cue validity modulates the neural correlates of covert endogenous orienting of attention in parietal and frontal cortex. *NeuroImage*, 32, 1257-1264.

[7]   Parton, A., Malhotra, P., & Husain, M. (2004). Hemispatial neglect. *Journal of Neurology, Neurosurgery and Psychiatry*, 75, 13-21.

[8]   Posner, M.I., Walker, J.A., Friedrich, F.J., & Rafal, R.D. (1984). Effects of parietal injury on covert orienting of attention. *Journal of Neuroscience*, 4, 1863-1874.

Correspondence. Simone Vossel, Institute of Neuroscience & Biophysics – Medicine (INB-3), Research Centre Jülich, Leo-Brandt-Str. 5, D-52425 Jülich; s.vossel(at)fz-juelich.de

Neuronal Nicotinic Acetylcholine Receptor α4 Subunit Gene CHRNA4 and Visuospatial Attention: An fMRI Study

Neber, T., Giessing, C. and Thiel, C.M.

Institute of Biology and Environmental Sciences, Cognitive Neurobiology, Carl von Ossietzky University Oldenburg

Introduction. Prior evidence suggests that the cholinergic agonist nicotine reduces reaction times in invalid trials in cued target detection tasks and neural activity in the posterior parietal cortex [1, 2]. We have previously found individual differences in the behavioural effects of nicotine and in the neural networks needed for reorienting visuospatial attention after invalid cuing [2, 3]. Variation in genes controlling aspects of cholinergic neurotransmission and/or attentional reorienting may contribute to these individual differences. Several polymorphisms have been identified within exon 5 of the alpha4 subunit of the nicotinic ACh receptor gene CHRNA 4 [4]. Recently, a C to T substitution (bp 1545) in CHRNA4 has been related to reorienting visuospatial attention in cued target detection tasks [5]. The present study was performed to elucidate the role of genetic differences in the CHRNA4 gene on attentional reorienting and attention-related brain activity.

Methods. Subjects: Young, healthy right handed subjects were tested for a C1545T polymorphism on exon 5 of the CHRNA4 gene. Based on genotyping 16 homozygous subjects were recruited for the study. Three subjects were excluded from further analysis due to movement artefacts during scanning or brain anomaly leaving a sample of 7 subjects with TT CHRNA4 genotype and a sample of 6 subjects with CC CHRNA4 genotype.

Genotyping: Genomic material was obtained via buccal cell brush. Samples were analysed for the C1545T polymorphism in the CHRNA4 gene with polymerase chain reaction (PCR) and restriction fragment length polymorphism (RFLP) technique according to [4].

Scanning and fMRI data analysis: A visually cued target detection task with valid, neutral and invalid trials was used. Trials were arranged in blocks in which short noise burst were either present ("high arousal") or absent ("low

arousal"). Echoplanar images (EPI) with blood oxygen level-dependent contrast were obtained using a 1.5 T Magnetom MRI system (Siemens). Data were analyzed with the Statistical Parametric Mapping software SPM5 for task by genotype and task by genotype by arousal interactions and are reported at p<.001, uncorrected.
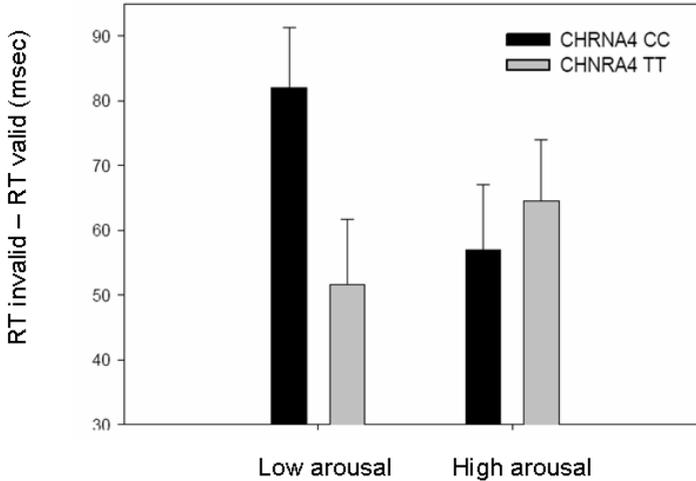
Figure 1. Validity effect (RT invalid - RT valid) as a function of genotype and arousal.

Results. Behavioral data: The repeated measures ANOVA revealed a significant main effect of validity ($F(1,11)=108.3$, $p<.001$) and a genotype x validity x arousal interaction ($F(1,11)=9.34$, $p<.05$). Fig. 1 illustrates the validity effect in both genotype groups as a function of arousal. Note the high validity effect in the CHRNA4 CC group under conditions of low arousal only. This suggests that difficulties in reorienting visuospatial attention in the CHRNA4 CC group are ameliorated by increasing arousal with noise bursts.

Imaging data: For both groups, increased neural activity was found for invalid as compared to valid trials in the right superior temporal gyrus, the right middle temporal gyrus und the right middle frontal gyrus. A significant

genotype x validity interaction was seen in the left inferior frontal gyrus (see fig. 2). There was no genotype x validity x arousal interaction.
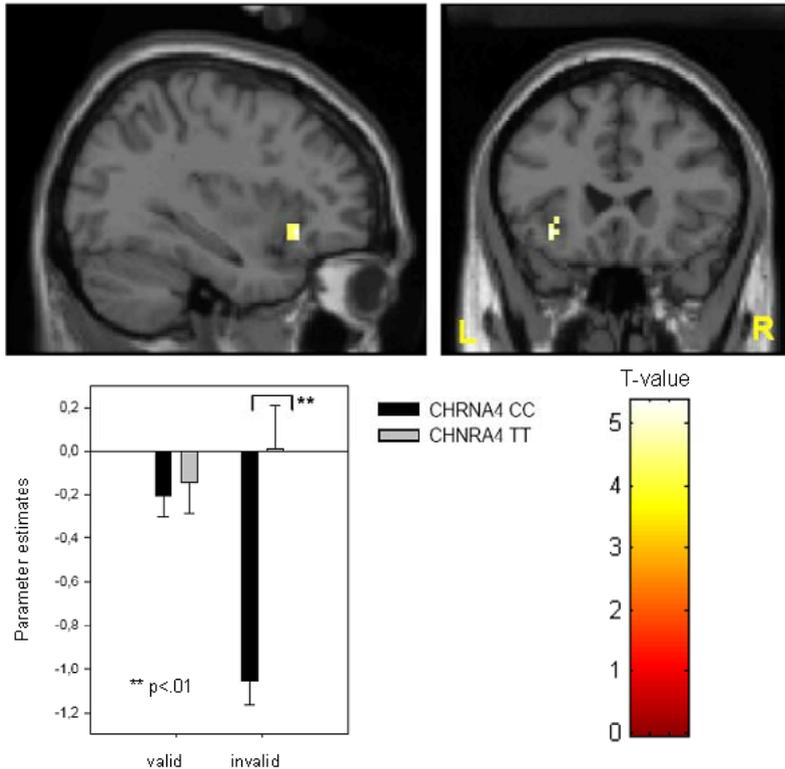
Figure 2. Genotype x Validity Interaction. Activations superimposed on an individual T1 image and plot of parameter estimates (mean and SEM) as a function of genotype and cue validity.

Discussion. Even though the data should be regarded as preliminary due to the small sample size, this is the first study to show that normal variation in a single gene coding for the nicotinic ACh receptor can contribute to individual differences in reorienting visuospatial attention and related brain activity.

[1]   Witte, E.A., Davidson, M.C., & Marrocco, R.T. (1997. Effects of altering brain cholinergic activity on covert orienting of attention: comparison of monkey and human performance. *Psychopharmacology,* 132, 324-334.

[2]   Thiel, C.M., Zilles, K., & Fink, G.R. (2005). Nicotine modulates reorienting of visuospatial attention and neural activity in human parietal cortex. *Neuropsychopharmacology*, 30, 810-820.

[3]   Giessing, C., Fink, G.R., Rösler, F., & Thiel, C.M. (2007, in press). fMRI data predict individual differences of behavioral effects of nicotine: A partial least square analysis. *J Cog Neurosci*.

[4]   Steinlein, O.K., Deckert, J., Nothen, M.M., Franke, P., Maier, W., Beckmann, H., & Propping, P. (1997) Neuronal nicotinic acetylcholine receptor alpha 4 subunit (CHRNA4) and panic disorder: an association study. *Am J Med Genet,* 74, 199-201.

[5]   Parasuraman, R., Greenwood, P.M., Kumar, R., & Fossella, J. (2005) Beyond heritability: neurotransmitter genes differentially modulate visuospatial attention and working memory. *Psychol Sci,* 16, 200-207.

Correspondence. Christiane Thiel, Institute of Biology and Environmental Sciences, Cognitive Neurobiology, Carl von Ossietzky University Oldenburg, 26111 Oldenburg; christiane.thiel(at)uni-oldenburg.de

VII. Executive Functions and Action Monitoring

Executive Functions and Action Monitoring

Herrmann, M.[1,2] and Kreiter, A.K.[2,3]

[1]Department of Neuropsychology and Behavioral Neurobiology, University of Bremen, [2]Center for Advanced Imaging (CAI) – Bremen, [3]Institute for Brain Research, University of Bremen

Cognitive control of human behavior has emerged as the central research topic of the combined Magdeburg-Bremen Center for Advanced Imaging (CAI) project. Cognitive control refers to the ability of humans to coordinate thoughts and actions with internal goals and concepts. Thus, the focus of our transdisciplinary and multi-methodological approach to cognitive control aimed at the identification of the neural mechanisms which transform (metacognitive) strategies into actions, which – vice versa – are controlled and evaluated by means of the executive system. Here, we present three studies closely related to the central CAI research topic, and an additional study that emerged from a cooperation between the CAI Bremen and the Cognition and Communication Research Center at Northumbria University (UK).

The investigations reported by Galashan and colleagues and Zinke and coworkers demonstrate preliminary results of a shape-tracking working memory (WM) task in humans and non-human primates. They introduce a delayed match-to-sample design based on morphing complex shapes that require continuous monitoring and updating of the WM content. Cognitive task load is modulated by systematic variation of the maintenance duration. The behavioral data clearly show that the task-related increase in cognitive load is mirrored by a significant decrease of the accuracy rate. In addition to a widespread activation pattern reflecting visuo-spatial WM performance, the maintenance and retrieval of complex figures also leads to a specific signal enhancement in bilateral area MT^+. This data indicates that activity of the area MT^+ – the human homologue of the well-studied monkey MT-MST region – not only reflects motion processing but also task-related WM demands.

To allow for direct comparison of the human fMRI data and the results from primate electrophysiology Zinke and colleagues trained macaque monkeys in order to perform a highly comparable task in fMRI experiments. Here they present first data that were collected during the accommodation period of an animal to the scanner environment. Applying independent component analysis they found spatial patterns of brain activations that reflect the dynamic change of brain networks involved in the different stages of the WM task. These results demonstrate the feasibility of highly demanding cognitive tasks with monkeys inside the scanner, that link and complement results from animal and human experiments.

The work by Wittfoth et al. summarize the part of the human data collected during the first period of the CAI project „Changes in brain activation patterns associated with top-down regulation of coherent motion perception". Interference resolution derived from two Simon tasks based on coherent motion perception results in distinct activation patterns depending on whether the conflict originated through stimulus location or motion direction. Detailed analysis of error-related activity in high- or low-conflict trials points to a task-related subdivision of the anterior cingulate cortex (ACC) and task-specific networks of conflict resolution.

Christophel and coworkers re-address the idea of an involvement of area MT^+ in human action monitoring. They were able to replicate the data from the Kanwisher lab at MIT showing that area MT^+ is also engaged in processing implied dynamic information derived from static pictures. Furthermore, the authors could demonstrate that it is indeed the functional relevance of implied motion processing rather than the objects with dynamic information per se.

Correspondence. Manfred Herrmann, Institute for Cognitive Neuroscience (ICN), University of Bremen, Grazerstr. 6, D-28359 Bremen; manfred.herrmann(at)uni-bremen.de; Andreas Kreiter, Institute for Brain, University of Bremen, Hochschulring 16a, D-28359 Bremen; kreiter(at)brain.uni-bremen.de

Neuronal Correlates of a Shape-Tracking Working Memory Task – Human Data

Galashan, D.[1,2], Zinke, W.[2,3], Schmuck, K.[1,2], Fehr, T.[1,2], Küstermann, E.[1,2], Kreiter, A.K.[2,3] and Herrmann, M.[1,2]

[1]Department of Neuropsychology and Behavioral Neurobiology, University of Bremen; [2]Center for Advanced Imaging (CAI) – Bremen; [3]Institute for Brain Research, University of Bremen

Introduction. Visuo-spatial working memory (WM) tasks involve a widespread network of brain areas including posterior parietal, superior and inferior frontal regions, premotor/supplementary motor regions, as well as inferior temporal regions [1]. Several frontal brain regions (mid-dorsolateral, mid-ventrolateral and dorsal anterior cingulate cortex) are recruited with increasing task complexity and cognitive demand [2]. Most visual WM tasks either use the N-back design, where subjects have to identify stimuli which are identical to the stimulus presented "N" trials before, or delayed match-to-sample design (DMTS), where subjects decide after a delay period whether the probe stimulus matches the previously presented sample stimulus. While the DMTS task primarily requires maintenance processes, the n-back task additionally involves monitoring and updating of the WM content. Cognitive load is mainly varied in WM tasks by manipulating either the number of items held in WM, or by the duration of the retention period. These manipulations lead to confounds of visual processing demands and accordingly maintenance length cognitive load. To disentangle the neural correlates of this WM effect we utilized a shape-tracking DMTS task requiring continuous matching-to-sample during the retention interval. Using complex and simple shapes allowed us to investigate differences in neural activation caused by increasing the cognitive load derived from four different durations of the maintenance period.

Methods. Nineteen healthy right-handed volunteers (10 female; range 20-30 yrs., mean age 24.79, SD 3.03) with no history of neurological and/or psychiatric disorders gave informed and written consent to participate in an fMRI experiment. Three female participants had to be excluded post-hoc

because of misunderstanding the instructions, severe head motion during scanning, or dozing off. We used 10 different curved complex shapes (hardly to be verbalized, see fig. 1) and one simple shape (circle) to generate 200 morphing sequences. Each sequence started with an encoding epoch (2.4 s) during which the target shape was presented. After this period the target stimulus began to continuously change its contours into the following shape (morph) over a 1.5 sec period. After a randomly assigned morphing period of 3, 6, 9 or 12 s the target shape re-appeared. Subjects had to indicate this re-appearance by pressing a button. During the intertrial interval lasting 2 s with a random jitter of ± 300 ms a smoothed fixation point was shown.

Figure 1. Stimulus material: targets 1 to 10: curved complex figures; target 11: circle (simple figure).

To identify area MT^+ in each subject a localizer stimulus (flow field vs. static field) was used in an additional scan. A 3T scanner (Siemens Magnetom Allegra®) was utilized to acquire $T2^*$-weighted functional images using a gradient EPI sequence. Statistical parametric maps were thresholded at $p<0.05$ using the false discovery rate approach (FDR) and with an extent threshold of 20 contiguous voxels.

Results. A repeated-measures two-way ANOVA with factors "stimulus complexity" (figure vs. circle) and "delay" (3s, 6s, 9s, 12s) showed that reaction times (RTs) in response to circles were significantly shorter than to shapes at each delay stage. An interaction "stimulus shape x delay" yielded decreasing RTs for circle trials with increasing delay period whereas no association was found for figure trials. Wilcoxon tests showed significantly higher error rates for figure compared to circle trials at 6s, 9s, and 12s delay periods. An increase in error rates for figure trials with increasing delay stage was significant in all but one comparison (6s vs. 9s delay), whereas no differences in accuracy were found for circle trials (see fig. 2). Contrasting the activation patterns of higher stimulus complexity (figure trials) with the simple shape (circle trials) combined over all delay stages resulted in an activation cluster spreading bilaterally from occipital gyri to middle and inferior temporal gyri on the one hand and to inferior and superior parietal

areas on the other hand (see fig. 3). Additional suprathreshold voxels were located bilateral in the inferior frontal gyrus (inferior FG) and in the right hemisphere middle, medial and inferior frontal gyri as well as in the dorsal anterior cingulate cortex (dorsal ACC).
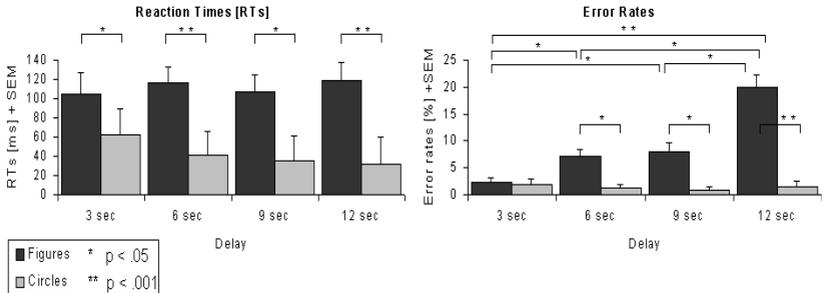
Figure 2. Reaction times and error rates for figure trials (dark bars) and circle trials (bright bars) for each delay period.

Area MT$^+$ (as functionally specified in each subject) showed significantly higher percent signal changes during the complex figure morph period compared to the low-complexity circle trials for each delay period.
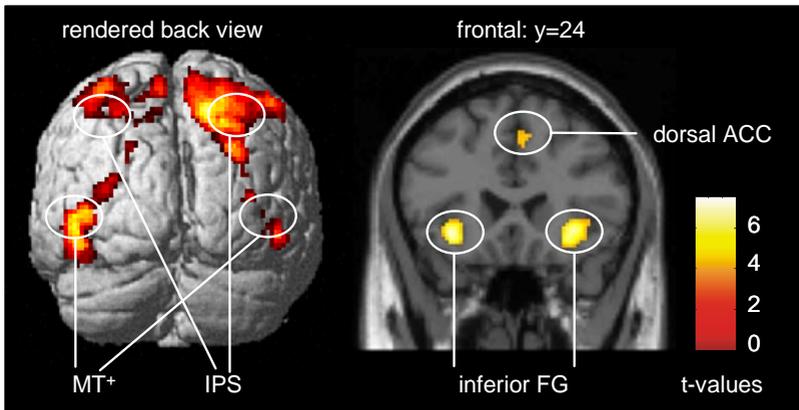
Figure 3. Conjunct activation of morph periods for complex figures vs. circles over all delay periods. (FDR = .01; IPS: intraparietal sulcus, ACC: anterior cingulate cortex, FG: frontal gyrus).

Discussion. The analysis of behavioral data confirmed our hypothesis that both task complexity and prolonged delay periods results in increasing demands. The comparison of maintenance periods with different cognitive load but similar visual processing and motor demands revealed a widespread activation pattern comprising brain areas usually assigned to the processing of visual stimuli. The present data indicate that areas attributed to (visuo-spatial) WM maintenance (temporal, posterior parietal regions, middle frontal gyrus) show enhanced activity with higher stimulus complexity for longer maintenance periods. Additionally, recruited brain regions (inferior frontal gyrus, dorsolateral prefrontal cortex, dorsal anterior cingulate cortex) correspond to areas usually linked to task difficulty [see 2, 3]. Our present data are in accordance with the results of Rypma et al. [4], demonstrating that higher task demands lead not just to an increased activation of the WM network, but also causes an additional recruitment of frontal brain areas, which are supposed to reflect increasing task demands. This activation pattern is displayed constantly over different maintenance intervals (3s, 6s, 9s and 12s). Furthermore, the BOLD signal in individually defined area MT$^+$ was modulated by task demands (complexity and delay periods). This suggests an involvement of area MT$^+$ in cognitive performance. We suppose that this effect, as well as the enhanced activity of other visual processing areas during maintenance of more complex stimuli, is evoked by the allocation of attentional resources.

[1]   Wager, T.D. & Smith, E.E. (2003). Neuroimaging studies of working memory: A meta-analysis. *Cognitive, Affective, & Behavioral Neuroscience*, 3, 255-274.

[2]   Duncan, J. & Owen, A.M. (2000). Common regions of the human frontal lobe recruited by diverse cognitive demands. *Trends in Neurosciences*, 23, 475-483.

[3]   Gould, R.L., Brown, R.G., Owen, A.M., Ffytche, D.H., & Howard, R.J. (2003). fMRI BOLD response to increasing task difficulty during successful paired associates learning. *NeuroImage*, 20, 1006-1019.

[4]   Rypma, B., Prabhakaran, V., Desmond, J.E., Glover, G.H., & Gabrieli, J.D.E. (1999). Load-dependent roles of frontal brain regions in the maintenance of working memory. *NeuroImage*, 9, 216-226.

Correspondence: Daniela Galashan, Department of Neuropsychology and Behavioral Neurobiology, Institute for Cognitive Neuroscience (ICN), University of Bremen, Grazerstr. 6, D-28359 Bremen; galashan(at)uni-bremen.de

Neuronal Correlates of a Shape-Tracking Working Memory Task – Macaque Data

Zinke, W.[1,2], Galashan, D.[2,3], Herrmann, M.[2,3] and Kreiter, A.K.[1,2]

[1]Institute for Brain Research, University of Bremen; [2]Center for Advanced Imaging (CAI) – Bremen; [3]Department of Neuropsychology and Behavioral Neurobiology, University of Bremen

Introduction. In a delayed match-to-sample (DMS) task the sample stimulus needs to be encoded and maintained until a matching stimulus appears in a series of subsequent test stimuli. The detection of a match is indicated by an appropriate response. Neurophysiological studies in monkeys identified the contribution of several brain structures to such working memory (WM) tasks [1]. Specific networks are recruited at different task stages, predicting a differential modulation of functional connectivity within these networks. Indeed, experiments with multi-electrode arrays demonstrated that distinct locations in the posterior infero-temporal cortex (IT) synchronized their neuronal activity while monkeys were successfully performing a short-term memory task [2]. However, such detailed neurophysiological investigations of interactions within distributed networks require precise knowledge about the anatomical distribution of the activated networks. Using fMRI with a monkey allows the identification of regions involved in the WM task throughout the whole brain in order to guide neurophysiological investigations. Furthermore, monkey fMRI allows to directly link human fMRI data with results from monkey electrophysiological studies.

To identify brain structures involved in encoding, delay or retrieval stages of WM tasks, event related designs are commonly used [3]. This model-driven approach does not necessarily capture the dynamics of the neural processes underlying the WM task. A data-driven method such as independent component analysis (ICA) [4] could be used to decompose the distributed activity patterns associated with the WM task. Here, we show the feasibility of this data driven approach to identify the detailed structure and the spatio-temporal modulation of networks in a monkey fMRI experiment.
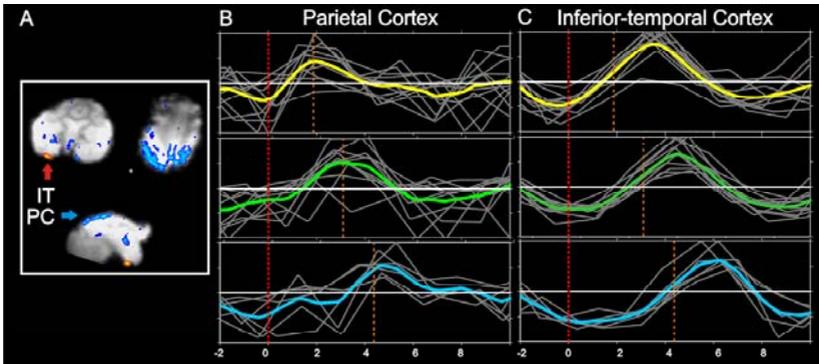
Figure 1. IC map and trial averaged IC time course: Two IC maps are rendered onto an EPI image (A). The blue arrow indicates a component covering mainly the parietal cortex (PC); the red arrow shows the distinct component found in inferior-temporal cortex (IT). The time course of the PC (B) and IT component (C) are averaged for trials with the target on the first (yellow), second (green) or third position (blue). Grey lines show the single time course, the red dotted line indicates the target onset and the orange lines the median response time.

Methods. A male macaque monkey was trained to perform a complex DMS task with multiple test stimulus presentations. A simplified version of the task was used to accustom the monkey to the scanner environment. The data presented here were acquired during this accommodation period. Throughout each trial the monkey was required to keep its gaze within a 1.8˚ x 2.6˚ window centered at the fixation spot. After 0.5 s one of three shapes (circle, triangle or star, size 2.7˚) was presented at an eccentricity of 3˚ in the upper right quadrant for 1 s. Subsequently, up to three shapes were shown for 0.75 s, each preceded by 0.5 s blank period. The animal had to release a lever within 600 ms when the matching shape appeared. Successful trials were rewarded with apple juice. Behavioral errors such as fixation breaks or false responses resulted in termination of the trial without reward. The imaging experiments were carried out within a 3T Siemens Allegra® scanner using an EPI sequence (TR 1.55 s, TE 30 ms, flip angle 70˚, 26 slices, phase encode L-R, resolution 1.5 x 1.5 x 2.0 mm). The monkey accomplished about 300 correct trials within a scanning session lasting two hours. Data were analyzed using the tools of the FSL software package

(www.fmrib.ox.ac.uk/fsl). Time series were motion corrected and smoothed with a 2 mm Gaussian kernel. Melodic [4] was applied in order to determine spatial independent components (IC). The time courses of the ICs were sorted according to the trial type and aligned to the stimulus onset. They were baseline corrected and normalized to the maximal absolute value, followed by linear interpolation and averaging.

Results. Data obtained during two scanning sessions, each lasting 2h, were used for the analysis presented here. ICA resulted in multiple components and allowed to separate noise from meaningful signals. Task-related components were characterized by a time course correlated to trial events and characteristic shifts in time depending on delay duration. Furthermore they showed the typical latency of a BOLD response, while task correlated movement artifacts occurred instantaneously. Some of the meaningful components comprised a set of distributed regions, whereas others were constrained to a distinct location (fig. 1). Averaging over successful trials of single runs shows clear differences between the time courses of different components (fig. 2). Comparable IC maps were extracted from all runs and both sessions. These maps are found in regions such as PC, IT and dorso-lateral prefrontal cortex that were already described in the context of working memory.
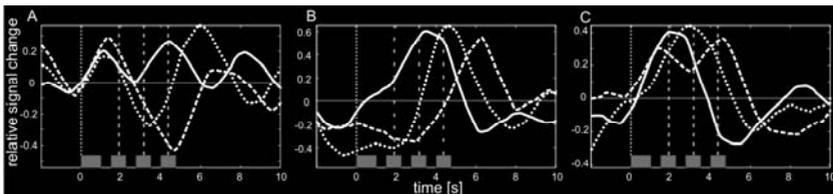
Figure 2. IC time course: Trial averaged time courses of three components (A-C) are shown for trials, where the target re-appeared at the first (solid), second (dotted) or last position (dashed). Grey rectangles indicate the stimulus presentation; dashed grey lines represent the median response time.

Discussion. The current results are based on a limited set of preliminary data. However, they demonstrate first, that successful fMRI recordings can be obtained from monkeys performing complex and demanding tasks within a scanner and second, that ICA followed by trial averaging of the IC time courses is a useful method to identify brain regions and networks dynamically recruited by the WM task. Since the IC time course is not

necessarily compatible with the time course predicted by a GLM approach, ICA provides additional information about the dynamic changes of the networks engaged in the different stages of the WM task. These dynamic changes may reflect modulations of functional connectivity between brain regions. Further investigations of the connectivity between the sub-regions of an IC map will use structural equation modeling as well as neurophysiological multi-channel recordings [5]. With respect to human brain function the same kind of data driven analysis done with corresponding human data (see Galashan et al. in this reader), will facilitate the identification of corresponding functional networks in both species based on the spatio-temporal characteristics of the ICs.

[1]   Constantinidis, C. & Procyk, E. (2004). The primate working memory networks. *Cognitive, Affective, & Behavioral Neuroscience*, 4 , 444-465.

[2]   Tallon-Baudry, C., Mandon, S., Freiwald, W.A., & Kreiter, A.K. (2004). Oscillatory synchrony in the monkey temporal lobe correlates with performance in a visual short-term memory task. *Cereb Cortex*, 14, 713-720.

[3]   D'Esposito, M.D., Postle, B.R., Jonides, J., & Smith EE (1999). The neural substrate and temporal dynamics of interference effects in working memory as revealed by event-related functional MRI. *Proceedings of the National Academy of Science*, 96, 7514-7519.

[4]   Beckmann, C.F. & Smith, S.M. (2004). Probabilistic independent component analysis for functional magnetic resonance imaging. *IEEE Transactions on Medical Imaging*, 23, 137-152.

[5]   Taylor, K., Mandon, S., & Kreiter, A.K. (2005). Oscillatory synchrony is modulated by attention in monkey area V1. *Society for Neuroscience*, No. 411.17

Correspondence. Wolf Zinke, Institute for Brain, University of Bremen, Hochschulring 16a, D-28359 Bremen; zinke(at)brain.uni-bremen.de

Cognitive Control and Error Processing in the Human Brain: Evidence from fMRI

Wittfoth, M.[1,2,3], Küstermann, E.[2,4], Galashan, D.[2,4], Fahle, M.[3] and Herrmann, M.[2,4]

[1]present address: Department of Neurology, Medical School Hannover; [2]Center for Advanced Imaging (CAI) – Bremen; [3]Department of Human Neurobiology, University of Bremen; [4]Department of Neuropsychology and Behavioral Neurobiology, University of Bremen

Introduction. Cumulating evidence suggests that performance monitoring comprises several sub-processes: on the one hand processes associated with the monitoring of pre-response conflict and uncertainty as well as control of cognitive conflict and on the other hand processes which are related to the detection of post-response errors. By using two variants of the Simon task which has been widely used to study conflict resolution in cognitive psychology, the present study was aimed to analyze conflict resolution induced by two interference tasks which only differed with respect to the source of conflicting information (i.e. motion direction / stimulus location). The Simon effect is a robust phenomenon which arises if stimulus and response location do not correspond, albeit stimulus location is task-irrelevant. This effect is interpreted as resulting from the automatic generation of a spatial code in response to stimulus location. Since the spatial code overlaps with the relevant response code derived from the non-spatial dimension (e.g. shape), it interferes with the speed of correct response selection. If a single neural network is engaged in conflict resolution then the activation patterns of response conflict induced by both motion direction and stimulus location should only differ with respect to the specific demands related to the processing of different types of incompatible information. Additionally, by comparing errors committed by high-conflict trials (which are forced due to task interference) to unforced errors committed by non-conflicting trials (in the absence of pre-response conflict) in the motion-based Simon task, we try to shed light on a possible influence of cognitive conflict and cognitive facilitation on error processing.

Methods. Twenty healthy subjects (3 male, 21 – 31 yrs., mean age: 25.5 yrs.) participated in the study. Subjects had to detect and identify form-from-motion stimuli in two different experiments which were conducted within one session. The stimuli consisted of either a triangle or a square containing approximately 200 coherently moving bright dots on a dark screen against a randomly moving background of a total of 4000 dots. The motion-based Simon task contained three conditions: (1) compatible trials (COMP) consisted of dots moving coherently to the side corresponding to a correct response (e.g., a triangle requires a right-hand button press and all dots within the triangle were moving to the right), (2) in incompatible trials (INCOMP) dots within the triangle or square were moving coherently in a direction opposite to the correct side (e.g. the correct response to a square was to press the left-hand button but the target-dots were moving to the right), and (3) during neutral trials (NEU) dots were moving upwards, therefore evoking neither interference nor facilitation. In 20 percent of all trials incompatible stimuli were presented. Neutral trials had the same probability of occurrence. This has been demonstrated to be a prerequisite of inducing interference effects [1]. Subjects had to press the left-hand button as fast and correct as possible if coherently moving dots formed a square and the right-hand button if a triangle was presented. Stimulus location was the task-irrelevant dimension in the second variant (location-based Simon task). The design of this task again included three conditions. Movement direction of the coherently moving dots in the NEU condition led to neither interference nor facilitation because the dots were moving upwards in all trials. All other parameters were identical to the motion-based Simon task, apart from the fact that stimuli appeared not centrally but at a 6° eccentricity to the left or to the right of the fixation point. The order of the two Simon tasks was counterbalanced across subjects. MRI data were acquired on a 3-T Magnetom Allegra® system (Siemens, Erlangen, Germany) equipped with a standard quadrature head coil. Changes in blood oxygenation level-dependent (BOLD) $T2^*$-weighted MR signal were measured using a gradient echo-planar imaging (EPI) sequence (38 slices, slice-thickness: 3 mm with a 0.3 mm gap, TR = 2.5 s, TE = 30 ms, flip angle = 90°, 64 x 64 matrix, FOV 192 x 192, interleaved acquisition). Data analysis was performed with SPM2 (Wellcome Department of Cognitive Neurology, London).

Results. Behavioral data revealed that both types of Simon tasks induced highly significant interference effects. Using event-related fMRI we could demonstrate that both tasks share a common cluster of activated brain

regions during conflict resolution (pre-supplementary motor area (pre-SMA), superior parietal lobule (SPL), and cuneus) but also show task-specific activation patterns (left superior temporal cortex in the motion-based, and the left fusiform gyrus in the location-based Simon task). For the analysis of error-related activation (which was limited to the motion-based Simon task), five participants were excluded due to low error rates (< 5 errors in each condition) or perfect accuracy. While errors related to incompatible trials (forced errors) were mainly associated with activation of the rostral anterior cingulate cortex (rACC) and the precuneus / posterior cingulate, errors related to trials without pre-response conflict (unforced errors) showed peak activation in right inferior frontal gyrus. In order to find common activations between unforced/ forced errors and high-conflict trials, we conducted conjunction tests which showed right inferior frontal gyrus and the bilateral inferior parietal lobule (BA 40) as areas being recruited during both the resolution of conflict and the processing of unforced errors. Common regions of forced errors and conflict processing were medial superior frontal cortex and small clusters in bilateral inferior frontal gyrus (see fig. 1).
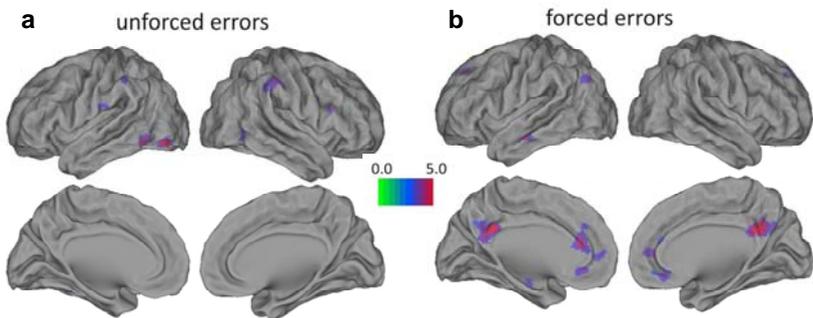
Figure 1. Specific brain activation related to (a) errors on compatible trials (unforced errors), and (b) errors on incompatible trials (forced errors) overlaid on a human PALS SPM2 template.

Discussion. The present data derived from two Simon tasks based on coherent motion perception indicate that both stimulus location and motion direction induce strong interference effects. Both types of conflict resolution resulted in shared activation as well as in task-specific activation patterns. Regarding functional subdivisions of the medial wall, the present data

corroborate the hypothesis that it is mainly the pre-SMA and not the anterior cingulate cortex (ACC) which triggers conflict resolution [2, 3]. Despite conceptual similarities of task design, the observed activation patterns significantly differ probably related to the source of task-irrelevant information, thus indicating the existence of different task-specific networks of conflict resolution [4]. The present findings regarding error-related activity emphasize functionally specific activation patterns in response to errors related to compatible and incompatible events. While the dorsal ACC/ medial superior frontal cortex and operculo-insular frontal cortices may serve as a common error-processing network, functionally specific regions contribute to the processing of errors in regard to whether these erroneous responses were made after the presentation of high- or low-conflict trials. Specifically, error-related dorsal ACC activity in the absence of simultaneously interfering processing streams (as in the case of unforced errors) seems to favor the assumption that the ACC acts as a detector of erroneous motor responses, instead of being a pure conflict monitoring system [5].

[1]   Braver, T.S., Barch, D.M., Gray, J.R., Molfese, D.L., & Snyder, A. (2001). Anterior cingulate cortex and response conflict: effects of frequency, inhibition and errors. *Cerebral Cortex*, 11, 825-836.

[2]   Ullsperger, M. & von Cramon, D.Y. (2001). Subprocesses of performance monitoring: a dissociation of error processing and response competition revealed by event-related fMRI and ERPs. *NeuroImage*, 14, 1387-1401.

[3]   Nachev, P., Rees, G., Parton, A., Kennard, C., & Husain, M. (2005). Volition and conflict in human medial frontal cortex. *Current Biology*, 15, 122-128.

[4]   Wittfoth, M., Buck, D., Fahle, M., & Herrmann, M. (2006). Comparison of two Simon tasks: Neuronal correlates of conflict resolution based on coherent motion perception. *NeuroImage,* 32, 921-929.

[5]   Wittfoth, M., Küstermann, E., Fahle, M., & Herrmann, M. (2007). The influence of response conflict on error processing: evidence from event-related fMRI, *Brain Research* (submitted).

Correspondence. Present address: Matthias Wittfoth, Department of Neurology, Medical School Hannover, Hannover, Germany; wittfoth.matthias(at)mh-hannover.de

MT$^+$ Activation During Spatial Language Processing

Christophel, T.[1,2], Fehr, T.[1,2], Valdes-Conroy, B.[3], Galashan, D.[1,2], Coventry, K.R.[3] and Herrmann, M.[1,2]

[1]Department of Neuropsychology and Behavioral Neurobiology, University of Bremen, [2]Center for Advanced Imaging (CAI) – Bremen, [3]Cognition and Communication Research Centre, Northumbria University, UK

Introduction. Spatial language comprehension, according to the 'functional geometric framework' [1], involves computing where objects are, what they are, and how they are interacting. For example, making a judgment that a bottle is over a glass not only involves computing where the bottle is in relation to the glass, but also involves mentally simulating how the bottle and glass typically interact or will interact over time (whether the bottle is in the correct position for the liquid to successfully reach the glass [2]). Individual spatial terms also vary in the extent to which their meaning is associated with static geometric versus dynamic-kinematic information ([1, 2]). A central functional structure for the processing of motion is area MT$^+$. Kourtzi and Kanwisher [3] reported significant activation of MT$^+$ for static images with implied motion. We tested whether such activations are driven by knowledge of individual objects or knowledge of how objects typically interact with each other, and if motion processing is affected by the by top-down modulation vis-à-vis spatial language consistent with predictions from the functional geometric framework.

Methods. Twelve healthy, right handed, native English speakers (3 female; mean = 30.25 yrs.) participated in the experiment and gave informed consent in accordance with institutional and federal guidelines. We examined spatial language processing using a sentence-picture verification task. Participants were asked to establish whether a sentence (e.g., 'The bottle is over the glass') presented prior to a picture was a true or false description of the picture following. Sentence and pictures were manipulated systematically in a 3 x 3 design. The language condition comprised three different object relations: two types of spatial prepositions ('over/under/above/below' and 'near/far') and a comparative relation of spatial object features ('bigger/

smaller'). The picture condition included three manipulations of typicality of functional interaction of objects: a) functional interaction relevant: one object (bottle, cereal box etc.) was shown releasing a fluid substance (water, cereals etc.) and was positioned higher than a container object (glass, bowl, etc.) consistent with typical interaction between the objects; b) functional interaction not relevant: same objects as in (a) but the releasing objects were positioned lower than the container object, inconsistent with how those objects typically interact; and c) non-functional controls: objects without any functional interaction (e.g. TV and apple) positioned as in (a) and (b).
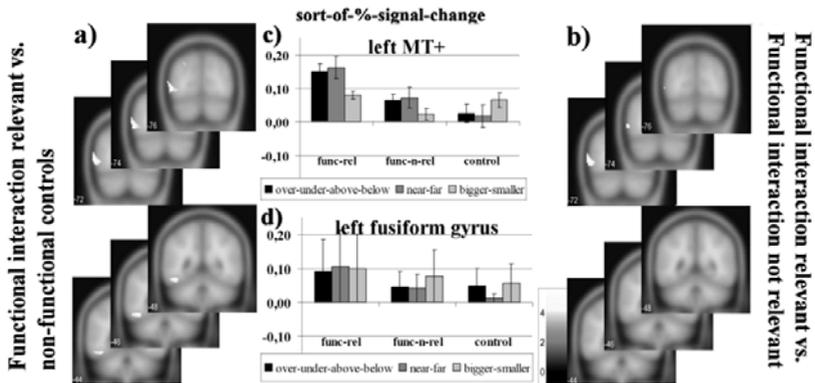
Figure 1. Activated clusters (FDR 0.05, k = 20) for (a) functional interaction relevant vs. non-functional control conditions and (b) functional interaction relevant vs. functional interaction not relevant conditions, coronal slices (MNI-space: -44; -46; -48; -72; -74; -78) and sort-of-%-signal-change data for the 3 x 3 design in (c) left MT^+ and (d) in the left fusiform gyrus, error bars indicate SEMs.

The order of the 9 (3 x 3) different conditions in the sentence-picture verification task was determined by a pseudorandomized non-stationary probabilistic design. Functional MRI data were obtained using an gradient EPI sequence (3T-Siemens Magnetom Allegra®) during the sentence-picture-verification, a baseline condition and a localizer task developed to define regions-of-interest (ROIs) for area MT^+. ROIs were defined by extracting the activated clusters at the temporo-parieto-occipital junction in a motion vs. no-motion contrast with individual thresholds, for the 10 subjects

who showed activations during this stimulation. Additional regions of interest were defined by group level results.

Results. For the picture condition, we found significant activation differences in left area MT$^+$ between functional interaction relevant and functional interaction not relevant conditions. Contrasted against the non-functional controls, the functional interaction relevant condition activated left MT+, the left fusiform gyrus, the left precuneus and bilateral areas of the visual association cortex (BA 18). The results for the left area MT$^+$ and the left fusiform gyrus were confirmed by a 3 x 3 ANOVA including sort-of-%-signal-change data (fig. 1). The comparison of spatial relations and spatial object features showed wide-spread activations. Applying a conjunction analysis, we found the right angular gyrus and a bihemispheric network of parietal and occipital areas (precuneus, cingulate gyrus and posterior cingulate) being activated. In addition, right MT$^+$ was activated for near/far vs. bigger/smaller, as well as bilateral medial and middle frontal gyrus, right inferior and precentral gyrus, left superior frontal gyrus, bilateral postcentral gyrus and inferior parietal lobule, bilateral middle and superior temporal gyrus and right claustrum.
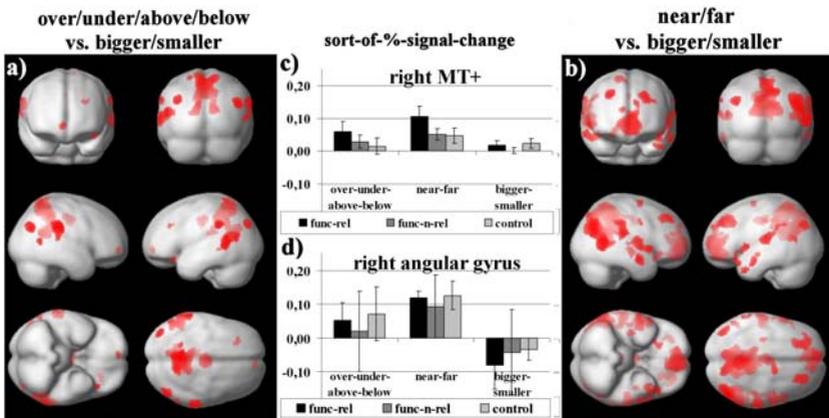
Figure 2. Activated clusters (FDR 0.05, k = 20) in (a) over/under/above/below vs. bigger/smaller, and (b) near/far vs. bigger/smaller (rendered on a smoothed standard MNI-brain) and sort-of-%-signal-change data for the 3 x 3 design in (c) the right angular gyrus, and (d) right MT$^+$ (error bars indicate SEMs).

Discrete activations for over/under/above/below vs. bigger/smaller included left inferior and middle frontal and right medial frontal gyrus, left superior occipital gyrus, bilateral inferior parietal lobule and left postcentral gyrus, and bilateral superior temporal and left middle temporal gyrus. The results in right MT$^+$ and the right angular gyrus were confirmed by a 3 x 3 ANOVA of sort-of-%-signal-change data (figs. 2c and 2d).

Discussion. Our findings indicate that motion processing in area MT$^+$ related to static images with implied motion is induced by whether the objects are placed in a typical functional situation rather than by the objects themselves. However, in contrast to Kourtzi and Kanwisher [3] the effect of implied motion is significant only in the left hemisphere. Differences in functional interaction between objects seem to be constituted in the fusiform gyrus, the precuneus and the visual association cortex. Furthermore, the relation described by the sentence for the same objects mediates MT$^+$ activation providing strong support for the functional-geometric framework [1], in contrast to the findings of Damasio et al. [4]. Differences in results can be explained by more specificity in the present study in the types of spatial relations and objects used.

[1]   Coventry, K.R. & Garrod, S.C. (2004). *Saying, seeing and acting. The psychological semantics of spatial prepositions*. Essays in Cognitive Psychology series, Psychology Press.

[2]   Coventry, K.R., Prat-Sala, M., & Richards, L.V. (2001). The interplay between geometry and function in the comprehension of 'over', 'under', 'above' and 'below'. *Journal of Memory and Language,* 44, 376-398.

[3]   Kourtzi, Z. & Kanwisher, N. (2000). Activation in human MT/MST by static images with implied movement. *Journal of Cognitive Neuroscience,* 12, 48-55.

[4]   Damasio, H., Grabowski, T.J., Tranel, D., Ponto, L.L.B., Hichwa, R.D., & Damasio, A.D. (2001). Neural correlates of naming actions and of naming spatial relations. *NeuroImage,* 13, 1053-1064.

Correspondence. Thomas Christophel, Department of Neuropsychology and Behavioral Neurobiology, Institute for Cognitive Neuroscience (ICN), University of Bremen, Grazer Strasse 6, D-28359 Bremen; tbcl(at)uni-bremen.de

VIII. Various Topics

Various Topics

Thiel, C.M.[1] and Herrmann, M.[2,3]

[1]Institute of Biology and Environmental Sciences, Cognitive Neurobiology, Carl von Ossietzky University Oldenburg, [2]Center for Advanced Imaging (CAI) – Bremen, [3]Department of Neuropsychology and Behavioral Neurobiology, University of Bremen

The majority of the studies presented in this chapter are not embedded in large-scale research projects but illustrate fMRI approaches to various topics outside of the research mainstream in cognitive neuroscience. Thus, many investigations are low-budget projects without continuous funding. The data presented here are often preliminary in nature and should be viewed as work in progress. They, nevertheless, bridge different disciplines such as clinical neurology and cognitive neuroscience or educational and neuroscience research and enrich the flavor of fMRI research at Bremen and Oldenburg universities.

The work of Özyurt and Thiel reflects the aim of the University of Oldenburg to foster interdisciplinary cooperations. The fMRI study presented here is part of a larger BMBF funded initiative that aims to combine educational and neuroscience research and deals with the effects of error feedback on learning in children. Preliminary data analyses show feedback-related neural activity in frontal brain regions and in the basal ganglia. The neuroscience data acquired in the project are expected to shed light on brain mechanisms involved in learning and error feedback in children. A long term goal of combining neuroscience and educational research is to build a scientific basis on which individualized means for teaching and learning for students and teacher education can be developed.

Küstermann and colleagues present a collaborative research project between the Neurology Department at the Clinical Center Bremen-Mitte and the Center for Advanced Imaging (CAI). The authors use fMRI to investigate the short-term functional reorganization of movement-related brain regions after therapeutical lumbar puncture in patients with normal pressure hydrocephalus (NPH). Preliminary data show that improvements in gait

disorders after lumbar puncture are associated with signal enhancements related to imagined movements particularly in the motor strip and parahippocampal region.

The study presented by Erhard and coworkers investigated seven highly trained and experienced Zen meditators and seven age-matched control subjects with respect to brain activation patterns evoked by the startle response. The study sample was characterized by a high drop-out rate due to missing behavioral correlates of the startle reflex. However, explorative data analysis demonstrates that startle-related amygdala activation in Zen meditators is absent during meditation, a finding which points to a neurobiological correlate of meditation induced coping with fear inducing stimuli.

Fehr and colleagues report part of a research cooperation with Sydney (Australia) and Exeter (UK) universities which dates back to the late 1990s when Chris Code started brain imaging studies in mental calculation and number processing [1]. The present work highlights a methodological issue of fMRI investigation in arithmetic operations. The authors show that both different operators as well as the modality of stimulus presentation (auditory or visually presented tasks) affect brain activation patterns during mental calculation. Visually presented tasks result in more widespread and bilaterally distributed brain activation patterns.

[1]   Cowell, S.F., Egan, G.F., Code, C., Harasty, J., & Watson, J.D. (2000). The functional neuroanatomy of simple calculation and number repetition: A parametric PET activation study. *NeuroImage*, 12, 565-73.

Correspondence. Christiane Thiel, Institute of Biology and Environmental Sciences, Cognitive Neurobiology, Carl von Ossietzky University Oldenburg, 26111 Oldenburg; christiane.thiel(at)uni-oldenburg.de; Manfred Herrmann, Institute for Cognitive Neuroscience (ICN), University of Bremen, Grazerstr. 6, D-28359 Bremen; manfred.herrmann(at)uni-bremen.de

The Influence of Immediate Feedback on Subsequent Learning in Children: An fMRI Study

Özyurt, J. and Thiel, C.

Cognitive Neurobiology Group, Department of Biology and Environmental Sciences, Carl von Ossietzky University Oldenburg, D-26111 Oldenburg

Introduction. The present event related fMRI study is part of a larger project that aims to combine educational and neuroscience research. An important debate in educational research on effective learning is the question whether errors should be corrected immediately. Although it is quite plausible that we need feedback about our mistakes in the learning process, it is also conceivable that emotional consequences of feedback might interfere with future learning. Here we investigate the effects of immediate error feedback on subsequent learning in children. To ensure comparability to institutional learning situations an associative learning paradigm that resembles vocabulary learning is used. The task requires formation of object-name associations which have to be retrieved after a short delay period. Children are randomly assigned either to a group receiving corrective feedback after retrieval or to a group receiving no feedback but a neutral stimulus. While in a parallel behavioral study, data of a large sample of children (N=200) enables to combine data of the learning task with data about individual differences (like memory capacity, attention, frustration tolerance, self concept), the fMRI study (N=40) primarily aims to focus on neural correlates of cognitive processes involved in feedback learning. We hypothesized that negative feedback will elicit anterior cingulate activity while positive feedback will elicit striatal activity. We further hypothesized that encoding related activity for specific items will differ in medial temporal and frontal brain regions depending on the direction of feedback received before (i.e. positive vs. negative) and on the group children were assigned to (with vs. without feedback).

Methods. Participants were right-handed children (10-12 yrs) attending the first two years of German secondary school. They had no history of neurologic or psychiatric disorders. Imaging was performed on a 1.5-T SIEMENS Sonata System (Siemens, Erlangen/Germany) using a T2*-weighted echo-planar imaging (EPI) sequence. The experimental tasks

consisted of 40 trials, presented in two sessions per 20 trials. Each trial involved an initial encoding phase, consisting of four object-name associations. Visual stimuli were man-made or natural objects presented for 1.500 msec, with an interstimulus interval of 500 msec. During the presentation of each visual stimulus a pseudoword was presented auditorily as the corresponding object name. Children were instructed to memorize the objects and their appropriate names. In a retrieval period starting after a jittered delay period (4-18 sec) one of the objects was presented with one of the pseudowords and children had to decide by button press with their right hand whether this pseudoword was the correct (index finger, left button) or incorrect name (middle finger, right button) for the object presented. The retrieval phase lasted for 3.500 msec. In the feedback group children received feedback for 1.000 msec (a positive or negative smiley) 500 msec after the end of the retrieval phase, indicating a correct and incorrect response respectively. Reaction times and errors were recorded during task performance in the MRI scanner. After completion of the task a T1-weighted anatomical image of the brain was taken. To reduce movement artifacts and to enhance compliance children were trained in a mock scanner with a similar task prior to the experimental session. Analysis of fMRI data presented here focuses on the group receiving corrective feedback. In order to investigate whether encoding-related activity differs after receiving positive vs. negative feedback we contrasted encoding related activity following positive vs. negative feedback. A second contrast concentrated on differential activation in the retrieval phase when comparing positive vs. negative feedback after successful or unsuccessful retrieval.

Results. Preliminary data of 10 children which received corrective feedback indicated that our task is well adapted to obtain a sufficient amount of correct and incorrect responses. Error rates in the learning paradigm were in the range of 20 to 45% (mean 34.3%). Reaction times of correct (1.596 msec) and incorrect responses (1.638 msec) did not differ significantly. The fMRI data during encoding revealed no significant differences between encoding-related neural activity after positive vs. negative feedback. During retrieval, we found significantly more activation in the left inferior frontal gyrus (BA 47, 38 voxel) and in the left ventral and medial globus pallidus (14 voxel) when children received negative feedback after the retrieval phase compared to events with positive feedback. Contrasting retrieval events including positive feedback with those including negative feedback, the left putamen (19 voxel) was shown to be more active as well as the left middle and

superior frontal gyrus (BA 8, 55 voxel) and a cluster in the left peristriate occipital area 19, extending to occipitotemporal area 37 (22 voxel).
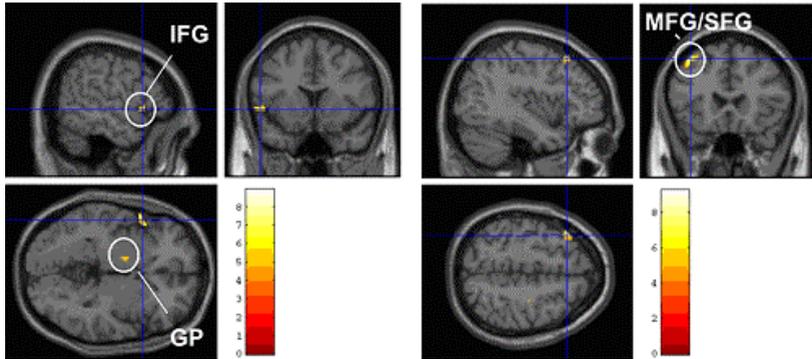
Figure 1. Neural activity during the retrieval phase. Left: differential activity for negative feedback vs. positive feedback. Right: differential activity for positive vs. negative feedback (p=.001, k=10). IFG=inferior frontal gyrus, MFG=middle frontal gyrus, SFG=superior frontal gyrus, GP=globus pallidus.

Discussion. The preliminary data analysis in 10 children receiving corrective feedback did not reveal differences in activation for encoding preceded by positive vs. negative feedback. This result is possibly due to the yet small sample size. Contrasting positive with negative feedback during retrieval revealed increased differential activation in several areas of the basal ganglia under both, positive and negative feedback. The striatum is known to be active in conditions with vs. without feedback [1]. The significantly stronger activation of the left inferior frontal gyrus (BA 47) for negative feedback vs. positive feedback during retrieval might be a neural correlate for error detection and error processing [2]. The stronger activation of the left superior frontal gyrus (BA 8) for positive feedback vs. negative feedback during retrieval might be a potential correlate for successful retrieval [3]. Clearly more data, especially when receiving no feedback is needed to isolate functional correlates of positive vs. negative feedback.

[1] Tricomi, E., Delgado, M.R., McCandliss, B.D., McClelland, J.L., & Fiez, J.A. (2006). Performance feedback drives caudate activation in a phonological learning task. *J Cogn Neurosci*, 18, 1029-1043.

[2] Menon, V., Adleman,.N.E., White, C.D., Glover, G.H., & Reiss, A.L. (2001). Error related brain activation during a go/nogo response inhibition task. *Hum Brain Mapp*, 12, 131-143.

[3] Lepage, M., Ghaffar, O., Nyberg, L., & Tulving, E. (2000). Prefrontal cortex and episodic memory retrieval mode. *PNAS*, 97, 506-511.

Correspondence: Jale Özyurt, Cognitive Neurobiology Group, Department of Biology and Environmental Sciences, Faculty V, Carl von Ossietzky University Oldenburg, D-26111 Oldenburg; jale.oezyurt(at)uni-oldenburg.de

Neuronal Correlates of Movement Disorders in Normal Pressure Hydrocephalus (NPH)

Küstermann, E.[1,2,3], Ebke, M.[4], Dolge, K.[2,3,4], Schwendemann, G.[4], Leibfritz, D.[1,3] and Herrmann M.[2,3]

[1]Institute of Organic Chemistry, University of Bremen, [2]Department of Neuropsychology and Behavioral Neurobiology, University of Bremen, [3]Center for Advanced Imaging (CAI) – Bremen, [4]Neurologische Klinik, Klinikum Bremen-Mitte

Introduction: Normal pressure hydrocephalus (NPH) affects predominantly elderly people and poses a major impact on their every day life. It is characterized by greatly enlarged ventricles at fairly normal pressure rates. Typical symptoms are gait problems which improve upon guidance. Still, little is known about the underlying pathophysiology. Lumbar puncture (LP) with removal of 30-50 ml cerebrospinal fluid (CSF) could treat NPH patients successfully. It has been hypothesized that reduced resorption of CSF leads to its penetration into the frontal and parietal lobe which leads to a reduced cerebral blood flow. Here we report blood-oxygen level dependent (BOLD)-signal changes with functional magnetic resonance imaging (fMRI) before and after lumbar puncture (LP) of about 50 ml CSF in NPH patients. In order to explore correlations between brain activity and gait, subjects were asked to perform imaginary foot movement and walking tasks similar to those published recently [1, 2]. We expected a changed brain activity pattern after therapeutic LP.

Methods. Experimental Protocol: eight patients (4 male, mean age=70.6 yrs., 65–80 yrs.,) with suspected NPH (Klinikum Bremen-Ost and -Mitte) were asked to volunteer for this study which was approved by the local ethics committee. FMRI scans were performed before and 3 days after LP. Before MR-scanning, subjects were prepared for the imagination tasks by walking with closed eyes (i) freely and (ii) guided by a supporter for about 40 m. During scanning, subjects were instructed via head phones to perform the following tasks: (a) move the right foot; (b) imagine moving the right foot; (c) imagine walking freely and (d) imagine guided walking as trained just before. Task duration as well as resting periods between tasks were 15 s. Subjects were requested to perform two runs of 11 min each.

MR-imaging: All experiments were performed at 3T (Allegra®, Siemens, Germany) using a circularly polarized birdcage head coil for transmit and receive. For fMRI a standard EPI-protocol (TE/TR =30/2600ms) was used covering the whole head with 45 slices at an isotropic resolution of 3mm. Brain morphology was assessed by a 3D-T1-weighted scan (MPRAGE, TE/TR/TI=4.38/2300/900ms, 8° exc. pulse) at 1mm isotropic resolution. Data analysis was performed with SPM5 (http://www.fil.ion.ucl.ac.uk/spm) under Matlab7 (The MathWorks, Natick, USA). Morphological and fMRI data were normalized to a custom made T1-weighted NPH-template data set fitting well on the standardized MNI-template. Eight NPH-subjects were scanned before and after LP; one was excluded from further analysis due to excessive foot movements. FMRI data were also obtained from 10 healthy young volunteers (3 male, mean age=31.9 yrs., 28-36 yrs.). Average BOLD responses to the foot movement task were calculated for individuals and groups based on extracted time courses from the most activated voxel and its neighbors in the motor cortex (http://marsbar.sourceforge.net/). Cumulative head movements during fMRI scans were estimated by integrating the magnitude of posthoc motion correction traces. were used to The cognitive performance of 6 NPH-patients was assessed by neuropsychological tests (tab. 1) before and after LP. Not all of them participated in MR-examination.

Results. Real and imagined foot movements as well as imagination of walking caused positive BOLD signal changes in a number of brain areas, predominantly in motor, premotor and pre-SMA, BA6, putamen and the cerebellum (fig. 1). These findings are consistent with results reported previously [1-3]. Although the principal patterns are fairly similar between groups, the size of activated areas in controls are larger. However, by lowering the threshold in the NPH data, similar patterns were obtained. Group specific features of the BOLD signal were assessed for the foot movement task. Maximal signal changes showed no significant signal changes between the NPH group(2.3±0.9%) and young controls (2.4±1.1%). Analysis of motion data revealed 2 to 4-fold more intense head movement of NPH-subjects than controls. After LP, the strongest increase in brain activity was observed after random effects analysis related to the imaginary walking task in the precentral gyrus (fig. 2A). Signal changes are also found at the parahippocampal gyrus, albeit at a much lower significance level. Other areas exhibiting LP-related signal changes are mostly located either at tissue/CSF interfaces, inside white matter, or outside the brain (fig. 2B).
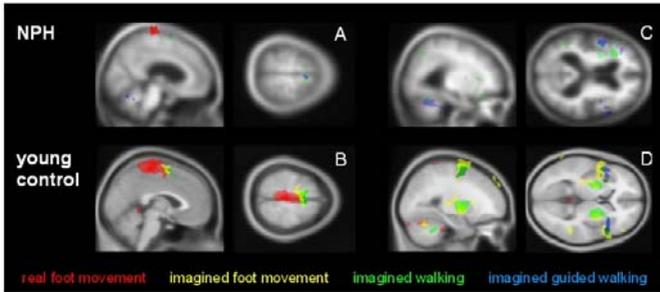
Figure 1. Activation patterns after random effects analysis of NPH (A+C, n=7) and young controls (B+D, n=10). For easier inspection, data are presented at different statistical thresholds. A+B: p=0.001, cluster > 5; C+D: p=0.005, cluster > 50.
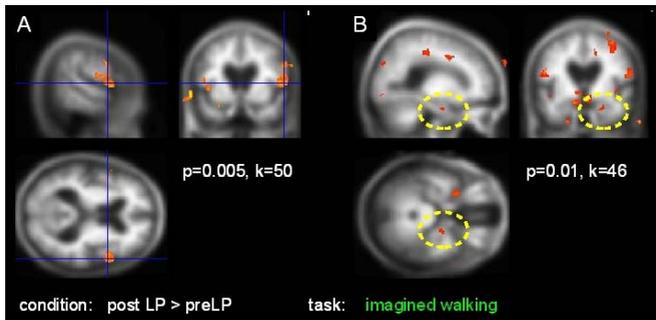
Figure 2. Areas of increased BOLD signal after LP are predominantly observed in the precentral gyrus (A) and at a lower level on the parahippocampal gyrus (B).

Test		pre-LP	post-LP	*P*
MMSE	(max. 30.0)	24.0	24.8	0.55
mental calculation	(max. 12.0)	9.7	9.7	1.00
memory	(max. 40.0)	16.5	14.8	0.73
time	(max. 8.0)	6.5	6.3	0.70
fragmented images	(max. 8.0)	5.7	5.7	1.00
lexical fluency	(words/min)	8.5	9.2	0.57
semantic fluency	(words/min)	15.0	13.5	0.40

Table 1. Mean neuropsychological test scores (raw data) before and after LP (n=6).

All patients experienced improvements in gait due to the LP intervention. However, the neuropsychological tests failed to demonstrate improvements upon the lumbar puncture (see tab. 1).

Discussion. The hypotheses of disturbances in liquor penetration into brain tissues as well as failures of resorption were challenged by clinical evidence of no improvements although drainage was effective. Increase of ventricles were seen although gait disturbances or cognitive dysfunctions improved after LP. Thus, fluid disturbances in liquor are unlikely responsible for NPH symptoms. Recent data by Tullberg [4] and others brought the focus on the hypothesis of neuronal dysfunction with high correlation between improvements in symptoms and restitution of axonal function. Our results are in line with this idea: the increased signal in the precentral gyrus, which is involved in neuronal circuitry for movements [5, 6], and the parahippocampal region during imagined walking is in line with the notion of facilitated neuronal processing. These changes seem to correlate with improvements of gait in all our tested NPH-subjects. Current efforts focus on the problem whether yet unexplained variance due to bulk head and physiological brain motion can be identified and removed from the data.

[1]   Jahn, K., et al. (2004). Brain activation patterns during imagined stance and locomotion in functional magnetic resonance imaging, *NeuroImage*, 22, 1722

[2]   Malouin, F. et al. (2003). Brain activations during motor imagery of locomotor-related tasks: a PET study, *Human Brain Mapping*, 19, 47-62.

[3]   Miyai, I., et al. (2001). Cortical mapping of gait in humans: a near-infrared spectroscopic topography study, *NeuroImage*, 14, 1186-92.

[4]   Tullberg, M., et al. (2007). Ventricular cerebrospinal fluid neurofilament protein levels decrease in parallel with white matter pathology after shunt surgery in normal pressure hydrocephalus, *Eur J Neurol,* 14, 248-54.

[5]   Schubotz, R.I. & von Cramon D.Y. (2004). Sequences of abstract nonbiological stimuli share ventral premotor cortex with action observation and imagery. *J Neurosci*, 24, 5467-74.

[6]   Ehrsson, H.H., et al., (2004). That's my hand! Activity in premotor cortex reflects feeling of ownership of a limb. *Science*, 305, 875-7.

Correspondence. Ekkehard Küstermann, c/o Department of Organic Chemistry, University of Bremen, Leobener Strasse NW2/C, D-28359 Bremen; ek(at)tomo.uni-bremen.de

The Effects of ZEN Meditation on the Cerebral Processing of the Startle Response

Erhard, P.[1,2], Tangeten, S.[3], Koch, M.[3], Leibfritz, D.[1,2] and Herrmann, M.[2,4]

[1]Institute of Organic Chemistry, University of Bremen, [2]Center for Advanced Imaging (CAI) - Bremen, [3]Institute for Brain Research, Department of Neurobiology/ Neuropharmacology, [4]Department of Neuropsychology and Behavioral Neurobiology, Bremen University

Introduction. Practicing meditation brings the brain into a state that differs considerably both from sleep and the normal awake state [1]. This state is not easily characterized in scientific terms. A number of different meditation methods has been described and a big variety of different effects on different physiological parameters such as resting state EEG, galvanic skin response (GSR), heart rate, respiration pattern and awareness of the environment has been observed [2]. The startle response is a defensive reflex evoked by unexpected and intense stimuli. We sought to investigate, if and how the cerebral processing of the well characterized auditory startle response [3] is altered in ZEN mediator both in normal awake state and during meditation. To this end we performed an fMRI startle experiment in our 3T Allegra (Siemens™) scanner. We hypothesized, that meditation can modulate the cerebral response to startle in areas that are part of the fear circuit. Experienced ZEN meditators and age matched controls with no experience or knowledge of meditation participated in this study.

Methods. The study was approved by the local ethics board. Seven male experienced ZEN meditators (ZM, 20 yrs. average, 10 yrs. minimum meditation practice) with no history of neurological or psychiatric illness and 7 age matched male volunteers with no history of meditation experience or knowledge participated (NM). The paradigm consisted of either meditating (ZEN meditation) or relaxing in the scanner. The startle sound was applied via a sound card, a commercial sound mixer and ConFon™ head-phones. The startle sound consisted of white noise with a randomized duration of 30 to 55ms and a sound pressure level of max 105 dBA and appeared pseudo-

randomized with an average ISI of 30s. In addition, the breathing pattern, heart rate and galvanic skin response (GSR) were recorded simultaneously and in sync with fMRI data acquisition. The GSR electrodes were attached to the palm of the left hand. The startle eye blink response was recorded on videotape via a camera behind the scanner and a mirror-setup. The duration of each of the experimental runs was approximately 9 to 11 min. Three runs were performed with every volunteer. ZM were instructed to refrain from meditation during the first functional run. An anatomical scan followed, during which ZM were asked to get into meditation as deep as possible. ZM were able to indicate how deep they are in meditation by pressing a button from one (beginning meditation) to four times (as deep as possible). Another button indicated gradually getting out of meditation e.g. due to distraction. Two functional scans followed where meditators were asked to continue meditating. Controls followed the same scheme, except that they were not advised to meditate. The data from control subjects were used to investigate an order effect. All subjects had to respond to the NEO-FFI questionnaire and ZM were also evaluated regarding their meditation habits. FMRI data acquisition parameters were: TE = 30ms, TR = 2500ms, 45 slices, flip angle = 90º, FOV = 192x168 mm, matrix: 64(read)x56, slice thickness: 3mm, prospective motion correction, 220 to 270 volumes per run. The SPM2 functional imaging analysis software was used for the entire fMRI data processing. Preprocessing included retrospective motion correction, slice time correction, normalization to the standard MNI brain and smoothing with a Gaussian kernel of 8 mm isotropic. Statistical analysis of each individual functional run on the first level was based on a model that included the startle stimuli and motion parameters. Random effects data analysis was performed with various subgroups of the cohort. The eye blink response to the startle sound was rated by careful observation of the video recordings. Physiological data was analyzed with the Spike2™ software and home written routines in MatLab™ and IDL™.

Results. No significant difference in head movement was found between ZM and NM. The breathing pattern turned out to be too slow for a robust analysis of correlation with the startle response, in some subjects, the startle sound induced an interruption in the breathing pattern. The heart rate was slightly increased following the startle stimuli, however no significant difference was observed between subjects and conditions. No order effect in non meditating volunteers was observed for heart rate and respiration frequency. Four out of seven controls showed no or very little response to the startle stimulus. Due

to not meeting this behavioral prerequisite these subjects were excluded from further statistical analysis. Likewise, two out of seven meditators had to be excluded for the same reason. The GSR measurement turned out to be extremely sensitive to hand motion, which in many cases was correlated with the occurrence of startle stimuli, and, depending on the position of the hand also sensitive to respiration and heartbeat. The reason for this behavior is the fact, that even minimal movements of the GSR leads induce relatively high currents inside the magnetic field of the MRI scanner. These are amplified by several orders of magnitude in the GSR electronics. Nevertheless in meditating subjects, the size of the GSR correlates with the rating of the eye blink effect. The fMRI data of ZM and NM showed strong activation in the auditory cortices bilaterally. The inferior parietal lobule was slightly more activated in NM across all runs. Medial wall activation in particular in the cingulate gyrus was more abundant in ZM (see fig. 1a). No activation above statistical threshold in the amygdala could be detected in NM. A clear bilateral activation in the amygdala showed up in ZM in the non meditating state (see fig. 1b). The amygdalae, however, were not activated due to startle in both meditation runs. No area was more activated due to startle during meditation than off meditation.
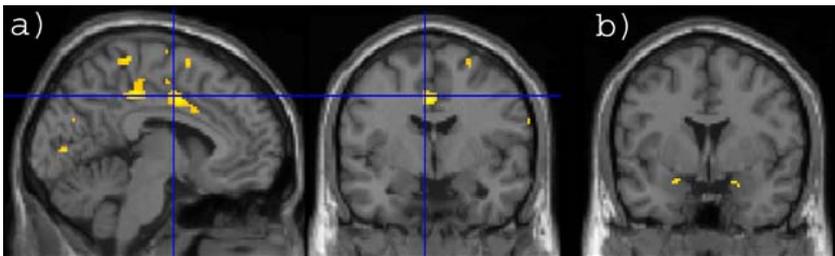
Figure 1. Second level data analysis: Cerebral activation patterns of startle events (a) medial processing is more extended in ZEN meditators than in the normal control (b) bilateral activation in amygdalae (MNI 22:2:-20; -22:-2:18) during rest (off meditation).

Conclusion. We conducted an fMRI study on the effect of startle sounds on long term meditators both during meditation and during normal awake state. We also acquired fMRI data on normal volunteers, despite the fact, that up to now we were unable to provide a sufficiently large cohort of these age matched subjects, we could show, that the acquisition order does not impact

the cerebral activation pattern evoked by startle stimuli. During fMRI we recorded physiological data such as respiration, heart rate and GSR. We found that the GSR to startle sounds is correlated with the eye blink reflex. The most important finding in our study is, that bilateral activation in ZM in the amygdalae was present before meditation but absent during meditation. The amygdala is at the core of the fear and anxiety circuit [4, 5]. This finding indicates, that meditation can modulate a near automatic response, that otherwise cannot be altered voluntarily. This, taken together with the fact that more areas of the medial wall, most pronounced in the posterior part of the cingulate cortex (which is also part of the fear circuit [6], are involved in startle processing in ZEN meditators hints, that these volunteers developed a better coping strategy regarding sudden fear inducing events.

[1]   Cahn, B.R. & Polich, J. (2006). Meditation states and traits: EEG, ERP, and neuroimaging studies. *Psychological Bulletin*, 132, 180-211.

[2]   Davidson, R.J., Kabat-Zinn, J., Schumacher, J., Rosenkranz, M., Muller, D., Santorelli, S.F., Urbanowski, F., Harrington, A., Bonus, K., & Sheridan, J.F. (2003). Alterations in brain and immune function produced by mindfulness meditation. *Psychosomatic Medicine,* 65, 564-570.

[3]   Orr, S.P., Lasko, N.B., Shalev, A.Y., & Pitman, R.K. (1995) Physiologic responses to loud tones in Vietnam veterans with posttraumatic stress disorder. *Journal Abnormality Psychology*, 104, 75-82.

[4]   Charney, D.S. & Deutch, A. (1996). A functional neuroanatomy of anxiety and fear: implications for the pathophysiology and treatment of anxiety disorders. *Critical Reviews in Neurobiology*, 10, 419-446.

[5]   LeDoux, J.E. (2000). Emotion circuits in the brain. *Review of Neuroscience,* 23, 155-184.

[6]   Vogt, B.A., Finch, D.M., & Olson, C.R. (1992). Functional heterogeneity in cingulate cortex: the anterior executive and posterior evaluative regions. *Cerebral Cortex*, 2, 435-443.

Correspondence. Peter Erhard, Institute of Organic Chemistry, University of Bremen, 28359 Bremen; pe(at)tomo.uni-bremen.de

Neuronal Correlates of Mental Calculation

Fehr, T.[1,2,3], Code, C.[4,5] and Herrmann, M.[1,2]

[1]Dept. of Neuropsychology / Behav. Neurobiology, University of Bremen, [2]Center for Advanced Imaging (CAI) - Bremen, [3]Dept. of Neurology II, Magdeburg University, [4]School of Psychology & Centre for Cognitive Neuroscience, University of Exeter, [5]School of Communication Sciences & Disorders, University of Sydney

Introduction. The issue of how arithmetic operations are represented in the brain has been addressed in numerous studies. Lesion studies suggest that a network of different brain areas (e.g. the left and/or right parietal lobe, frontal cortex, and basal ganglia) is involved in mental calculation processes. Neuroimaging studies have reported inferior parietal and lateral frontal activations during mental arithmetic using tasks of different complexities. For psychophysiological aspects of mental calculation an influential theoretical framework has been suggested by Dehaene [1]. He proposed a model that assumes that different brain regions are responsible for the processing of spoken numbers, recalling numerical knowledge, calculation, and comparing magnitudes. Indeed, there is scarce information about the comparability of brain activation associated with different operators and task presentation modalities. The present study investigated fMRI-BOLD activity during mental arithmetic processing after visual and auditory task presentation.

Methods. FMRI data acquisition: Functional magnetic resonance imaging (GE Signa LX 1.5 T Scanner, Milwaukee, WI, gradient EPI sequence covering 23 axial (AC-PC), interleaved slices (5 mm thickness, 1 mm gap) encompassing the entire cerebrum and cerebellum (TR/TE = 2000/40 ms; FOV 20 cm, 600 volumes in each run) recordings were obtained from 11 healthy adults (6 female; mean age: 26.8±4.6 yrs.; 22-40 yrs.) Arithmetic tasks were presented sequentially in visual and auditory form including digits and the operators '+', '-', '/', and 'x' as task elements (fig. 1). Forty tasks for each operator were presented. Fifty percent of the task solutions ranged between 1 and 9 (= simple tasks) and 50 percent ranged between 10 and 100 (= complex tasks).

FMRI data analysis: After standard pre-processing (re-alignment, slice timing, normalizing and smoothing) data sets were analyzed using a second-level random effects analysis. To accomplish this second-level analysis, predetermined condition effects at each voxel were calculated using a t-statistic for each participant and session, and producing a statistical image for the complex vs. simple calculation contrast. These contrast images were then

Figure 1. Sequential presentation of task elements.

used to identify main effects of task using a one sample t-test. To identify common brain regions reflecting processing of all operators and for subtraction tasks across modalities conjunction (null) [2] analyses were applied.

Results. Behavioral data: For all tasks and modalities complex tasks showed longer reaction times than simple tasks (Greenhouse-Geisser (GG) adjusted; all post hoc tests were calculated according Fisher´s LSD; visual (all operators): Task ($F_{[8,80]}$=90.9; p<.01); visual and auditory subtraction: Task ($F_{[3,30]}$=95.4; p<.01,); Presentation Modality ($F_{[1,10]}$=36.8; p<.01). For the visual modality only, simple tasks showed shorter RTs than complex tasks (all p<.01). Complex subtraction resulted in longer RTs compared to all other complex operators (all p<.01). Auditory presentation produced longer RTs for complex subtraction (all p<.01) and simple tasks, but the difference for simple tasks did not reach statistical significance (p=.05).

FMRI data: Contrasting complex vs. simple tasks showed widespread network activation in prominently fronto-temporal, inferior parietal and other regions including basal ganglia and cerebellum (fig. 2). Mental processing of different operators and modalities showed conjunct activations in prominently right frontal and inferior parietal regions (fig. 3).

Figure 2. Glass-brain views of complex vs. simple contrasts for (a) all visual operators and (b) auditory subtraction.

Discussion. Mental processing of different operators recruited partly common and partly different brain areas. Furthermore different presentation modalities of calculation tasks seem to influence mental arithmetic processing. Conjunct activation for subtraction tasks after auditory or visually presented tasks showed prominently right frontal and parietal distribution. The calculation of visually presented tasks seemed to recruit larger and more bilateral distributed neural networks. At the same time, response times were faster for complex subtraction after visual presented tasks suggesting more efficient parallel processing after visual in comparison

to mental arithmetic after auditory task presentation. Right frontal brain regions - possibly indicating working memory involvement - were commonly recruited during mental calculation independent of operator or task presentation modality. Task- and modality-dependent activation of basal ganglia and cerebellum might indicate an involvement of motor components in mental arithmetic. Furthermore, different patterns of task- and modality-dependent activations in parietal regions might indicate a modality and task-specific involvement of parietal sub-regions in mental arithmetic.
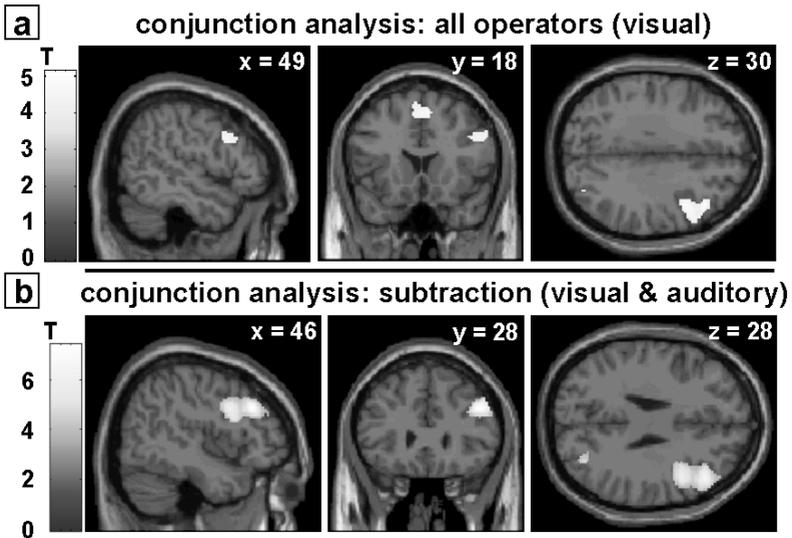
Figure 3. Conjunction analyses for (a) all operators and (b) auditory & visually presented tasks superimposed on an individual normalized brain.

[1] Dehaene, S. (1992). Varieties of numerical abilities. *Cognition*, 44, 1-42.

[2] Nichols, T., Brett, M., Andersson, J., Wager, T., & Poline, J.B. (2005). Valid conjunction inference with the minimum statistic. *NeuroImage*, 25, 653-660.

Correspondence. Thorsten Fehr, Department of Neuropsychology and Behavioral Neurobiology, Institute for Cognitive Neuroscience (ICN), University of Bremen, Grazer Strasse 6, D-28359 Bremen; fehr(at)uni-bremen.de